RECEPTOR FOR ADVANCED GLYCATION END PRODUCTS (RAGE) IN PULMONARY FIBROSIS

by

Lana Elaine Hanford

BS, Western Washington University, 2000

Submitted to the Graduate Faculty of

The School of Medicine in partial fulfillment

of the requirements for the degree of

Doctor of Philosophy

University of Pittsburgh

2005

UNIVERSITY OF PITTSBURGH

SCHOOL OF MEDICINE

This dissertation was presented

by

Lana Elaine Hanford

It was defended on

May 6, 2005

and approved by

Dr. Charleen T. Chu, MD, PhD
Department of Pathology

Dr. Augustine M. Choi, MD
Department of Medicine

Dr. George K. Michalopoulos, MD, PhD
Department of Pathology

Dr. Bruce R. Pitt, PhD
Department of Environmental and Occupational Health

Dr. Tim D. Oury, MD, PhD
Dissertation Director
Department of Pathology

COPYRIGHT

RECEPTOR FOR ADVANCED GLYCATION END PRODUCTS (RAGE)
IN PULMONARY FIBROSIS

Lana Elaine Hanford, PhD

University of Pittsburgh, 2005

ABSTRACT

Idiopathic pulmonary fibrosis (IPF) is a debilitating disease that involves a severe reduction in respiratory function, essentially culminating in the loss of the ability to sufficiently breathe. Current therapies are largely ineffective, and many of the molecular details of the pathogenesis of IPF remain unknown. Thus, new therapeutic targets need to be identified.

We investigated a possible role for the receptor for advanced glycation end products (RAGE) in the pathogenesis of IPF. RAGE is a multiligand member of the immunoglobulin superfamily of cell surface receptors. It is generally associated with cellular perturbation in that RAGE-ligand interactions initiate a signaling cascade that ends with the activation of the pro-inflammatory transcription factor NF-κB. In most adult healthy tissues RAGE is expressed at low levels, but it is highly upregulated at sites of various pathologies, where it is thought to act as a propagation factor for disease.

Notably, the exception to low RAGE expression in healthy adult tissues is the lung, the organ shown to have the highest RAGE transcript levels in humans and rats. This suggests that RAGE may have a role in lung homeostasis, implying that RAGE serves a function in the lung distinct from that in other tissues.

RAGE has a secreted isoform, sRAGE, that acts as a decoy receptor. In humans, sRAGE is a product of alternative splicing. In contrast, we found that sRAGE in mice is produced by proteolytic truncation of cell surface RAGE.

The focus of this project was to investigate *the hypotheses that RAGE and sRAGE regulation are altered during the pathogenesis of pulmonary fibrosis, and that this alteration is a key step in the pathogenesis of pulmonary fibrosis*. To address these hypotheses, we utilized the bleomycin and asbestos mouse models of pulmonary fibrosis as well as human IPF tissues. We found that in both animal models and in IPF tissues, RAGE and sRAGE protein levels are significantly reduced during the pathogenesis of pulmonary fibrosis. Observations from RAGE knockout mice suggest that absence of pulmonary RAGE is itself pro-fibrotic. These studies reveal RAGE as a novel therapeutic target in the pathogenesis of idiopathic pulmonary fibrosis.

TABLE OF CONTENTS

LIST OF TABLES

LIST OF FIGURES

ABBREVIATIONS

α-SMA	α-smooth muscle actin
Aβ	Amyloid β peptide
AE-I	Alveolar epithelial type-I cells
AE-II	Alveolar Epithelial Type-II cells
AGE	Advanced glycation end products
AM	Alveolar macrophage
BALF	Bronchoalveolar Lavage Fluid
DN-RAGE	Dominant-negative RAGE mutant
DTT	Dithiothreitol
ECM	Extracellular Matrix
EN-RAGE	S100A12 (Extracellular newly-identified RAGE ligand)
ERK1/2	Extracellular signal-regulated Kinase
HMGB1	High Mobility Group Protein 1
husRAGE	Human sRAGE (recombinant)
ICAM-1	Intercellular Adhesion Molecule-1
IL-1β	Interleukin-1β
IL-6	Interleukin-6
IPF	Idiopathic Pulmonary Fibrosis
LC-MS/MS	Liquid chromatography tandem mass spectrometry
MALDI-MS	Matrix-assisted laser desorption ionixation mass spectrometry
PAGE	Polyacrylamide Gel Electrophoresis
PF	Pulmonary Fibrosis
RAGE	Receptor for Advanced Glycation End Products
ROI	Reactive Oxygen Intermediates
RP-HPLC	Reverse phase high pressure liquid chromatography
SDS	Sodium dodecyl sulfate
sRAGE	Soluble RAGE
TGF-β	Transforming Growth Factor β
TNF-α	Tumor Necrosis Factor α
UIP	Usual Interstitial Pneumonia
VCAM-1	Vascular Cell Adhesion Molecule-1

ACKNOWLEDGEMENTS

I would like to thank my mentor, Tim Oury, for his excellent guidance, as well as his strong encouragement, unending enthusiasm and constant support. In addition to teaching me so much about science and the importance of W.A.G.'s, I have also learned from him what it means to be a great mentor.

I would also like to thank the other members of my dissertation committee, Dr. Charleen Chu, Dr. Augustine Choi, Dr. George Michalopoulos and Dr. Bruce Pitt, for their helpful suggestions, insightful discussions, and encouragement, as well as for their patience during times when I was trying to schedule a committee meeting. Their valuable input is appreciated.

The many hours that I have logged in lab as a graduate student would not have been nearly as fun had there not been such great people to work with. So I must thank everyone who has worked with me in lab over the years: Lisa Schaefer, Toni Termin, Cheryl Fattman, Rod Tan, Jake Tobolewski, Gina Randa and, of course, Tim. You all made days in lab so much more fun.

I am fortunate to have a family that is so supportive, even from across the country. I am grateful to have not two, not even four, but six parents who have all supported me in different ways and from whom I am constantly learning, as well as two sisters who are also some of my best friends.

I am also fortunate to have the best husband in the entire world, Marc, who is the epitomy of support and who is a rich source of inspiration and intellect as well as humor. He makes every day of my life better and I can not express my appreciation of him in words, except to say that he is my royal flush on the flop.

1. INTRODUCTION

Idiopathic pulmonary fibrosis (IPF) is an extremely debilitating disease that culminates essentially in the loss of the ability to breathe. Current therapies are largely ineffective and the only cure is lung transplantation, which comes with its own complications. Being that many details of the molecular pathogenesis of IPF are still unknown, further research in the pathogenesis of this disease will bring into light novel therapeutic targets, with hopes to improve afflicted patients' care and quality of life.

1.1. PULMONARY FIBROSIS

1.1.1. Highlights of Normal Lung Architecture

The primary function of the lung is gas exchange. Molecular oxygen from the air must enter into the circulation to be delivered to tissues throughout the body in order for them to generate energy. Simultaneously, carbon dioxide must be released from the blood as a waste product from cellular respiration. The elegant design of the lung allows this organ to perform this vital exchange.

Oxygen and carbon dioxide move between the blood and air by diffusion, necessitating an exceedlingly thin barrier between blood and air. At the same time, in order to deliver sufficient oxygen to all tissues of the body, the gas exchange surface area must be extremely large. In humans, this large surface area is obtained by the development of 300 million tiny sacs, called

alveoli, each surrounded by a dense network of capillaries [1]. Remarkably, the combined surface area of all of the alveoli within an adult human lung is approximately equivalent to the size of a tennis court. Over ninety percent of the alveolar surface is lined by thin, expanded squamous alveolar epithelial-type I cells (AE-I) [2]. This cell and its thin underlying basement membrane make up the only barrier between the air and the pulmonary capillaries; in some areas of the lung, this air-blood barrier is just 0.3 μm thick [3]. The thin, delicate nature of the alveolar wall is *essential* for the lung to carry out its vital gas exchange function.

Another important feature of the lung is its elasticity. During inhalation, the lung expands in order to take in a large volume of air and maximize respiratory exchange. This property is referred to as compliance, and diseases that severely limit pulmonary compliance, such as pulmonary fibrosis, are termed *restrictive*. When we exhale, the lung recoils to push out expired air, and this property is called elastance. Diseases that reduce elastance of the lung, such as emphysema, are referred to as *obstructive*.

1.1.2. The Fibrotic Lung

Idiopathic pulmonary fibrosis is a restrictive type of lung disease that involves irreversible damage to the lung parenchyma, including marked impairment of lung compliance and severe thickening of normally thin alveolar walls, and eventually results in respiratory insufficiency. Known causes of pulmonary fibrosis (PF) include environmental particulates (asbestos and silica [4, 5]), chemicals (the antineoplastic drug bleomycin [6]), and radiation [7]. Familial pulmonary fibrosis, evidently due to mutations in surfactant protein C [8-11], has also been described. However, the majority of clinical PF cases are idiopathic (IPF), indicating that the fibrotic stimulus is unknown.

Prevalence rates of IPF have been estimated to be 3-5 per 100,000 population [12], although many consider this an underestimation. The diagnosis of IPF is suggested after X-ray and high resolution computed tomography are utilized to rule out all other restrictive lung diseases. However, the gold standard for IPF diagnosis is lung biopsy analysis [13]. Mainstay therapy consists of corticosteroid administration, to which only 10-30% of patients show an initial favorable response [14]. In addition, there is no proof that corticosteroids alter survival and they are associated with significant side effects including insomnia, irritability, depression, weight gain, and increased susceptibility to infections [15, 16].

Idiopathic pulmonary fibrosis onset occurs later in life, usually in the fifth or sixth decade, with a slight male predominance [17]. Patients typically present with increasing exertional dyspnea often associated with a dry, nonproductive cough [18]. Advancement of IPF is marked by progressive reductions in lung volume, worsening of resting and exercise hypoxia, and a widening gap between alveolar and arterial oxygen levels, which necessitates increased supplemental oxygen. The median survival time after biopsy-confirmed IPF is approximately 3 years [19]. The major cause of death in IPF patients is respiratory failure, followed by cardiovascular conditions including heart failure, ischemic heart disease and stroke [18].

1.1.2.1. Histologic Characteristics

In terms of histology, IPF is described as usual interstitial pneumonia (UIP). The hallmark of UIP is heterogeneity of lesions, both temporally and spatially [13]. In other words, relatively normal lung architecture is found interspersed with regions at various stages along the fibrotic pathway. Advanced stages include areas of dense fibrosis, where lung architecture is distorted, noted by the collapse of alveolar airspaces and capillaries. Areas of recent alveolar injury are thought to be marked by fibroblastic foci, composed of myofibroblasts and fibroblasts

undergoing intense proliferation and synthesis and secretion of extracellular matrix (ECM) components [13]. Patches of mild interstitial inflammation are also observed. Initially, lesions are predominantly found in the peripheral subpleural parenchyma of the lung, and encroach centrally with disease progression.

1.1.2.2. Pathogenesis of IPF

Histological changes associated with pulmonary fibrosis include loss of alveolar epithelial type I cells (AE-I), repopulation of alveolar surfaces with alveolar epithelial type II cells (AE-II) and some bronchiolar epithelial cells, edema, leukocyte infiltration, fibroblast proliferation, and excess extracellular matrix (ECM) deposition which leads to progressive alveolar interstitial thickening [20, 21]. Key events in the pathogenesis of IPF are severe injury to the alveolar epithelial cells and destruction of the underlying basement membrane. As AE-I cells are injured and undergo necrosis or apoptosis they are sloughed off, resulting in a denuded basement membrane [22, 23]. Another early target of injury is the pulmonary endothelium, which becomes leaky. Once the epithelial and endothelial barriers are compromised, proteinaceous edema accumulates in the airspaces. In attempt to repair the denuded epithelial basement membrane, AE-II cells divide and migrate to cover the surface [20]. In addition, fibroblasts divide and penetrate the denuded basement membrane to invade the airspaces, where serum proteins including fibrin act as a scaffold for invading fibroblasts [24]. These fibroblasts synthesize ECM components, including collagen types I and III [25, 26]. Areas of fibroblast proliferation and synthesis of ECM components evolve into fibroblastic foci, which are the hallmark lesions of IPF [27]. Fibroblastic foci are considered by some to be prognostic indicators, such that a higher number of fibroblastic foci corresponds to worse prognosis.

During the evolution of fibroblastic foci, fibroblasts differentiate into myofibroblasts, expressing α-smooth muscle actin (α-SMA) and increasing further their ECM synthesis. Myofibroblasts share properties with fibroblasts, smooth muscle cells and inflammatory cells [28]. Like fibroblasts, myofibroblasts are capable of synthesizing and secreting extracellular matrix. They are thought to be the main source of collagen type I in the fibrotic lung [29]. Myofibroblasts have a contractile phenotype as do smooth muscle cells, and this property contributes to the loss of lung compliance in IPF [28, 30]. Finally, myofibroblasts are capable of producing cytokines including transforming growth factor-β (TGF-β) and monocyte chemotactic protein-1, imparting on them the potential to stimulate further matrix deposition and recruit inflammatory cells [28, 31, 32]. Most of the cells in a fibroblastic focus are myofibroblasts, aligned in a parallel manner, presumably contributing to active contraction and deformed lung architecture [33].

There is also an inflammatory component evident in cases of IPF. Bronchoalveolar lavage fluid (BALF) from IPF patients has been noted to contain increased numbers of activated neutrophils and eosinophils [34], which release oxidants and proteases that can further damage the parenchyma [35]. It has been suggested that these cells are recruited directly by alveolar macrophage (AM)-released chemoattractants, or indirectly by chemoattractants released by parenchymal cells (epithelial cells and fibroblasts) in response to AM-generated cytokines, including TNF-α and IL-1. Pulmonary macrophages also secrete pro-fibrotic cytokines including TGF-β, PDGF, and IGF-1 [20, 36], allowing macrophages to participate in both pro-inflammatory and pro-fibrotic mechanisms.

One point of controversy in the pathogenesis of idiopathic pulmonary fibrosis is the issue of whether inflammation is a key driving force of the fibrotic response. Until relatively recently,

it had been widely believed that IPF resulted from chronic inflammation [37]. This hypothesis has been contested by many investigators due to several lines of evidence (reviewed in [38]). One point is that dissociation of the inflammatory response from the fibrotic response has been shown in transgenic animal models. For example, mice null of αvβ6 integrin (a protein capable of activating TGF-β) develop exaggerated inflammation, but are protected from pulmonary fibrosis [39]. Second, inflammation is not necessarily more predominant during the early stages of IPF [27]. Also, clinical indicators of inflammation fail to correlate with disease stage or IPF outcome. Finally, therapy that is anti-inflammatory in nature (i.e. corticosteroids) generally does not improve illness or survival [14]. Those who do not believe that inflammation is key in IPF pathogenesis study the hypothesis that UIP is an example of abnormal wound healing in the lung due to absence of proper reepithelialization and irregular myofibroblast behavior [38].

The consensus, regardless of the importance or lack thereof of inflammation in IPF pathogenesis, seems to be that IPF represents a sort of dysfunctional healing mechanism. Key early events are AE-I cell death and disruption of the underlying basement membrane [35, 38]. Hallmark lesions are fibroblastic foci [27], which demonstrate high expression of TGF-β and connective tissue growth factor, molecules typically associated with wound healing [40, 41].

1.1.3. Animal Models of Idiopathic Pulmonary Fibrosis

There is no perfect animal model for IPF. However, animal models are an essential tool for elucidating the mechanisms involved in this disease. Animal models in use include pulmonary fibrosis induced by bleomycin, asbestos, silica, hyperoxia, and irradiation, as well as transgenic approaches. Here, the bleomycin and asbestos models of pulmonary fibrosis will be described.

1.1.3.1. Intratracheal Instillation of Bleomycin

Bleomycin is a chemotherapeutic drug that has the notable side effect of causing pulmonary toxicity [42]. It is a mixture of DNA-intercalating glycopeptides that forms equimolar complexes with Cu^{2+} or Fe^{2+}. When bleomycin forms a ternary complex with Fe^{2+} and O_2 in the presence of DNA, it causes oxidative damage via single- and double-strand breaks in DNA [43, 44]. Most tissues express the cysteine protease bleomycin hydrolase, the enzyme responsible for bleomycin degradation, with an exception being the lung which expresses little to no bleomycin hydrolase in bleomycin-sensitive animals [45]. It has been used extensively for animal models of pulmonary fibrosis when administered via intratracheal, intravenous, or intraperitoneal injection [20]. Some advantages of the intratracheal route are that a lower dose of bleomycin is necessary to elicit substantial injury, the disease develops with quicker kinetics, and the time of injury is precisely defined [20, 46, 47]. Notably, sensitivity of mice to pulmonary bleomycin injury depends on the strain; for example, the C57Bl/6 strain has been classified as a high responder, while the BALB/c strain is highly resistant [48].

After a single bleomycin insult, bleomycin-sensitive mice develop lung fibrosis within two weeks. The first week is dominated by an inflammatory phase [49]. Following disruption of the epithelial and endothelial barriers, influx of inflammatory cells including neutrophils, mononuclear phagocytes and lymphocytes, as well as fibroblasts, into the alveoli and interstitium occurs. The second week is dominated by a fibrotic repair phase in which excess ECM is synthesized and deposited by fibroblasts and myofibroblasts [20]. This results in patchy areas of parenchymal reorganization and extensive intra-alveolar and interstitial fibrosis.

There are drawbacks to the bleomycin model, however. One drawback is that the injury is biphasic with an inflammatory phase consistently preceding the fibrotic phase. Thus, it does

not necessarily reflect the complexity of the pathogenesis of human IPF. Also, fibroblastic foci, the hallmark lesions of IPF, do not develop after bleomycin injury in mice. Although bleomycin does cause a significant increase in the number of lung myofibroblasts compared to control animals [50], the characteristic foci observed in IPF are not observed in response to bleomycin. Finally, whereas lung damage in IPF is irreversible, bleomycin injury in a mouse is reversible [51]. After a significant period of time following cessation of bleomycin administration, pulmonary lesions regress.

1.1.3.2. Intratracheal Instillation of Asbestos Fibers

Asbestos is a fibrous, naturally occurring mineral dust. Inhalation of a sufficient load of asbestos fibers leads to asbestosis, a type of interstitial lung disease characterized by chronic inflammation and pulmonary fibrosis. Fibers are classified as serpentines or amphiboles, depending on their chemical composition and structure, but all types of fibers have high tensile strength and heat and chemical stability, explaining their high usage in various industrial applications [20]. In humans, there is a latency period between exposure to asbestos and full development of asbestosis of approximately 20-40 years [52].

Animal studies have shown that the pathogenicity of asbestos fibers depends upon the quantity and length of the fibers [53-55] as well as the class of fiber, with amphibole forms, including crocidolite, being the more fibrogenic class [56, 57]. For animal models, asbestos can be administered by inhalation or by intratracheal instillation. An advantage of the latter approach is that the asbestos fibers are more contained because they are not aerosolized. Fibers deposited in the distal lung are taken up by alveolar macrophages and AE-I cells [58], followed by death of AE-I cells, hyperplasia of AE-II cells, influx of alveolar and interstitial macrophages, neutrophils, lymphocytes and eosinophils, then fibroblast proliferation and collagen

accumulation [59]. Similar to IPF, asbestosis lesions are unevenly distributed and patchy, with the appearance of focal lesions reminiscent of fibroblastic foci.

1.2. THE RECEPTOR FOR ADVANCED GLYCATION END PRODUCTS (RAGE)

The receptor for advanced glycation end products (RAGE) was first described in 1992 by Schmidt and colleagues [60] during attempts to identify the protein responsible for mediating advanced glycation end product (AGE)-induced effects on the endothelium. In these studies, RAGE was found to be noncovalently associated with lactoferrin-like peptide (LF-L). However, since it was reported that RAGE is the signaling component of this complex and LF-L does not affect RAGE-AGE binding [61], LF-L has generated less interest in terms of RAGE biology.

RAGE is a member of the immunoglobulin superfamily of cell surface receptors [62]. It is composed of three extracellular immunoglobulin domains (one aminoterminal V-type and two C-type domains) followed by a single-pass transmembrane domain, and a short, highly-charged cytoplasmic tail that is essential for RAGE signaling [62, 63]. RAGE is a highly conserved protein, showing 78% amino acid identity between humans and mice. It is expressed in a number of cell types, including monocytes/macrophages, neutrophils, smooth muscle cells, endothelial cells, AE-I cells, fibroblasts and neurons [60, 64-69]. Notably, there is a secreted isoform of RAGE, soluble RAGE or sRAGE, which lacks a transmembrane domain and thus is secreted. In humans, sRAGE has been shown to result from alternative splicing [70]. An additional isoform has been detected in human pericytes that lacks part of the aminoterminal immunoglobulin domain (the domain involved in ligand binding [71]), but the function of this isoform is not presently known [72]. It is possible that this isoform may retain the ability to bind

β2 integrins since this interaction does not appear to utilize the same RAGE epitope as utilized by the other RAGE ligands [73] (see below).

RAGE is expressed at high levels in the nervous system during development, when it participates in neurite outgrowth and cell differentiation [74, 75]. Thereafter RAGE is expressed at very low levels in normal adult tissues, with the exception being the lung, where there are high levels of RAGE transcripts under normal circumstances [64, 76]. RAGE expression is upregulated in a number of pathologies, however, including diabetic complications (atherosclerosis and nephropathy), acute and chronic inflammation, tumor invasion and metastasis, and Alzheimer's disease [77-83], in which RAGE is considered a *propagator* of disease pathogenesis (reviewed in [84]).

1.2.1. RAGE-mediated Signaling

RAGE has a 43-amino acid cytoplasmic tail that is highly acidic [60]. It lacks classical signaling domains such as phosphorylation sites or kinase domains [84], but is essential for RAGE-mediated signaling. Indeed, many studies have utilized a cytoplasmic deletion mutant of RAGE that acts in a dominant-negative manner (DN-RAGE) [63, 81, 85].

RAGE is more effective at mediating cellular activation and perturbation than at mediating endocytosis and degradation of its bound ligands. Interestingly, it has been reported that when endocytosis does occur via RAGE, rather than causing pathogenic ligand degradation, RAGE mediates transcytosis of its ligands (including AGEs and amyloid-β) to the basal cell surface [86, 87], where these ligands can interact with RAGE and other mediators in the subluminal tissue.

RAGE ligation is capable of triggering a number of cell signaling pathways, depending on the cell type and ligand involved. However, these pathways have not been fully elucidated.

Perhaps the most-studied pathway is one that is initiated by AGE-RAGE ligation in vascular endothelial cells, smooth muscle cells, and monocytes. This signaling pathway involves ERK1/2, the only signaling component shown to bind directly to the cytoplasmic tail of RAGE [88], reactive oxygen intermediates (ROI), $p21^{ras}$, and p38 MAPK, and culminates in the activation of the transcription factor NF-κB [63, 71, 89, 90] (Figure 1). One source of the signaling ROI is evidently NADPH oxidase [91].

Notably, the promoter of RAGE contains two active NF-κB-responsive elements [92], such that when RAGE binds a ligand and mediates signaling that involves NF-κB activation, RAGE itself is upregulated [93], along with various other immune and inflammatory NF-κB-responsive genes. Thus, RAGE ligation initiates a positive feedback loop. There is also evidence that RAGE ligation induces sustained activation of NF-κB [94], further propagating the cycle. This built-in amplification is thought to be the mechanism to explain the observation that at sites where RAGE ligands accumulate (i.e. the diseases listed in the previous section), RAGE also accumulates; in other words, RAGE and its ligands demonstrate sustained colocalization [64, 80, 81, 95-97]. Indeed, the only way to stop the cycle of RAGE stimulation and ensuing cellular perturbation appears to be to block RAGE ligation, for example using soluble RAGE [84]. The identification of an apparent negative regulator of RAGE expression has been made only recently, when overexpression of an alternative AGE receptor, oligosaccharyl transferase-48 (AGE-R1), was found to downregulate RAGE [98].

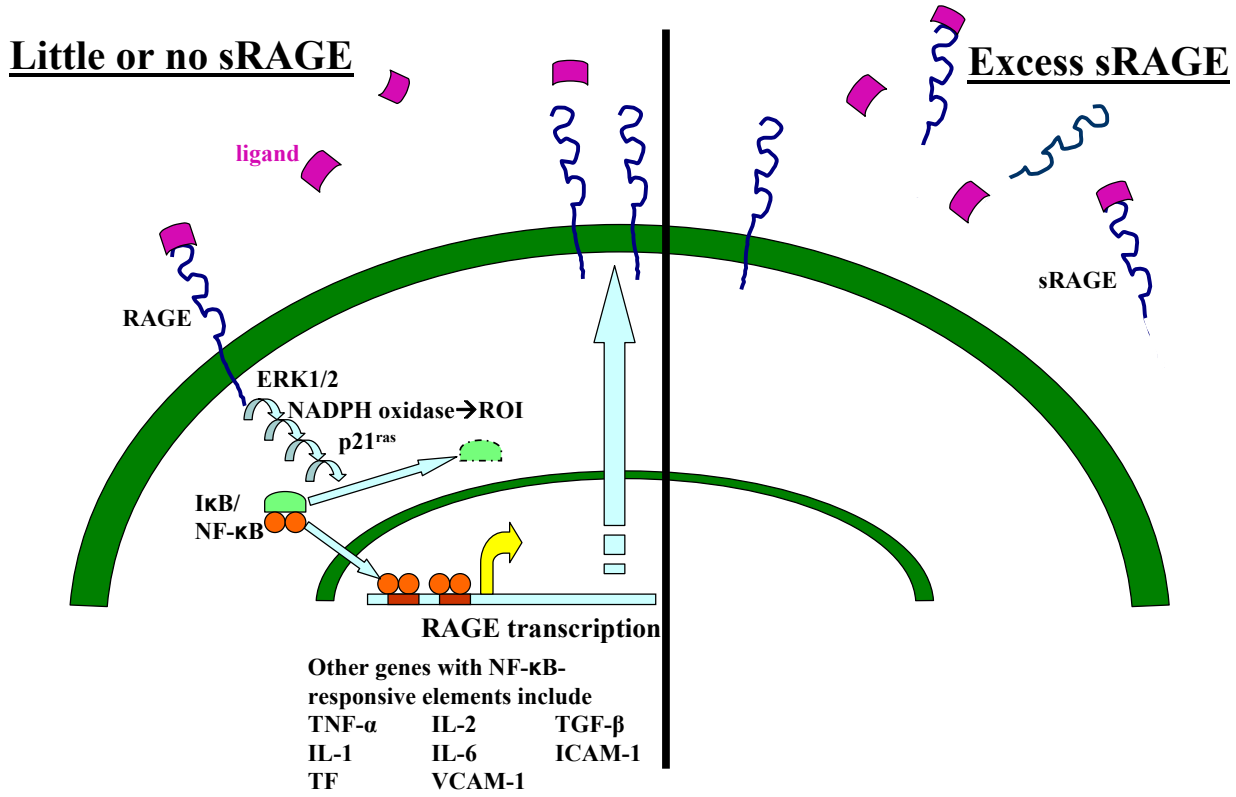

Figure 1. RAGE initiates a positive feedback loop.

The signaling pathway depicted here is the best characterized RAGE signaling pathway. Other signaling pathways initiated by RAGE ligation involve SAPK/JNK and Rho GTPases; or JAK2; or p44/42 MAPK, p38 MAPK and SAP/JNK. The pathway triggered by RAGE depends on the cell type and ligand class involved. (Left) RAGE ligation leads to inflammatory mediator upregulation and upregulation of RAGE itself. (Right) When RAGE ligation is blocked, here by the presence of sRAGE, upregulation of inflammatory mediators and RAGE are prevented.

Other signaling pathways that have been described involve the SAPK/JNK and Rho GTPases (Rac and cdc42), activated by amphoterin-RAGE interaction on neurons to stimulate neurite outgrowth [63, 81], and another pathway involving JAK2, activated by S100B in vascular smooth muscle cells [99]. In addition, amphoterin-RAGE interactions activate p44/42 MAPK, p38 MAPK, and SAP/JNK in glioma cells [81].

1.2.2. Ligands of RAGE and Their Associated Pathologies

One interesting characteristic of RAGE is its affinity for *families* of ligands; RAGE is a promiscuous receptor. Its ligands, listed in Table 1, include advanced glycation end products (AGEs), HMGB1/amphoterin, S100/calgranulins, and amyloid peptides (reviewed in [84]). These ligands are discussed in more detail below. Interestingly, the same RAGE domain (aminoterminal V-like immunoglobulin domain) has been shown to be essential for ligand binding, and each class of ligands has been shown to compete with one another for RAGE binding [80, 82, 100]. In addition, RAGE has more recently been shown to bind β2 integrins, such as Mac-1, which are involved in leukocyte adhesion to the endothelium [73]. However, this interaction appears to occur in a different RAGE domain because AGE-binding does not affect Mac-1 binding, while S100 binding augments Mac-1 binding to RAGE.

Table 1. Summary of RAGE ligands and their associated pathologies.

RAGE ligand	Description	Associated pathology
Advanced glycation end products (AGEs)	• Proteins, lipids or nucleic acids with sugar adducts as a result of nonenzymatic glycation • Form during normal ageing and at an accelerated rate in diabetic tissues and in oxidative environments	Tissue rigidity (crosslinks) [101] Diabetic atherosclerosis and nephropathy [77, 79] Macrophage activation [68, 102]
HMGB1 (amphoterin)	• Nuclear non-histone binding protein; gains access to extracellular space by an unknown mechanism • Released by activated macrophages and necrotic cells • Participates in neurite outgrowth during development	Trigger of inflammation [103, 104] Acute lung inflammation [105] Tumor growth/metastasis [81]
S100/Calgranulin family (EN-RAGE, S100B, etc.)	• Small Ca^{2+}-binding proteins secreted by activated inflammatory cells (macrophages, neutrophils, lymphocytes) • Hallmark: accumulation at chronic inflammatory sites	Acute and chronic inflammation [80]
Amyloid fibrils (amyloid-β)	• β-sheet rich pathogenic conformation of certain proteins • Cause of native→amyloid conversion is unknown	Alzheimer's disease [82] Systemic amyloidosis [106]
β2 Integrins (Mac-1)	• Integrins expressed by leukocytes • Involved in firm adhesion of leukocytes to the endothelium	Leukocyte recruitment [73]

1.2.2.1. Advanced Glycation End Products

Advanced glycation end products (AGEs) are an heterogeneous group of proteins (or lipids or nucleic acids) with covalently-bound sugar adducts. Glycation occurs nonenzymatically, beginning with a condensation reaction of the sugar with a free amino group, often a lysine or arginine side group, to form a Schiff base [107]. The rate of this first step is proportional to the concentration of sugar in the open chain form and time [108]. The Schiff base undergoes rearrangement via acid-base catalysis to form the more stable Amadori product. A series of incompletely defined oxidation reactions further rearranges these products to eventually result in AGEs, irreversibly glycated products [107, 109]. AGEs can be formed extracellularly and intracellularly [110], and form naturally with ageing and at an accelerated rate in hyperglycemic or oxidative environments [101, 111, 112]. They have a brown pigment and inherent fluorescence, and show a propensity to form crosslinks [109, 113]. In addition to RAGE, other AGE receptors include oligosaccharyl transferase-48 (AGE-R1), 80K-H phosphoprotein (AGE-R2), galectin-3 (AGE-R3), and macrophage scavenger class A receptors (reviewed in [114]). RAGE binds AGEs with a K_d of 50-100 nM [62, 115].

AGEs have pathological effects that are both receptor-dependent and –independent [116]. AGE adducts on intracellular proteins can alter their ability to function properly [117]. Due partially to their propensity to form crosslinks, AGEs can alter vessel wall and basement membrane structure by increasing tissue rigidity and affecting matrix-matrix or matrix-cell interactions [118, 119]. In addition, AGEs can quench nitric oxide to cause defects in vasodilation [120]. The primary means of receptor-dependent AGE pathological effects appear to be via RAGE signaling.

AGE-RAGE INTERACTIONS ON THE ENDOTHELIUM

AGEs are found in tissues as well as in plasma. Aged and diabetic red blood cell membranes are modified with AGEs [121, 122]. Because the endothelium expresses RAGE [60, 61], when AGE load in the bloodstream is considerable, endothelial physiology is affected.

One way in which the endothelium has been shown to react to AGEs via RAGE is to increase production of pro-inflammatory mediators, including VCAM-1, ICAM-1, E-selectin, IL-6, and tissue factor [86, 91, 97]. Further, it has been postulated that myeloperoxidase activation can cause increased AGE formation, so that in an inflammatory milieau where activated neutrophils are undergoing oxidative bursts, more RAGE ligands may accumulate [97]. Thus, AGEs have the potential to both initiate and perpetuate pro-inflammatory mechanisms.

Another facet of the endothelial response to AGEs mediated via RAGE is vessel hyperpermeability [121], a characteristic of diabetic vasculopathy [123]. Diabetic red blood cells have been used as a model AGE entity, *in vivo* and *in vitro*. In the presence of the diabetic red blood cells, endothelial barrier function is compromised. This is largely reversed by either blockade of RAGE signaling or by the presence of antioxidants, supporting the importance of cellular oxidant stress, likely due at least in part to RAGE signaling mechanisms.

AGE-RAGE INTERACTIONS IN INFLAMMATORY CELLS

In addition to the pro-inflammatory signaling that AGEs stimulate via RAGE ligation to produce ROI, TNF-α, IL-6 and nitric oxide in mononuclear phagocytes [91, 102], AGEs also induce chemotaxis of these cells. Using chemotaxis chambers and an *in vivo* model of immobilized AGEs, Schmidt and colleagues reported that soluble AGEs induce macrophage chemotaxis, while immobilized AGEs prevent their chemotaxis [68]. In addition, RAGE is capable of mediating AGE deposition in tissues [86, 124]. One can imagine a situation in which

macrophages are attracted to a site due to an AGE concentration gradient, then once they migrate into the tissue where AGEs are immobile components of the basement membrane, they are unable to migrate further, becoming activated while stationary and thereby incurring damage to the surrounding tissue.

Neutrophils have also been shown to express RAGE and internalize AGEs [66]. Interestingly, however, AGE pretreatment of neutrophils leads to an increase in phagocytic index, but a decrease in diapedesis, ROS production and bacterial killing. Thus, AGE pretreatment of neutrophils leads to a higher number of ingested bacteria, but impaired ability to kill the bacteria.

AGE-RAGE INTERACTIONS IN OTHER CELLS

Using *in vitro* models, it has been shown that AGE-RAGE interactions can cause myofibroblast differentiation from renal epithelial cells [125, 126]; in addition, RAGE is upregulated during myofibroblast differentiation from hepatic stellate cells [127].

Finally, RAGE expressed by vascular smooth muscle cells is responsible for neointimal expansion subsequent to arterial injury [128, 129]. AGEs and S100/calgranulins (see below) are the ligands implicated to interact with RAGE in neointimal formation.

1.2.2.2. HMGB1/Amphoterin

High mobility group protein-1, or HMGB1, is a nonhistone chromosomal protein that is capable of modulating transcription by binding the minor groove of AT-rich sequences and bending DNA to facilitate binding of transcription factors [130]. It is highly conserved, with over 95% amino acid identity between humans and rodents. HMGB1 is also found as a membrane-associated form, referred to as amphoterin [131]. Amphoterin is highly expressed in the central and peripheral nervous systems during later stages of embryonic development, where

it promotes neurite outgrowth [132, 133], at least partially due to amphoterin interactions with RAGE [63, 74]. RAGE is reported to bind amphoterin with a K_d of approximately 9 nM [74]. Other receptors for HMGB1/amphoterin are toll-like receptors 2 and 4 [134].

In 1999, HMGB1 was rediscovered as a cytokine when Wang and colleagues reported that it is a late mediator of endotoxin lethality [104], as it is released after the initial spikes of TNF-α and IL-1 have returned to baseline. HMGB1 is released from macrophages, mostly from pre-formed pools [135], and can be detected in the serum of critically ill patients with sepsis [104]. HMGB1 in turn activates the endothelium via RAGE ligation, indicated by increased expression of cell surface adhesion molecules VCAM-1 and ICAM-1, and increased neutrophil adhesion [136, 137]. The role of endothelial cell RAGE ligation in sepsis is supported by the fact that RAGE-/- mice are protected from septic lethality, but their susceptibility is reconstituted when RAGE is expressed only on endothelial cells and hematopoetic cells [138].

HMGB1 also has an established role in lung pathology as a mediator of acute lung inflammation [105]. Similar to the case in sepsis, the HMGB1 spike appears subsequent to the TNF-α and IL-1 spikes. Intratracheal injection of purified HMGB1 alone induced edema and neutrophil influx into the lungs, which were inhibited with administration of anti-HMGB1 antibody. The role of RAGE in this situation has not yet been described.

HMGB1 also has the role of a diffusible signal of necrotic cell death to neighboring cells [103]. Necrotic cells passively release HMGB1, while in apoptotic cells, HMGB1 remains firmly anchored to chromatin. Thus, an HMGB1-dependent inflammatory response is mounted in response to necrotic cells, but not by cells undergoing programmed cell death. The role of RAGE in the ensuing inflammatory response has not yet been shown.

1.2.2.3. S100/Calgranulins

S100/calgranulins are a family of EF-hand calcium-binding proteins. These proteins are typically localized in the cytosol or nucleus of resting cells, where they bind protein targets in a calcium-dependent manner to regulate intracellular functions including protein phosphorylation, enzymatic activation, interaction with cytoskeletal components, and calcium homeostasis [139, 140]. However, some members can be released from activated inflammatory cells, where they have been shown to participate in a range of responses from inflammation to neurite outgrowth [80, 141, 142]. A number of members of this family have been shown to bind RAGE including S100A12 (EN-RAGE), S100A4, S100A13, S100B, and S100P [80, 140, 143]. RAGE binds one S100 protein (EN-RAGE) with a K_d of approximately 91 nM [80]. Although there is evidence that not all extracellular S100-mediated effects are RAGE-dependent [140, 144], another receptor for S100 proteins has not yet been identified.

Although S100A13 demonstrates somewhat ubiquitous expression [145, 146], other S100 proteins are expressed in a cell- and tissue-specific manner. For example, EN-RAGE is expressed exclusively by granulocytes [147], while S100B is expressed primarily in the nervous system by astrocytes and Schwann cells [148]. Interestingly, consequences of S100B are concentration-dependent. Nanomolar concentrations of S100B are trophic, stimulating neurite outgrowth and neuronal survival during development, whereas micromolar concentrations are toxic, causing astrocyte and neuronal death [149-151]. Both trophic and toxic response types have been shown to be mediated by RAGE ligation [141].

RAGE—EN-RAGE interactions have been implicated in both acute and chronic inflammatory milieau [80, 152], causing increased expression of VCAM-1 and ICAM-1 and increased NF-κB activity in the endothelium, and migration and cytokine secretion in

mononuclear phagocytes. Elevated EN-RAGE expression has also been reported in chronic active inflammatory bowel disease [153].

Certain S100 proteins have been reported in the lung. EN-RAGE levels in serum and sputum are significantly elevated in patients with cystic fibrosis experiencing acute infectious exacerbations [154]. In addition, there is evidence that S100A8 and S100A9 levels are elevated in bronchoalveolar lavage fluid from patients with IPF versus patients with sarcoidosis [155].

1.2.2.4. Amyloid Fibrils

The most-studied amyloid ligand of RAGE is amyloid-β peptide (Aβ), the main component of extracellular plaques in the Alzheimer's disease brain parenchyma and vasculature [82, 156, 157]. Aβ contributes to Alzheimer's disease pathogenesis due to its neurotoxicity [82, 158, 159], its ability to generate oxidant stress, both inherently and via RAGE signaling [82, 160], and its ability to activate microglia [82]. Consistent with the idea that RAGE ligand accumulation leads to RAGE upregulation (see Figure 1), RAGE expression in Alzheimer's disease brains is upregulated approximately 2.5-fold, particularly in neurons showing signs of oxidative stress near Aβ plaques, as well as in vessel walls and microglia near Aβ deposits [82]. RAGE binds Aβ with a K_d of approximately 57 nM [82]. In addition to RAGE, Aβ can bind to several other biomolecules, including scavenger receptors and ECM components (reviewed in [161]).

RAGE has been found to mediate several pathological effects of Aβ. Aβ crossing of the blood-brain barrier is RAGE dependent [87, 162]. In a mechanism involving NF-κB activation, RAGE-Aβ interactions induce oxidant stress in the endothelium and in neuronal cells [82]. RAGE has also been shown to mediate Aβ-induced microglial migration and activation,

indicated by increased TNF-α production and NF-κB activation [82]. Similar to the case of AGEs discussed above, soluble Aβ leads to microglial chemotaxis while immobilized Aβ inhibits migration, potentially promoting chronic activation of microglia once they reach Aβ plaques [82]. Finally, there is evidence that RAGE mediates, at least in part, Aβ neuronal toxicity. Hadding and colleagues [159] found that cells overexpressing RAGE were hypersensitized to Aβ-mediated death, even at low concentrations that were previously found to be neuroprotective [158]. Thus, whereas Aβ-RAGE interactions induce apoptosis of neurons, these interactions promote sustained cellular activation of microglia, a mechanism that may contribute to the underlying chronic inflammatory component of Alzheimer's disease [82, 84].

Another disease involving amyloid peptides is Creutzfeldt-Jakob disease, in which the central mediator is prion protein, which accumulates to form amyloid plaques [163]. Interestingly, RAGE (and AGEs) colocalize with prion protein in brains from Creutzfeldt-Jakob disease [164]. The functional significance of RAGE in this disease has not yet been described.

1.2.3. Soluble RAGE

Soluble RAGE, sRAGE, is the naturally-occuring, secreted isoform of RAGE. It is found at low levels (approximately 1 ng/ml) in plasma [77]. For this reason sRAGE can be administered to animals, even up to six months, without eliciting an immune response [84]. sRAGE-ligand complexes can be detected in the plasma [77, 162]. These complexes, however, are not extensively eliminated in the urine [124], so are thought to be degraded by an unknown mechanism.

It has been shown by two groups that sRAGE in humans results from alternative splicing [70, 72]. Although their cDNA sequences for sRAGE were not completely identical, they

reached the same conclusion: alternative splicing occurs just upstream of the transmembrane domain-encoding sequence, causing a translational frameshift such that there is no transmembrane domain encoded in these alternative transcripts. As a result, the carboxyterminal amino acid sequence of human sRAGE is distinct from that of RAGE.

sRAGE has been used in several models of RAGE-mediated diseases as a decoy to prevent disease progression (see Figure 1). sRAGE can block or reduce vascular hyperpermeability and atherosclerosis in diabetic vessels [77, 121], chronic inflammation in a colitis model [80], tumor growth and metastasis [81], impaired wound healing in diabetic animals [152], sustained NF-κB activation in diabetic peripheral blood mononuclear phagocytes [94], and Aβ deposits in brain tissue [162], among others. It is important to note that the effectiveness of sRAGE treatment is not necessarily due to RAGE blockade, because sRAGE can also prevent its ligands from binding other pathogenic receptors. In fact, Liliensiek and colleagues found that sRAGE prevented a delayed-type hypersensitivity response equally well in RAGE null and wild-type mice [138]. However, in most of these cases, neutralizing RAGE antibodies were used in parallel to show the same effects, thus supporting the proposition that RAGE is a key mediator in each type of pathology.

It is interesting to note that sRAGE does not always act in an anti-inflammatory manner. In cases where controlled inflammation is beneficial, for example for regeneration after massive hepatectomy [85] or for proper wound healing in diabetics [152], sRAGE acts to promote a limited inflammatory response. In the former instance, sRAGE prevents the downregulation of the pro-regenerative molecules TNF-α, IL-6 and active NF-κB. In the latter case, sRAGE prevents the RAGE-bearing macrophages from becoming immobilized in the perivascular tissue

where they encounter AGEs, thereby allowing them to migrate more rapidly to the wound where repair is needed.

1.3. CONCLUSIONS

Idiopathic pulmonary fibrosis is a debilitating disease associated with a dismal prognosis and poorly understood molecular pathogenesis. Current therapy is ineffective, and while the only real cure is lung transplantation, there is just a 64% 2-year survival rate associated with transplantation [165]. More research on the pathogenesis of pulmonary fibrosis using cell culture and animal models should be aimed at identifying new therapeutic targets in hopes of slowing disease progression and improving patients' quality of life.

The receptor for advanced glycation end products is a molecule that has been receiving attention over the past decade for promoting the pathogenesis of several diseases, from diabetic complications to cancer progression to Alzheimer's disease. RAGE is a promiscuous receptor, recognizing families of ligands. Incidentally, RAGE has a soluble isoform that acts as a decoy to prevent RAGE signaling. As sRAGE is alternatively spliced in humans [70, 72], it is possible that pathogenesis of RAGE-mediated diseases involves an imbalance between these two isoforms. Perhaps if, at some point during pathogenesis, the splicing machinery in an individual is directed to favor RAGE expression over sRAGE expression, that individual is more susceptible to disease progression. To our knowledge, there have been no studies focusing on the differential expression of these two RAGE isoforms in RAGE-mediated disease.

2. RATIONALE AND HYPOTHESIS

In most healthy adult tissues, RAGE expression is low [64], but becomes highly upregulated during the pathogenesis of several diseases. This upregulation of RAGE is thought to be explained by the accumulation of its ligands at the site of pathology, thereby initiating the positive feedback loop that drives RAGE expression (see Figure 1) [92, 111]. Because RAGE signaling is generally inflammatory and promotes sustained cellular activation, RAGE is considered a propagator of cellular dysfunction [84, 111, 166]. It has been suggested that RAGE is a pleiotropic antagonistic gene, one whose expression is beneficial during the early phases of life (including nervous system development) but becomes deleterious in later stages of life [167].

Notably, the exception to low RAGE expression in healthy adult tissues is the lung. The normal human and rat lung have been shown to contain exceptionally high levels of RAGE transcripts [64, 76]. In fact, many groups have used the lung as a source for purifying RAGE/sRAGE and for discovering RAGE ligands [60, 62, 74, 82, 121]. Despite the fact that the lung is relatively rich in RAGE expression, research on RAGE in the lung has been limited. High RAGE expression in the lung suggests that RAGE plays an important homeostatic role specifically in this organ, and raises the possibility that *RAGE is regulated differently in the lung compared to other tissues*.

In the lung, the cell type that seems to be responsible for the bulk of RAGE expression is the alveolar epithelial type I cell [67, 168]. RAGE has even been suggested as a marker for AE-I cells [169]. One of the early steps in injury leading to pulmonary fibrosis is the death of AE-I

cells. Thus, it is possible that loss of RAGE expression due to death of AE-I cells occurs in the pathogenesis of pulmonary fibrosis.

However, RAGE ligands are evidently present in IPF, and as illustrated in Figure 1, research in other tissues suggests that the presence of RAGE ligands would induce an upregulation of RAGE. Oxidative stress is considered a significant component to IPF pathogenesis [170-172] and AGEs form at an accelerated rate in oxidative environments [109, 111, 173]. In fact, elevated AGE immunoreactivity has been reported in lungs from IPF patients [174], and there is evidence of an association between diabetes, a disorder involving highly increased AGE levels, and pulmonary fibrosis [175, 176]. HMGB1 is also expressed in the lung [74], although there have been no studies describing its regulation in pulmonary fibrosis. Thus, due to upregulation of at least one RAGE ligand, it is possible that RAGE will be upregulated in IPF, if pulmonary RAGE expression increases in response to its ligands as it does in other tissues.

Based on what is known about RAGE from previous studies described in the Introduction, we might expect that RAGE consistently plays a pathogenic role. However, the few studies that have been done on RAGE in the lung suggest that RAGE-mediated responses in this tissue may be quite different than expected based on results from studies in other tissues. First, RAGE expression in the lung is normally high, while its expression in other tissuesis low and only increases under pathologic conditions. Furthermore, if one considers studies of RAGE in the field of cancer, it is evident that RAGE signaling responses in the lung are unique compared to other tisses. For example, RAGE expression has been shown to positively correlate with cancer cell growth as well as migration and invasion potential in glioma cells, colon cancer cells, gastric cancer cells, pancreatic cancer cells, and renal carcinoma cells [81, 83, 177-179].

On the other hand, studies on lung carcinoma have shown decreased RAGE expression in cancer cells [180-182]. Bartling and colleagues additionally found that overexpression of RAGE in a human lung cancer cell line led to decreased proliferation [181]. They reported that RAGE is apparently involved in intercellular contacts that are lost during tumorigenesis. These data demonstrate that the role of RAGE in lung carcinoma directly opposes the trends found in other tissues, further highlighting the proposition that *RAGE function and regulation may be unique in the lung* compared to other tissues.

Like cancer, idiopathic pulmonary fibrosis involves the heightened proliferation of a population of cells, mainly fibroblasts and myofibroblasts. RAGE has been implicated in the propagation of other fibrotic conditions, including diabetic renal fibrosis and liver fibrosis [79, 125-127, 183, 184]. In addition, RAGE has been shown to modulate collagen production by fibroblasts. In human skin fibroblasts, AGE-RAGE interactions decrease collagen synthesis [65], while in rat kidney fibroblasts, AGE-RAGE interactions led to an increase in collagen release [69]. Thus, RAGE is capable of influencing fibrotic outcomes. This also demonstrates that RAGE signaling in similar cell types can have different outcomes in different tissues.

Because of the suggested homeostatic role of RAGE in the lung, *we hypothesize that RAGE and sRAGE regulation is altered in response to injuries leading to pulmonary fibrosis.* To investigate this hypothesis, we have used animal models as well as human IPF tissue. As discussed above, RAGE-ligand interactions have been shown to be capable of modulating fibrotic responses. Thus, *we further hypothesize that altered RAGE and sRAGE regulation is a key event in the pathogenesis of idiopathic pulmonary fibrosis.*

3. MATERIALS AND METHODS

3.1. PROTEIN PREPARATIONS AND WESTERN BLOTTING

3.1.1. Mouse tissue preparations

Soluble Preparations. Indicated tissues were obtained from each of two untreated C57Bl/6 mice and homogenized in 500-1000µl of cold Homogenization Buffer (50mM potassium phosphate, pH 7.4, 0.3M potassium bromide, 3mM diethylenetriaminepentaacetic acid, 0.5mM phenylmethylsulfonylfluoride) and briefly sonicated. Samples were centrifuged at 20,000 x *g* for 20 minutes at 4°C. Supernatant protein concentration was determined using the Coomassie Plus Protein Assay Reagent (Pierce, Rockford, IL).

Membrane Preparations. Insoluble pellets from tissue homogenates were resuspended in 500 µl of PBS containing 1% Triton X-100, 0.15 U/ml aprotinin, 1mM phenylmethylsulfonylfluoride, 10µM E-64, and 10mM ethylenediaminetetraacetic acid, and briefly sonicated. Samples were then rocked at 4°C for approximately 30 minutes, followed by centrifugation at 20,000 x *g* for 10 minutes at 4°C. Supernatant protein concentration was determined using the Coomassie Plus Protein Assay Reagent (Pierce).

BALF and Sera Collection. Bronchoalveolar lavage fluid (BALF) was collected by injecting intratracheally and withdrawing 0.8 ml of 0.9% saline. BALF was then centrifuged at 16,000 x *g* for ten minutes at room temperature and the supernatant was used for western blot analysis. Blood was obtained from mice and allowed to clot for two hours at room temperature. Serum

was then collected as the supernatant from a 16,000 x g centrifugation for 10 minutes at room temperature.

3.1.2. PAGE and western blotting

SDS-PAGE. Equal amounts of total protein from each preparation were combined with dithiothreitol (50mM final) and denaturing sample buffer (1% SDS final) and boiled for 10 minutes. Samples were then electrophoresed in a 5-15% gradient acrylamide gel using a Mini-Slab gel system (Idea Scientific, Minneapolis, MN) at 20 mAmp for approximately 1.5 hours. Gels that were not to be used for western blot analysis were stained using Coomassie Staining Solution (40% methanol, 13.3% glacial acetic acid, 0.1% Coomassie Brilliant Blue).

Western Blotting. Proteins separated in the gel were transferred to a PVDF membrane by electroblotting at 500 mAmp for 50 minutes in cold buffer. PVDF membranes were blocked overnight in PBS containing 0.3% Tween-20 and 5% milk at 4^{o}C. Primary and biotinylated secondary antibody incubations each occurred at room temperature for one hour using antibody dilutions listed in Table 2. Visualization of immunoreactive bands was performed using enhanced chemiluminescence detection reagents (Amersham Biosciences).

Table 2. Information for antibodies used in western blot analyses.

Ab Target	Vendor	Source Species	Dilution	Secondary Ab Conditions
RAGE (mouse)* (AN750)	Anaspec	Rabbit	1:5,000	α-rabbit 1:5,000 5% milk
RAGE (human) (H-300)	Santa Cruz Biotechnology	Rabbit	1:5,000	α-rabbit 1:5,000 1% milk
β-actin	Sigma	Mouse	1:5,000	α-mouse 1:10,000
Albumin	ICN Biomedicals	Rabbit	1:20,000 5% milk	α-rabbit 1:5,000
α-SMA	Sigma	Mouse	1:5,000	α-mouse 1:10,000
HMGB1	BD Pharmingen	Rabbit	1:2,000	α-rabbit 1:5,000 1% milk

*** The epitope used to generate the AN750 anti-RAGE as chosen by CL Fattman and TD Oury was RSELTVIPTQGGTTHPTFSC, corresponding to extracellular domain residues 188-207 of the mouse RAGE sequence (accession number Q62151).**

3.2. MOUSE sRAGE PURIFICATION AND CHARACTERIZATION

3.2.1. Purification of sRAGE

Frozen mouse lungs from Pel-Freez Biologicals (Rogers, AZ) were used as starting material. Lungs were homogenized in 10 ml/g of Homogenizing Buffer (see Section 3.1.1) and briefly sonicated. Homogenates were centrifuged at 20,000 x *g* for 20 minutes at 4°C. Polyethyleneimine (0.01% final) (ICN Biomedicals, Aurora, OH) was added to the supernatant to precipitate nucleic acids [185], and samples were centrifuged again as described above.

Concanavalin A Batch Extraction. Concanavalin A-sepharose 4B (Sigma) (100 ml) was added to the cleared homogenate and gently stirred overnight at 4°C. Matrix with bound protein was collected using a scinted glass funnel and packed into a column (2.5 X 20 cm). The column was washed with HEPES buffer (50mM HEPES, pH 7.0, 0.25M sodium chloride) until A_{280} reached

approximately 0. Bound protein was batch eluted with 50mM HEPES, pH 7.0, 0.25M sodium chloride, 200mM methyl α-mannopyranoside at a flow rate of 10 ml/min.

Heparin-Sepharose Chromatography. Bulk eluate from the concanavalin A batch extraction was dialyzed into Buffer A (50mM Tris, pH 7.5, 50mM sodium chloride) and concentrated to 50 ml using an Amicon concentrator (10,000 Da cutoff). The concentrated sample was applied to a column packed with Affi-Gel heparin (Bio-Rad) (80 ml column material, 2.5 X 20 cm column) and washed with Buffer A until A_{280} reached approximately 0. Heparin-binding proteins were eluted with a 0.6%/min gradient of Buffer B (50mM Tris, pH 7.5, 1.0M sodium chloride) into 130 fractions at a flow rate of 5 ml/min. Fractions containing sRAGE were identified by western blotting, then pooled and dialyzed in Buffer A.

Anion-exchange Chromatography. Pooled fractions from heparin-sepharose chromatography were concentrated to 50 ml as detailed above and applied to a 1-ml Mono Q column (Amersham Biosciences). The column was washed with Buffer A until A_{280} reached approximately 0. Proteins were eluted with Buffer B using the following elution profile: 0.5%/min Buffer B for the first 60 ml; 1%/min Buffer B for the next 30 ml; and thereafter 100% Buffer B at a flow rate of 1 ml/min. Ninety-five fractions were collected, and sRAGE-containing fractions were identified by western blotting and pooled. All chromatography was performed on a Pharmacia fast protein liquid chromatography system.

3.2.2. Structural characterization of mouse sRAGE

Amino-terminal Sequencing. Samples were applied to a Biobrene precycled glass-fiber filter (Applied Biosystems) and subjected to automated Edman degradation in an Applied Biosystems Model 477A sequencer with online phenylthiohydantoin analysis using an Applied Biosystems

Model 120A HPLC system. Spectra from each Edman degradation cycle were compared to a standard in order to determine the amino acid residue released with each cycle.

Removal of Amino-terminal Blocking Group. Ten micrograms of purified mouse sRAGE suspended in 20mM Tris/HCl was combined with 0.5 mU *Pfu* pyroglutamate aminopeptidase (Takara Bio Inc., Shiga, Japan) and the supplied reaction buffer. The sample was incubated at 75^{o}C for four hours, then adsorbed to a PVDF membrane using ProSorb cartridges (Applied Biosystems) and sequenced as described above.

PCR and RT-PCR. While attempting to clone an alternatively spliced mouse RAGE cDNA that could encode sRAGE, RT-PCR or PCR was performed with total mouse lung RNA or a mouse lung cDNA library (Spring Bioscience, Fremont, CA). Figure 7 shows the approximate sites along the mouse RAGE cDNA (GenBank^{TM} accession number L33412.1) to which primers were targeted (primer sequences are listed in Table 3). RT-PCR was performed using EZ rTth RNA PCR kit (Applied Biosystems, Branchburn, NJ). Conditions were as follows: RT step at 60.0^{o}C for 30 min and 94.0^{o}C for 2 min; 40 cycles of 94.0^{o}C for 15 sec, 60.0^{o}C for 30 sec, and 70.0^{o}C for 1 min 30 sec; and a final extension step at 65.0^{o}C for 7 min. PCR was performed using *Taq* DNA polymerase (Fisher Scientific) and PCR nucleotide mixture (Roche Applied Science). Cycling conditions were as follows: denaturation at 94.0^{o}C for 5 min; 35 cycles of 94.0^{o}C for 30 sec, 58.0^{o}C for 30 sec, and 72.0^{o}C for 2 min; and a final extension step at 72.0^{o}C for 8 min.

Table 3. Primer sequences used in attempt to detect an alternative mouse RAGE transcript.

Primer‡	Sequence (5'….3')
A§	CTGGCATTCTCTGACAGAACGAGATG
B§	AGAAGATGGAGNCTGGGAAGGAA
C*	ATGCCAGCGGGGACAGCAGCTA
D	CAAGTCCAACTACCGAG
E	AAGAGACCAGGAGACACCCT
F	TCCAGAGGGCATTCAGCTGTT
G	CATTCAGCTGTTGGTTGAGCCTG
H	GACTGATTCAGCTCTGCACGTTC
I	TTTACTCAGCATGGATCATGTGGGC
J	CGTATCAAATGTTTACTCAGCAT
K*§	GTGCCACTCTGACCAGCCTGGTATG
L§	GTCTCTTTCCATCCCTCACTACCTC

‡Primer designations and their relative positions are indicated in Figure 7.
*Primers used to successfully amplify mouse membrane RAGE
§For primers designed to target sequences outside of the RAGE coding sequence, GenBank accession # AF030001.1 (nucleotides 74101-77630) was used.

RNA Isolation from mouse lungs. RNA isolation was performed as previously described [186]. Briefly, lungs were homogenized in Solution A (4M guanidine isothiocyanate, 25mM sodium citrate, pH 7.0, 0.5% n-lauryl sarcosine, 0.1M β-mercaptoethanol) and briefly sonicated, then centrifuged at 14,000 rpm for 10 minutes at 4^{o}C. The supernatant was subjected to two successive phenol-chloroform extractions, then overnight isopropanol precipitation. Samples were centrifuged as above and resulting pellets were washed with 75% ethanol and centrifuged as described above. Pellets were dried and resuspended in Resuspension Buffer (40mM Tris, pH 7.9, 10mM sodium chloride, 6mM magnesium chloride, 10mM calcium chloride) with RNase-free DNase. After an incubation at 37^{o}C for 20 minutes, Solution A was added to each sample and another phenol-chloroform extraction was performed, followed by overnight isopropanol

precipitation. Samples were centrifuged as above, and pellets were washed with 75% ethanol, centrifuged, and dried. RNA pellets were resuspended in sterile water.

Protease Digestion of sRAGE for Liquid Chromatography Tandem Mass Spectrometry (LC-MS/MS). For each reaction, 5 μg of purified sRAGE was lyophilized and reduced (30 min incubation at room temperature in the dark with 8M urea and 5mM dithiothreitol) and alkylated (30 min incubation in the dark at room temperature with 10mM iodoacetamide). Protein was then suspended in 100mM Tris, pH 7.5 to dilute the urea and incubated with 0.1 μg trypsin (Promega, Madsion, WI) or 0.1 μg thermolysine (Sigma) with 2mM calcium chloride or 0.1 μg chymotrypsin (Sigma) for 4 hours at 37^{o}C.

LC-MS/MS. The LC-MS/MS analyses were performed using a Micromass Q-TOF Ultima Global mass spectrometer (Micromass/Waters, Manchester, UK) connected to an LC-Packings UltiMate nanoLC system (LC-Packings, Amsterdam, The Netherlands). A nanospray ion source was used to hold the packed PicoFrit^{TM} columns (New Objective, Inc., Woburn, MA) and apply capillary voltage through a Valco union. The PicoFrit columns (75 μm inner diameter X 10 cm) were packed with Zorbax SB C_{18} 3.5 μm reverse phase column material (Agilent, Palo Alto, CA) using a high pressure column loader (Proxeon Biosystems, Odense, Denmark). The column was developed at a flow rate of 200 nl/min and linear gradients from 0.02% heptafluorobutyric acid/0.5% acetic acid in water to 0.02% heptafluorobutyric acid/0.5% acetic acid in 75% acetonitrile/24.5% water. After data acquisition, the individual MS/MS spectra acquired for each of the precursors were centroided using the Micromass Masslynx data processing software and output as a single Mascot-searchable peak list. The peak list files were used to query the Swiss-Prot database using the Mascot program [187].

Matrix-assisted Laser Desorption Ionization Mass Spectrometry (MALDI-MS). Buffer salts were removed from sRAGE using ZipTips (Millipore Corporation, Danvers, MA). MALDI-MS was performed using a Micromass Q-TOF Ultima Global mass spectrometer operated in MALDI-MS mode. Spectra were recorded in linear mode (mass determination) or reflector mode (glycosylation studies).

Disulfide Characterization. A tryptic map of mouse RAGE was generated by GPMAW (General Protein/Mass Analysis for Windows) software (Lighthouse Data, Odense, Denmark). Approximately 400 μg of native purified sRAGE was incubated with 8 μg trypsin overnight at room temperature. The reaction was then analyzed by SDS-PAGE to confirm reaction completion. After trypsinization of nonreduced sRAGE, the peptides were separated by gel filtration (Superdex peptide HR10/30 column (Amersham Biosciences)) in 20mM sodium phosphate, pH 7.2, 250mM sodium chloride. Each peak from gel filtration was further separated by reverse-phase high pressure liquid chromatography (RP-HPLC) on an Aquapore RP-300 column (Solvent A, 0.1% trifluoroacetic acid; Solvent B, 90% acetonitrile, 0.08% trifluoroacetic acid; elution profile, 2% solvent B/min linear gradient at 200 μl/min). Both chromatography steps were performed using a Pharmacia SMART system (Amersham Biosciences). Peaks from RP-HPLC were subjected to 3-6 cycles of Edman degradation, and these residues were used to identify the corresponding peptide on the tryptic map. If two cysteine-containing peptides were identified from a single RP-HPLC peak with an approximately 1:1 intensity, this was taken as evidence of their linkage by a disulfide bond. For confirmation, each of these peaks was subjected to MALDI-MS to verify that the mass corresponded to the combined mass of the two peptides. Finally, protein from each peak was reduced with 5mM dithiothreitol and again

analyzed by MALDI-MS to see whether two distinct masses resulted after reduction. If so, this result would confirm that the two peptides are linked by a disulfide bond.

Deglycosylation of Mouse sRAGE. 100μg of purified sRAGE was boiled for 5 min in denaturation buffer (50mM sodium phosphate, pH 7.5, 0.1% SDS, 50mM β-mercaptoethanol) and cooled. Triton X-100 was added (0.5% final concentration) followed by the addition of 9 U PNGase F (Calbiochem), and the reaction was incubated at 37^{o}C for 3 hours. For *O*-deglycosylation, 100μg of sRAGE in 50mM sodium acetate, pH 5.0, was incubated with 0.1 U of neuraminidase (Roche) at 37^{o}C for 18 hours. Following this incubation, 1.5 mU of *O*-glycosidase (Roche) was added with reaction buffer (50mM sodium phosphate, pH 7.5), and the reaction was incubated at 37^{o}C for 18 hours. Where indicated, sRAGE underwent PNGase F treatment followed by neuraminidase treatment and *O*-glycosidase treatment as detailed above. Reactions were terminated by the addition of SDS sample buffer (containing 4% SDS). One microgram of sRAGE from each reaction was subjected to SDS-PAGE and western blotting as described above.

***N*-linked Glycan Characterization.** An aliquot of each RP-HPLC fraction determined to contain the peptides with Asn_2 and Asn_{27} (potential *N*-glycosylation sites) was subjected to MALDI-MS before and after deglycosylation by PNGase F. Glycan components were identified from MALDI-MS analysis using GlycoMod on Expasy (us.expasy.org/tools/glycomod/).

3.3. RAGE AND sRAGE REGULATION STUDIES

3.3.1. Lung protein preparations and western blot analysis

Lungs were extracted from mice and soluble and membrane protein preparations were made as detailed above (Section 3.1.1). Typically, 30 μg of total lung protein was subjected to SDS-PAGE and western blot analysis as described above (Section 3.1.2).

3.3.2. Bleomycin mouse model of PF

C57Bl/6 mice (6-8 weeks old) (Taconic, Germantown, NY) were anesthetized with Isoflurane (Abbot Laboratories, North Chicago, IL) and given one intratracheal instillation of bleomycin (MP Biomedicals, Irvine, CA, or Bedford Laboratories, Bedford, OH) or an equivalent volume of 0.9% sterile saline on day 0. The effective dose of bleomycin varies with each drug lot, but typically the dose used was between 0.12 U and 0.06 U of bleomycin, dissolved in 50 μl of 0.9% sterile saline. Mice were sacrificed after the indicated amount of time post-treatment by lethal injection of pentobarbital (Sigma).

3.3.3. Asbestos mouse model of PF

C57Bl/6 mice (6-8 weeks old) (Taconic) were anesthetized with Isoflurane (Abbot Laboratories) and given one intratracheal instillation of 0.1 mg crocidolyte asbestos (>10 μm in length, provided by Andrew Ghio, Environmental Protection Agency) or 0.1 mg titanium dioxide (Sigma) on day 0. Instillation volume was 50 μl, and each treatment reagent was dissolved in 0.9% sterile saline. After the indicated amounts of time post-treatment, mice were sacrificed by lethal injection of pentobarbital (Sigma).

3.3.4. Human IPF tissue

IPF tissues. Lung tissue from IPF patients was obtained from the Department of Pathology Tissue Bank (University of Pittsburgh). Tissues were from surgical remnants of biopsies or

lungs explanted from IPF patients that received a pulmonary transplant. The use of archived tissue has been approved by the local Institutional Review Board. Diagnosis of IPF was supported by history, physical examination, pulmonary function studies, chest high-resolution computed tomography, bronchoalveolar lavage findings, and corroborated by open lung biopsy. The morphologic diagnosis of IPF was based on typical microscopic findings consistent with usual interstitial pneumonia [27]. Control samples included normal histology lung samples resected from patients with lung cancer obtained from the University of Pittsburgh Tissue Bank.

IPF microarray analysis. Total RNA was extracted using the RNeasy Mini Kit (Qiagen) and used as a template to generate double-stranded cDNA and biotin-labeled cRNA as recommended by the manufacturer of the arrays (Amersham Biosciences) and previously described [188]. Briefly, first-strand cDNA was synthesized from total RNA using T7 oligo(dT) primers in a reverse transcriptase reaction for 2 hours at 42^{o}C. Second-strand cDNA was then synthesized using the first-strand cDNA as a template (2 hours at 16^{o}C). Purified double-stranded cDNA was then used as a template for *in vitro* transcription in the presence of biotin-labeled nucleotides (14 hours at 37^{o}C). Biotin-labeled cRNA was then fragmented and hybridized (18 hours at 37^{o}C) to CodeLink UniSet Human I Bioarray slides (Amersham Biosciences). After hybridization, arrays were washed and stained with Streptavidin-Alexa Fluor® 647. The arrays were scanned using a Genepix 4000B microarray scanner (Molecular Devices) and images were analyzed using CodeLink Expression II Analysis Suite (Amersham Biosciences). The array slides were visually inspected for defects and quality control parameters as recommended by the manufacturer. Data files were imported into a microarray database and linked with updated gene annotations using SOURCE (http://genome-www5.stanford.edu/cgi-bin/SMD/source/sourceSearch) and then median scaled. Based on previous experience, all

expression levels below 0.01 were brought to 0.01. Statistical analysis was performed using Scoregene gene expression package (http://www.cs.huji.ac.il/labs/compbio/scoregenes), and data visualization was performed using Genexpress (http://genexpress.stanford.edu) and Spotfire DecisionSite 8.0 (Spotfire Inc., Göteborg, Sweden). The complete set of gene array data has been deposited in the Gene Expression Omnibus database with GEO serial accession number GSE2052 (http://www.ncbi.nlm.nih.gov/geo).

IPF protein preparations and western blot analysis. Soluble protein preparations were done as detailed for mouse tissues above (Section 3.1.1). For membrane protein preparations, the pellet leftover from the soluble preparation centrifugation was resuspended in CHAPS buffer (50mM Tris-HCl, pH 7.4, 150mM sodium chloride, 10mM CHAPS detergent) and briefly sonicated. Samples were rocked at 4^{o}C for 2 hours, then centrifuged at 20,000 x g for 20 minutes at 4^{o}C. Protein concentration in the supernatant was determined using the Coomassie Plus Protein Assay Reagent (Pierce).

3.3.5. RAGE knockout lung phenotype

RAGE knockout mice were generated in the laboratory of Dr. Bernd Arnold (German Cancer Research Center, Heidelberg, Germany) [189]. Immunohistochemical studies were performed on RAGE-/- mice (19-24 months old) in collaboration with Dr. Michael Kasper (Technical University of Dresden, Germany) and Dr. Angelika Bierhaus (University of Heidelberg, Germany). Lungs were isolated from RAGE-/- mice and age-matched RAGE+/+ controls and fixed with Schaffer's solution or 4% formaldehyde followed by paraffin embedding. Five micron sections were cut from paraffin blocks and immunostained as indicated below after pretreatment with either microwave irradiation (750 W, 2 times for 5 minutes) in 0.01M sodium citrate buffer, pH 6.0, or 0.05% aqueous saponin (30 minute incubation, room temperature).

Sections were stained with the following primary antibodies for 1 hour at room temperature: goat anti-RAGE (Merck and Dhome, Essex, UK) (1:2,000), rabbit anti-collagen type I (Quarttet Immunodiagnostica, Berlin, Germany) (1:20), mouse anti-TNF-α (Santa Cruz Biotechnology) (1:3), mouse anti-α-smooth muscle actin (Immunotech, Marseille, France) (1:50), and rabbit anti-galectin-3 (Boehringer Mannheim, Mannheim, Germany) (1:200). Biotinylated secondary antibody Elite kits (Vector Laboratories, Burlingame, CA) were incubated with sections for 1 hour at room temperature, and antibody binding was detected using the ABC complex (Vector Laboratories) and visualized using 3,3'-diaminobenzidine (Vector Laboratories), followed by counterstaining with hematoxylin.

3.4. CELL CULTURE STUDIES

3.4.1. A549 Epithelial cell line

Culture conditions. The A549 cell line was purchased from the American Type Culture Collection. It is a human lung epithelial cell line derived from lung carcinoma. A549 cells are cultured in Ham's F12K medium supplemented with 10% fetal calf serum ('culture medium') at 37^{o}C in the presence of 5% CO_2.

Cell treatments. Cells were plated in 6-well plates (190,000 cells per well) in culture medium. Cells were grown to approximately 70% confluence, then rinsed once with serum-free medium, then treated with 5 μg/cm^2 (or 48.1 μg/well) of endotoxin-free crocidolyte asbestos or titanium dioxide, or an equivalent volume of sterile 0.9% saline (vehicle) suspended in serum-free medium. Twenty-four hours after treatment, wells were washed three times with cold phosphate-buffered saline, then scraped in cold phosphate-buffered saline containing 0.5mM phenylmethylsulfonylfluoride and transferred to a fresh tube. Cell suspensions were centrifuged

at 4,000 rpm for 4 minutes at room temperature and supernatant was removed. The cell pellet was resuspended in Lysis Buffer (50mM Trizma-HCl, 150mM sodium chloride, 1% Triton X-100, 0.5mM phenylmethylsulfonylfluoride), briefly sonicated, then rocked at 4^{o}C for approximately one hour. Samples were centrifuged at 10,000 rpm for one minute to pellet cell debris, and supernatant was transferred to a new tube. Supernatant protein concentration was determined using the Coomassie Plus Protein Assay Reagent (Pierce). Western blot analysis was performed as detailed in Section 3.1.2.

3.4.2. MH-S Macrophage cell line

Culture conditions. The MH-S cell line was purchased from the American Type Culture Collection. It is a mouse alveolar macrophage cell line that is mixed, with adherent cells and cells in suspension. MH-S cells are cultured in RPMI 1640 medium with 2 mM L-glutamine supplemented to contain 1.5 g/L sodium bicarbonate, 4.5 g/L glucose, 10 mM HEPES, 1.0 mM sodium pyruvate, 0.05 mM β-mercaptoethanol and 10% fetal calf serum ('culture medium'). Cells are grown at 37^{o}C in the presence of 5% CO_2.

Cell treatments. Cells were plated in 6-well plates (600,000 cells per well) in culture medium. Cells were grown to approximately 85% confluence before treatment. To retain cells in suspension so they would be included in the treatments, medium was collected from each well and centrifuged at 1,000 rpm for 3 minutes at room temperature. Cell pellets were suspended in serum-free medium (without β-mercaptoethanol) and transferred back to their original wells, which had been rinsed once with serum-free medium. 5 μg/cm^2 of crocidolyte asbestos or titanium dioxide, or 5.0 mU Bleomycin, or an equivalent volume of sterile 0.9% saline was added to each well. Twenty-four hours after treatment, medium was collected from each well

and centrifuged at 2,000 rpm for 3 minutes to pellet cells. Cell-free media were used in western blot analyses (equivalent volumes of media were loaded into gels).

3.4.3. Pulmonary fibroblast cell lines

Culture conditions. The LL-47 and LL-29 cell lines were purchased from the American Type Culture Collection. They are human lung fibroblast cell lines. LL-47 was derived from a normal area of a human lung, while LL-29 was derived from from an IPF lung. Both cell lines are cultured in Ham's F12K medium supplemented with 10% fetal calf serum ('culture medium') at 37^{o}C in the presence of 5% CO_2.

Cell treatments. Cells were plated in 6-well plates (290,000 cells per well) in culture medium. Cells were grown to 40-50% confluence, then treated with 40μM AGE-BSA (prepared with glucose, see below) or nonglycated (control) BSA in culture medium, or culture medium alone (day 0). On days 2 and 4, the medium in each well was replaced with fresh medium containing the same components used to begin treatment on day 0. Thus, cells were treated with indicated components for 6 days total with fresh media replacement every two days. On day 6, cells were harvested. Cells in each well were trypsinized, then centrifuged at 10,000 rpm for 2 minutes. Cell pellets were resuspended in 4X SDS Sample Buffer (containing 4% SDS), briefly sonicated and boiled for 5 minutes. Protein concentrations were determined using the Coomassie Plus Protein Assay Reagent (Pierce).

3.4.4. Generation of AGE-BSA

Most experiments using AGE-BSA up to this point have been done using glucose-derived AGE-BSA. However, in a recent study [190] it was reported that ribose-derived AGE-BSA may bind RAGE better, so we have begun generating AGE-BSA with ribose. Both methods are included here.

Glucose-derived AGE-BSA. In a sterile 50 ml conical tube, the following components were added to sterile-filtered phosphate-buffered saline for a total volume of 20 ml: bovine serum albumin (BSA, final 1mM), D-glucose (final 1M), 3,4-dichloroisocoumarin (10μM final), E-64 (0.1mM final), ethylenediaminetetraacetic acid (1mM final), phenylmethylsulfonylfluoride (1.5mM final), diethylenetriaminepentaacetic acid (3mM final), and sodium azide (1mM final). For the control (nonglycated) BSA reaction, the glucose was omitted. Reactions were incubated in a 37^{o}C water bath for 10 weeks. By the end of ten weeks, the AGE-BSA reaction was brownish while the control BSA reaction remained yellow. Reactions were extensively dialyzed (into a total of 40 L of phosphate-buffered saline) to eliminate free glucose and sodium azide. AGEs have an approximately ten-fold increase in fluorescence [125, 191], so the fluorescence (excitation 370nm, emission 440 nm) of the two reactions was measured, thus we confirmed AGE formation in the AGE-BSA reaction.

Ribose-derived AGE-BSA. The following components were combined in a sterile 50 ml conical tube using aseptic technique: 20 ml sodium phosphate, pH 7.4 (400mM final), 3.75 g ribose (500mM final), 8.3 ml of 30% BSA solution (50 mg/ml final), and 21 ml sterile water. For the control (nonglycated) BSA reaction, ribose was omitted. The solutions were sterile filtered (0.22 μm filter) into a new sterile tube before placing into a 37^{o}C water bath, protected from light, for 4 weeks. A small aliquot was removed aseptically once per week from each reaction to monitor the pH of each solution to make sure it remained between 7-7.4. Unincorporated ribose was removed by extensive dialysis into a total of 20 L of sterile phosphate-buffered saline.

4. RAGE AND sRAGE ARE HIGHLY EXPRESSED IN THE MOUSE LUNG

Previous studies [64, 76] have shown high levels of RAGE/sRAGE transcripts in the human and rat lungs, compared to other tissues examined. This suggests that RAGE and sRAGE have a unique role in homeostasis of the lung in these organisms. Because we planned to use the bleomycin and asbestos mouse models to examine the role of RAGE in pulmonary fibrosis, we wanted to determine if RAGE and sRAGE expression are high in the lung of the mouse as well. We hypothesized that RAGE/sRAGE protein expression would be elevated in the lungs of mice compared to other mouse tissues.

4.1. HIGH EXPRESSION OF MEMBRANE-BOUND RAGE IN THE MOUSE LUNG

To determine if RAGE is expressed highly in the mouse lung, implicating a role for it in homeostasis of this organ, we wanted to compare amounts of this protein present in various tissues in mice. We chose to study tissues from untreated C57Bl/6 mice because this is the strain used in our mouse models of pulmonary fibrosis. Western blot analysis shows that indeed, RAGE protein is expressed at the highest level in the lungs of mice compared to the other tissues studied (Figure 2).

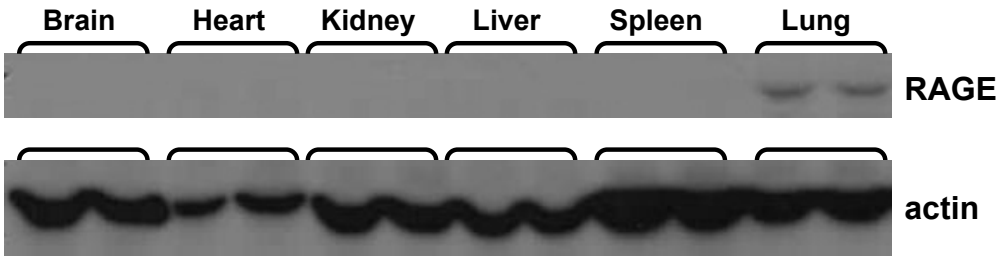

Figure 2. High expression of RAGE in mouse lungs.

Membrane protein fractions were isolated from the indicated tissues of two untreated C57Bl/6 mice. Forty micrograms of each preparation were subjected to western blot analysis, probing for RAGE (upper panel). The PVDF membrane was then stripped and re-probed for β-actin (lower panel) as a loading control. Note that RAGE is only detectable in the lungs of normal adult mice.

4.2. HIGH EXPRESSION OF SOLUBLE RAGE (sRAGE) IN THE MOUSE LUNG

We next wanted to determine if sRAGE is also expressed at its highest levels in the lung. In this case, it was essential to look on the protein level because, as it is a secreted protein, mRNA transcript levels may not reflect the location of the protein itself. Soluble protein fractions were prepared from several tissues from untreated C57Bl/6 mice and analyzed for sRAGE expression by western blotting. As Figure 3 shows, sRAGE is expressed at the highest levels in the mouse lung.

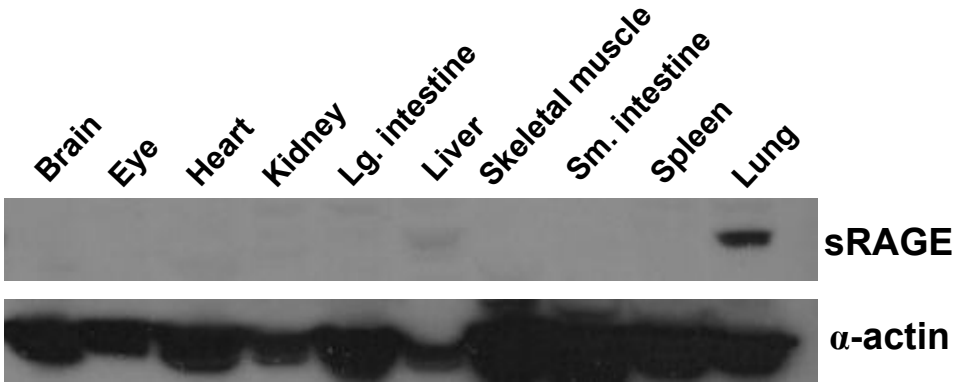

Figure 3. High expression of sRAGE in mouse lungs.

(Figure 3, cont.) Soluble protein fractions were isolated from each of the indicated tissues from two untreated C57Bl/6 mice. Forty micrograms of each preparation were subjected to western blot analysis, probing for sRAGE (upper panel). The PVDF membrane was then stripped and re-probed for α-actin (lower panel) as a loading control. Results are representative of two independent experiments. Note the high level of sRAGE in the lungs of healthy adult mice compared to other tissues.

4.3. sRAGE IS NOT LOCALIZED IN BALF OR SERUM

The protein preparations used to determine the tissue expression of RAGE and sRAGE in Figure 2 and Figure 3 do not distinguish between compartments of the lung. Thus, to further characterize the localization of sRAGE, we wanted to determine if it is detectable in the bronchoalveolar lining fluid (BALF) or in the serum since a secreted protein could potentially reside in these compartments. Serum and BALF were obtained from untreated mice and subjected to western blotting analysis to detect sRAGE. Figure 4 shows that sRAGE is undetectable in the BALF and serum.

Figure 4. sRAGE is not localized in the BALF or serum.

BALF and serum were extracted from five control C57Bl/6 mice. Thirty micrograms of total protein from each sample was subjected to western blot analysis probing for sRAGE. Positive control (+ lane), purified sRAGE.

4.4. CONCLUSIONS

Previous findings indicating that RAGE/sRAGE transcripts are highest in the lung compared to other human and rat tissues [64, 76] are supported by our data here on RAGE and sRAGE *protein* in mouse tissues. We found that both protein isoforms are expressed at the highest levels in the lung. This implicates these proteins in a conserved homeostatic function unique to the lung in these organisms, and likely other mammals, and supports our use of the mouse models for describing the role of RAGE/sRAGE in human IPF pathogenesis.

The only other tissue in which sRAGE could be detected in our studies was the liver. RAGE has been detected in the liver by other groups [64] as well, specifically in rat hepatic stellate cells and hepatic myofibroblasts [127]. However, RAGE in the liver seems to have a pathogenic link. RAGE is upregulated during stellate cell transdifferentiation to myofibroblasts (a critical step in liver fibrogenesis) [127], and in addition the presence of RAGE has been reported to limit regenerative capacity after massive hepatectomy [85].

We determined that the soluble RAGE isoform, sRAGE, is not localized to the BALF or serum compartments of the lung, suggesting that sRAGE resides in the pulmonary parenchyma. We have found that sRAGE has heparin affinity, which may have implications for its tissue localization (see Chapter 5).

5. PURIFICATION AND BIOCHEMICAL CHARACTERIZATION OF MOUSE sRAGE

To investigate the role of RAGE and sRAGE in pulmonary fibrosis, we planned to use the bleomycin- and asbestos-induced mouse models of pulmonary fibrosis and examine the differential regulation of RAGE and sRAGE expression in this disease. However, to distinguish between these two isoforms on the mRNA level, we first needed to determine if sRAGE in the mouse is produced by alternative splicing of the RAGE transcript, as is the case in humans [70, 72]. Furthermore, because mouse sRAGE would potentially be a valuable tool in future studies, we set out to identify a purification strategy for this protein, as well as biochemically characterize it to describe its structure.

5.1. sRAGE IS PURIFIED FROM MOUSE LUNGS IN THREE STEPS

The lung was determined to contain the highest concentration of sRAGE protein in the mouse (see Figure 3). Thus, mouse lungs were used as starting material for sRAGE purification.

Purification of mouse sRAGE was carried out by first homogenizing lung tissue in buffer containing protease inhibitors (see Section 3.2.1). Following homogenization, protein was subjected to batch extraction with concanavalin A-sepharose followed by Affi-Gel heparin affinity chromatography and finally Mono Q ion-exchange chromatography. Figure 5 shows the step-wise purification of sRAGE from mouse lungs.

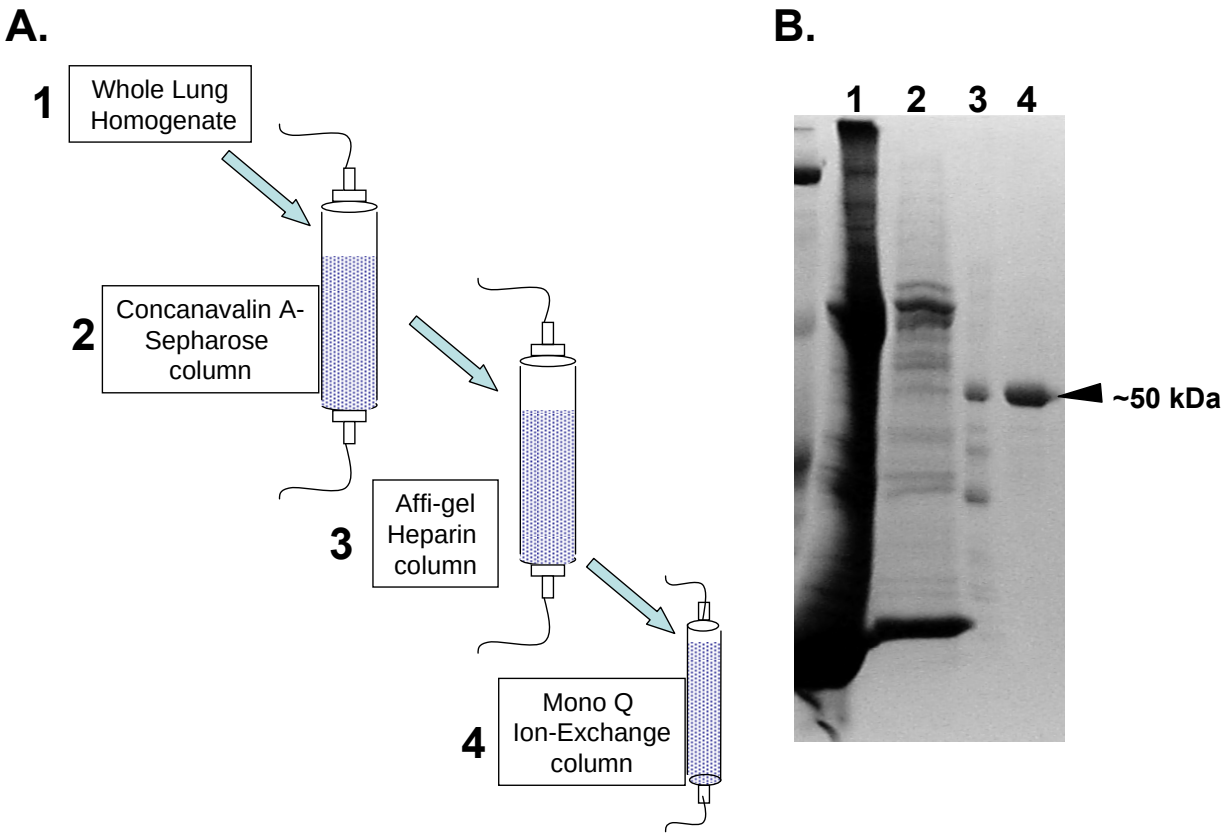

Figure 5. Three-step purification of sRAGE from mouse lungs.

(A) Purification scheme for mouse sRAGE. Mouse lungs were homogenized, then subjected to three chromatographic steps: Concanavalin A-sepharose, Affi-gel Heparin affinity chromatography, and Mono Q-sepharose ion-exchange. (B) Twenty-six microliters of protein after each step in *A* was separated by SDS-PAGE and the gel was stained with Coomassie Brilliant Blue. Lane markers indicate corresponding step in *A*.

5.2. BLOCKAGE OF THE AMINO-TERMINUS OF MOUSE sRAGE

We were unable to determine the amino-terminal sequence of the native purified mouse sRAGE using Edman degradation, so we hypothesized that the amino-terminus of sRAGE is blocked. After intracellular removal of the signal peptide (Met-Pro-Ala…Ala-Gly-Gly, the first 23 residues of the mouse RAGE polypeptide, GenBank™ accession number 6671525), the amino-terminal sequence becomes Gln_1-Asn-Ile-Thr-Ala-Arg… (see Figure 6). When Gln is the amino-terminal amino acid residue, it may spontaneously undergo deamidation and cyclization

to form the cyclic amino acid pyroglutamate (pGlu), which is unreactive in Edman degradation. To determine if pyroglutamate is the blocking group at the amino-terminus of mouse sRAGE, the purified protein was incubated with *Pfu* pyroglutamate aminopeptidase, then subjected to Edman degradation. The resulting amino-terminal sequence was determined to begin with Xxx-Ile-Thr-Ala-Arg… This sequence corresponds to an unidentified amino acid residue (Xxx) followed by the third residue after the signal peptide (Ile_3), and so on. Notably, Asn_2 was not identified as the aminoterminal amino acid residue after treatment with *Pfu* because it is glycosylated (see below). Thus, these studies indicate that after removal of the sRAGE signal peptide, the aminoterminal Gln is modified to form pGlu (depicted in Figure 9B).

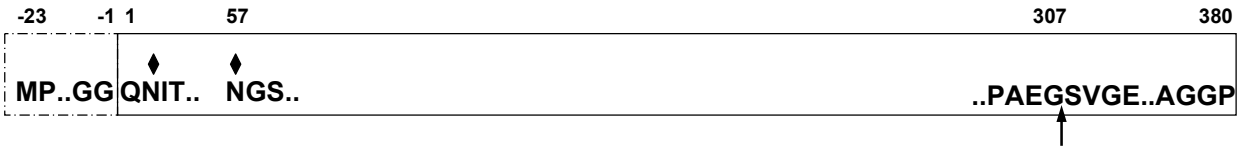

Figure 6. Mass spectroscopy sequencing highlights for mouse sRAGE.

Mouse sRAGE was proteolyzed with trypsin, chymotrypsin, or thermolysine, and resultant peptides were subjected to LC-MS/MS for sequencing. Summarized here is the composite sequencing of all three peptide sets. *Numbers* indicate amino acid positions relative to the first residue after the removal of the signal peptide. The portion of the sequence bordered with a *dashed line* indicates the signal peptide. The *arrow* indicates the residue at which our sequence data terminated (proposed carboxyl-terminus of sRAGE). *Diamonds* indicate *N*-glycosylation sites.

5.3. MOUSE sRAGE IS NOT A PRODUCT OF ALTERNATIVE SPLICING

Previous studies [70, 72] have shown that human sRAGE is a product of alternative splicing of RAGE mRNA. The alternative splice site is located just upstream of the transmembrane domain and results in a frameshift so that a transmembrane domain is no longer encoded for sRAGE. Thus, human RAGE and sRAGE have distinct carboxy-terminal amino acid sequences. To see if

mouse sRAGE is also produced by alternative splicing, we attempted to detect an alternative RAGE transcript. We used either mouse lung RNA or a mouse lung cDNA library as a template in RT-PCR or PCR. Primers were targeted to each end of the RAGE transcript, as well as various internal sites including sequences directly flanking the region homologous to the sequence spliced out in humans (see Figure 7 and Table 3, page 31), in attempt to detect a smaller amplicon that would indicate alternative splicing analogous to that seen in humans. We found no evidence of an alternative RAGE transcript. However, we were able to amplify mouse membrane RAGE (see Figure 7 and Table 3, primers indicated by *). Furthermore, we also were able to amplify and clone sRAGE from a human cDNA library whose sequence closely matched that found by Malherbe et al. [70], indicating that our failure to find an alternative mouse RAGE transcript is not due to failure of our primers to amplify RAGE cDNA.

Figure 7. Primers used in attempt to detect an alternatively spliced form of RAGE mRNA. **The translated portion of the mouse RAGE cDNA sequence is represented by the *rectangle*, whereas 5'- and 3'-untranslated regions are represented by *horizontal lines* (GenBank accession number AF030001.1 for nucleotides 74101-77630). Each *arrowhead* indicates the position of one primer sequence and the direction in which it was designed to amplify along the cDNA. Primer sequences are shown in Table 3 (page 31). The *dashed outline* represents the sequence homologous to that spliced out in the human sRAGE cDNA [70]. The *diagonally striped* sequence encodes the transmembrane domain of RAGE. The *vertical arrow* indicates the position at which the frameshift occurs in human sRAGE. Thus, after this codon, the amino acid sequences of human RAGE and sRAGE become distinct from one another. *Asterisks* indicate the primers used to successfully amplify and clone full-length mouse RAGE.**

To investigate the mouse sRAGE amino acid sequence, we used LC-MS/MS. Purified mouse sRAGE was digested with trypsin, chymotrypsin or thermolysine, and peptides were analyzed by LC-MS/MS. We chose to use three proteases so that peptides would overlap and thus sequence data from one digestion would complement that from the others. Figure 6 shows highlights from our sequencing data. 81.8% of the sequence between residues Gln_1-Gly_{307} was covered by the LC-MS/MS analyses. Notably, the carboxyl-terminal point at which our sequence data end is homologous to the point at which the human sRAGE amino acid sequence becomes distinct from that of human RAGE determined by Yonekura et al. [72] (see Figure 7, *vertical arrow*).

To determine if the mass of sRAGE corroborates this putative carboxyl-terminus (Gly_{307}), sRAGE was deglycosylated and subjected to MALDI-MS. If mouse sRAGE indeed ends at the last amino acid residue detected in our LC-MS/MS analysis (…Pro-Ala-Glu-Gly_{307}), then its expected (calculated) size would be approximately 32.736 kDa after removal of the signal peptide. We found that after deglycosylation, mass spectroscopy size determination of mouse sRAGE yielded approximately 32.854 kDa (Table 4). Such a small discrepancy supports the hypothesis that mouse sRAGE is truncated and does not have a distinct amino acid sequence from mouse membrane-bound RAGE.

Table 4. Mouse sRAGE masses determined by indicated methods.

Description	Method	Mass
	Calculation, based on amino acid sequence‡	32736.28 Da
Reduced, Denatured	SDS-PAGE	~45000 Da
Native	MALDI-MS	36033.00 Da
Deglycosylated (PNGase F)	MALDI-MS	34165.03 Da* 32854.15 Da

‡ Amino acid residues 1-307, see Figure 6
* Likely due to incomplete deglycosylation of sRAGE

5.4. DISULFIDE BRIDGE PATTERN OF MOUSE sRAGE

We investigated the disulfide pattern of mouse sRAGE to further characterize its structure. Initial studies indicated the presence of intrachain disulfide bonds in sRAGE due to differences in its mobility in SDS-PAGE before and after chemical reduction (Figure 8). Increased mobility on SDS-PAGE in the absence of the reducing agent indicates that sRAGE is more compact before reduction, suggesting that it contains at least one intrachain disulfide bond. This method will not quantify or localize the disulfide bonds, however.

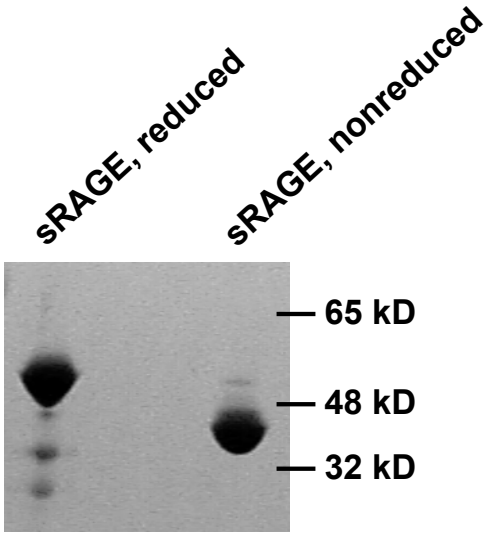

Figure 8. Mouse sRAGE contains intrachain disulfide bonds.

sRAGE purified from mouse lungs was subjected to SDS-PAGE (5-15% gradient acrylamide) in the presence or absence of 50 mM dithiothreitol, a reducing agent. The acrylamide gel was stained with Coomassie Brilliant Blue. Increased mobility in the nonreduced sRAGE indicates that before reduction sRAGE is more compact, and thus it contains at least one disulfide bond.

To further describe the disulfide bonding pattern of mouse sRAGE, trypsin was used because the tryptic digest map predicted that there would be no more than one cysteine in any single peptide. Tryptic peptides from purified, native mouse sRAGE were subjected to gel filtration. Peak fractions from gel filtration were subsequently subjected to RP-HPLC to further separate the peptides. Fractions from RP-HPLC were then sequenced using Edman degradation. Two peptides were presumed to be linked by a disulfide bond when sequence analysis of one RP-HPLC peak revealed two distinct amino-terminal peptide sequences and both peptides were identified by the tryptic map to contain cysteine residues. To confirm that the peptides were linked by a disulfide bond, a portion of the RP-HPLC fraction of interest was subjected to MALDI-MS to verify that the mass corresponded to two peptides. Another portion of the fraction of interest was then reduced and analyzed by MALDI-MS to determine if reduction

resulted in two masses that matched the predicted masses of the relevant peptides. Mouse sRAGE has six cysteines, and using this method we found that all six cysteines are engaged in disulfide bonds: Cys_{15} shares a disulfide bond with Cys_{75}, as does Cys_{120} with Cys_{184}, and Cys_{235} with Cys_{277} (depicted in Figure 9).

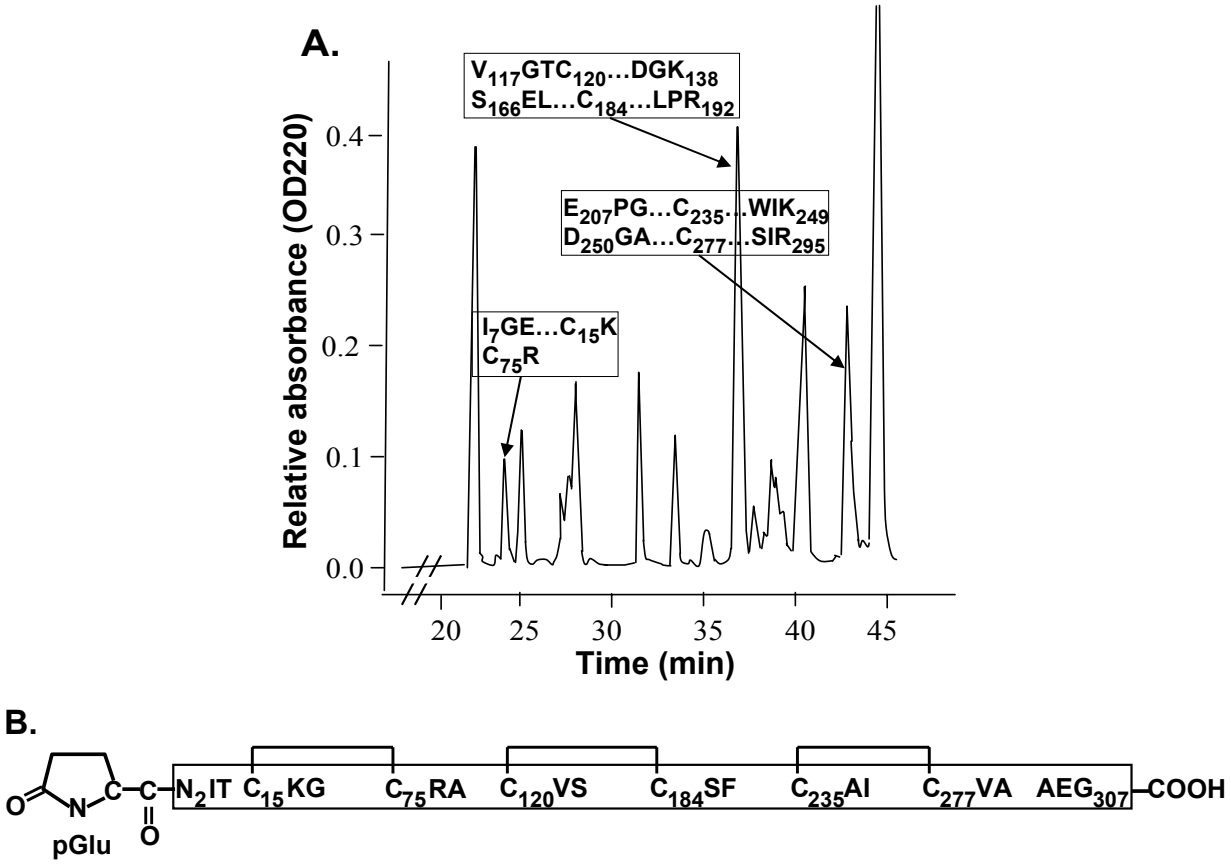

Figure 9. Disulfide pattern of mouse sRAGE.

(A) A representative RP-HPLC trace is shown. Native mouse sRAGE was trypsinized, and the resulting peptides were separated by RP-HPLC. Edman degradation was used to determine which peaks contained the indicated pairs of cysteine-containing peptides, and MALDI-MS analysis was used to confirm that the pair of the peptides in each of these peaks is joined by a disulfide bond (see *Methods*). The disulfide pattern within sRAGE is shown in (B) with *horizontal brackets* indicating each pair of cysteine residues joined by a disulfide bond. *pGlu*, pyroglutamate, the amino-terminal blocking group on sRAGE.

5.5. MOUSE sRAGE IS *N*-GLYCOSYLATED

The importance of RAGE glycosylation was shown by Srikrishna et al. [192] when they found a reduction in amphoterin-RAGE binding after RAGE deglycosylation. Presumably, the same is true for sRAGE because it has the same ligand specificity as RAGE. To determine if mouse sRAGE has *N*-linked and *O*-linked carbohydrates, purified mouse sRAGE was digested with *O*-glycosidase, *N*-glycosidase F (PNGase F), or a combination of the two enzymes. Analysis of sRAGE after deglycosylation by western blotting (Figure 10A) shows that mouse sRAGE is *N*-glycosylated but not *O*-glycosylated. To confirm this, sRAGE was subjected to amine monosaccharide analysis, but no *N*-acetylgalactosamine was detected (not illustrated), which supports the conclusion that mouse sRAGE is not *O*-glycosylated. Mouse sRAGE contains two potential *N*-glycosylation sites (Figure 6), and Figure 10A suggests that both of them are used because two sRAGE bands appear after deglycosylation (likely corresponding to partially and completely deglycosylated forms). In addition, mass spectroscopic size analysis of mouse sRAGE before and after PNGase F treatment (36033 Da and 32854 Da, respectively) (Table 4) indicates a reduction in size of approximately 3.2 kD, corresponding to two glycan groups.

To further confirm this and identify the components of these glycans, each of the two sRAGE tryptic peptides that were determined to contain one of the possible *N*-glycosylation sites by Edman degradation were analyzed by MALDI-MS in reflector mode before and after PNGase F treatment. MALDI-MS data (Table 5) was used with the GlycoMod program to identify components of each *N*-linked carbohydrate. Figure 10B summarizes this data, illustrating that Asn_2 likely has a di-antennary complex-type glycosylation with core fucosylation, and Asn_{57} has a compex or hybrid-type glycan.

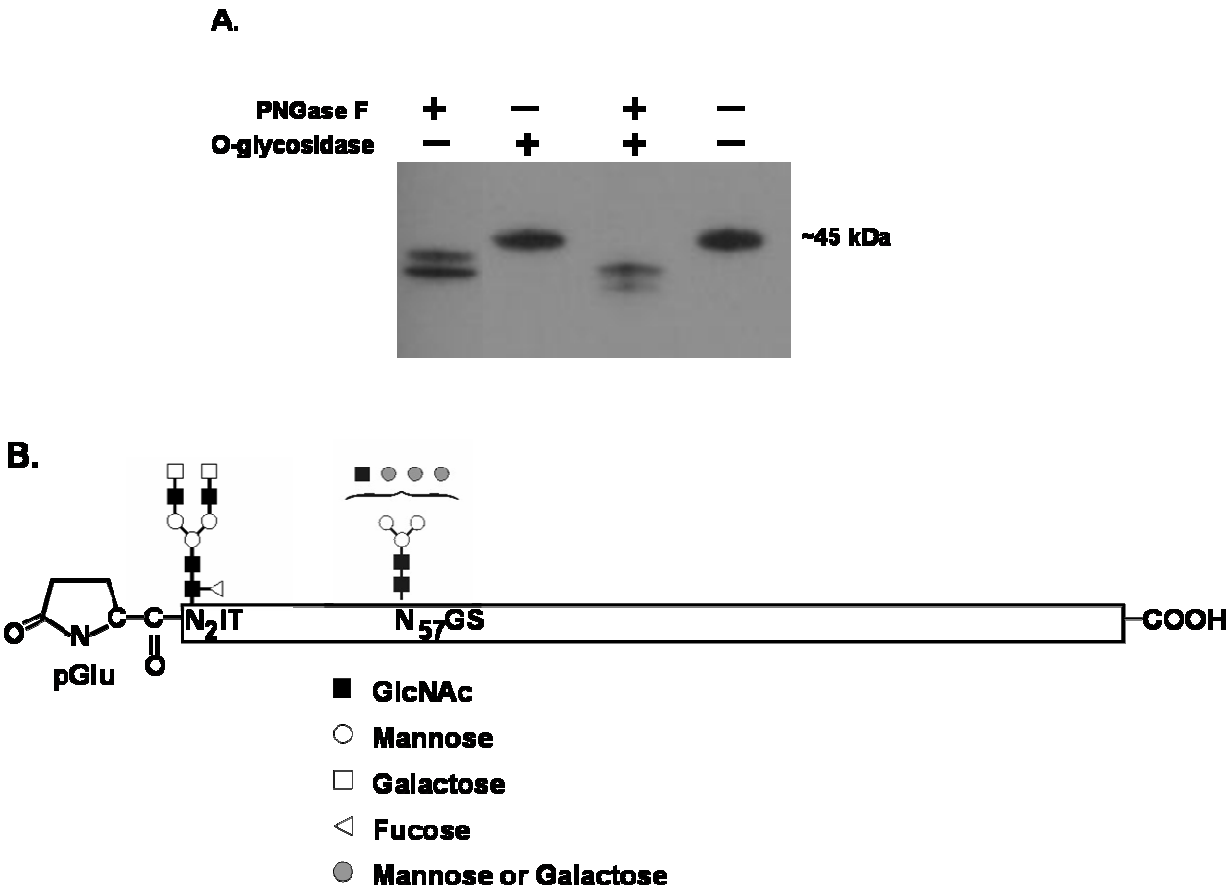

Figure 10. sRAGE is *N*-glycosylated.

(A) Purified sRAGE was incubated with *O*-glycosidase and/or PNGase F and subjected to western blot analysis probing for sRAGE. (B) Mouse sRAGE tryptic peptides that contained a possible *N*-glycosylation site were subjected to MALDI-MS for mass determination before and after deglycosylation. Data from MALDI-MS (see Table 4) were used in conjunction with the GlycoMod program to determine the composition of the *N*-linked sugar groups.

Table 5. MALDI-MS data for *N*-glycosylated peptides.

Peptide range	Glycosylated residue	Mass* (glycosylated)	Mass* after deglycosylation	Mass* of N-glycan‡
$pGlu_1$-Arg_6	Asn_2	2454.0029	686.3291	1768.7
Val_{40}-Arg_{74}	Asn_{57}	5189.8867	3608.2102	1582.7

*Masses are reported in Da.
‡Difference between peptide mass before and after deglycosylation by PNGase F treatment, plus 1 Da to account for the conversion of Asn to Asp resulting from PNGase F treatment.

5.6. CONCLUSIONS

We described a novel purification strategy for sRAGE from mouse lungs. This purification strategy includes a heparin affinity chromatography step. Heparin affinity, and the observation that sRAGE is undetectable in the BALF and serum (Figure 4), has important implications for the localization of sRAGE. It is likely that sRAGE is bound to heparan sulfate in the ECM and/or on cell membranes. There sRAGE may act as a decoy receptor by binding ligands and preventing them from binding membrane RAGE. Heparin affinity of RAGE has been reported by others [82], however the domain of RAGE/sRAGE that binds heparin has not been identified.

Our data suggest that, in contrast to sRAGE in humans, sRAGE in mice is not produced by alternative splicing. We found no evidence of an alternative transcript of RAGE in mouse lung RNA or a lung cDNA library. sRAGE from the mouse is likely to be a product of proteolytic truncation of RAGE (see Figure 11). Notably, matrix metalloproteinase-9 has been found to cause murine pulmonary epithelial cells to shed sRAGE into the culture medium [193], implicating this protease in the production of sRAGE from RAGE in the mouse. These findings may also suggest that human sRAGE has two levels of regulation. Human sRAGE may be

produced from proteolytic truncation in addition to the alternative splicing mechanisms already described [70, 72].

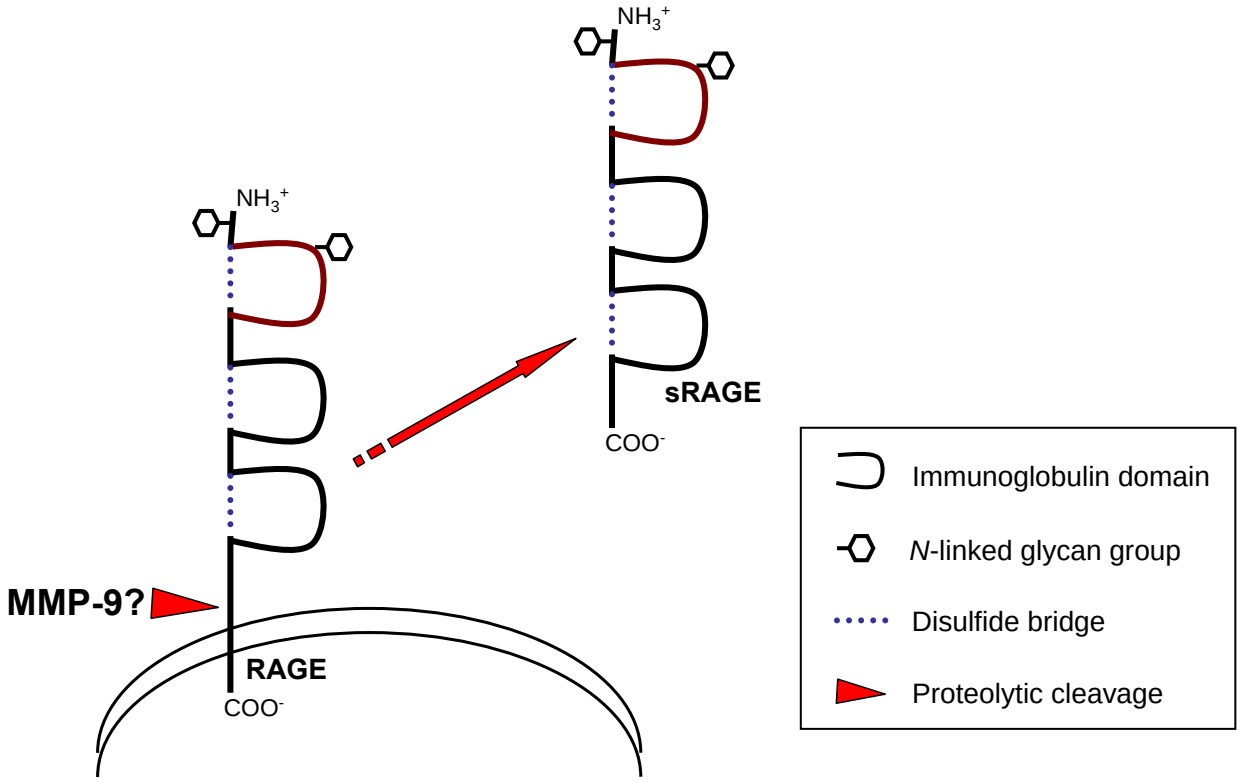

Figure 11. Summary of mouse sRAGE characterization.

sRAGE in the mouse is produced by proteolytic cleavage at a site proximal to the transmembrane domain, allowing sRAGE to be released from cell membranes. MMP-9 has been shown by others [193] to mediate release of sRAGE from cells. Mouse sRAGE contains three disulfide bonds and two *N*-linked glycosylation groups (positions are indicated above, see legend). The amino-terminal immunoglobulin domain involved in ligand binding is colored in brown.

Of the three extracellular immunoglobulin domains of sRAGE, the most amino-terminal one (V-like domain) (see Figure 11) has been shown to be necessary for ligand binding [71]. Because sRAGE is glycosylated at two sites in this domain, it is likely that glycosylation is important for the ability of sRAGE to bind its ligands, which would be in agreement with previous observations made by Srikrishna et al. [192] regarding bovine RAGE. This is important to consider when planning a protein expression system because protein expressed in a bacterial

system may lack post-translational modifications, such as glycosylation, that are critical for normal protein function.

In summary, we found that mouse sRAGE has affinity for heparin, which may play a key role in its extracellular localization. We also found evidence that the biosynthesis of sRAGE in mice contrasts to that in humans, in that mouse sRAGE seems to be a result of proteolytic truncation. Our observations are supported by the work of others who have identified matrix metalloproteinase-9 as a protease that is capable of executing this proteolysis [193].

6. RAGE AND sRAGE ARE DOWNREGULATED IN PULMONARY FIBROSIS

Because expression of RAGE and sRAGE are markedly higher in the lungs of mice (Figure 2 and Figure 3) and humans [64], we speculate that RAGE and sRAGE have important roles in pulmonary homeostasis. Thus, injury leading to the dysregulation of these proteins may be detrimental to lung homeostasis and promote pulmonary pathology. We hypothesized that injuries leading to the development of pulmonary fibrosis cause alterations in RAGE and/or sRAGE protein expression, which promotes further lung injury. To investigate this hypothesis we used the bleomycin- and asbestos-induced pulmonary fibrosis models in mice, as well as examining human IPF samples.

6.1. BLEOMYCIN MODEL OF PULMONARY FIBROSIS: RAGE AND sRAGE EXPRESSION

To investigate the regulation of RAGE and sRAGE expression during the pathogenesis of pulmonary fibrosis, we utilized the bleomycin model of pulmonary fibrosis. In this model, C57Bl/6 mice are treated with an intratracheal instillation of bleomycin sulfate while under anesthesia. During the first week after bleomycin insult, mice develop an intense inflammatory cell influx into the airspaces and interstitium with collapse of some airspaces and deposition of ECM [49]. By the second week after bleomycin injury, interstitial thickening and dense fibrosis are prominent.

To determine the effect that bleomycin has on the protein levels of RAGE, we first looked at seven days post-bleomycin treatment. This point marks the transition from the inflammatory phase into the fibrotic phase, and thus represents the point at which fibrogenesis becomes prominent. Western blotting shows that RAGE protein levels are significantly decreased in the lungs of mice seven days after bleomycin injury (Figure 12).

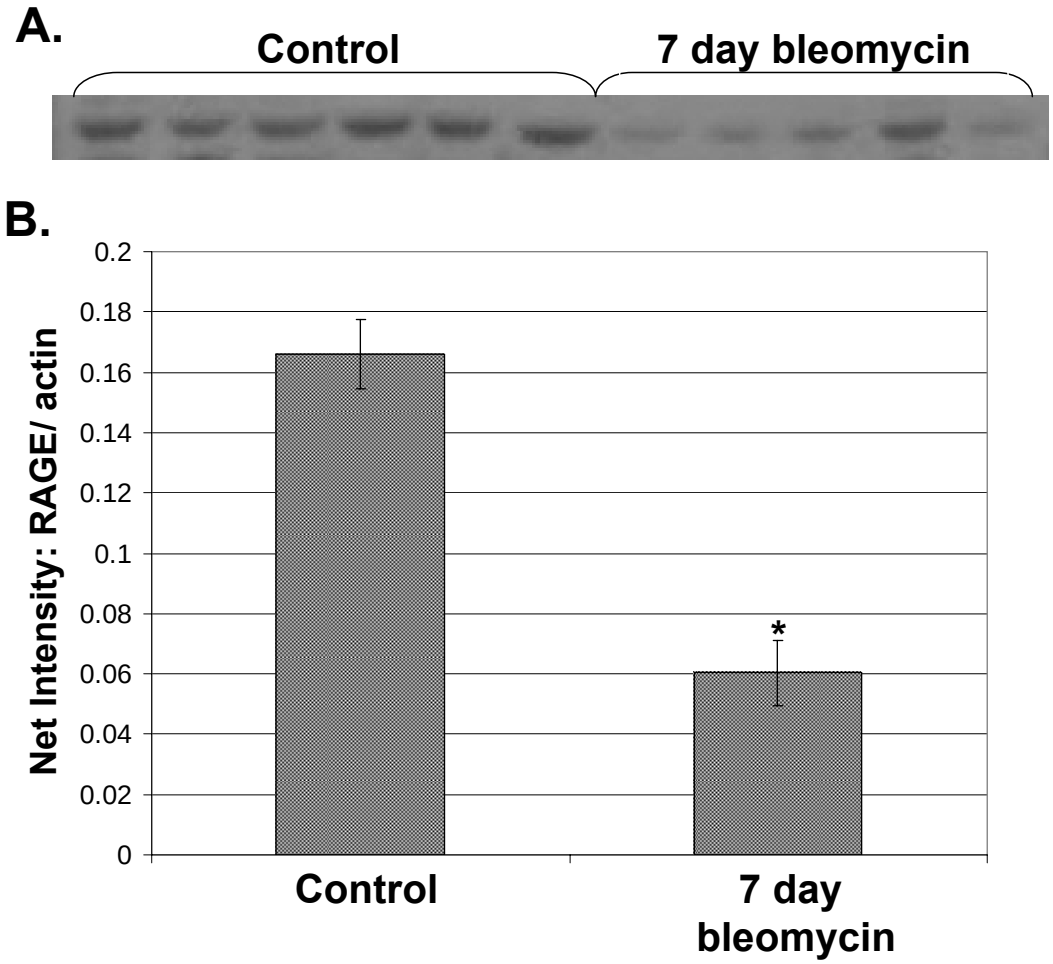

Figure 12. Reduction of RAGE protein 7 days after bleomycin treatment.

C57Bl/6 mice were treated with 0.1 U bleomycin and seven days later were sacrificed. Membrane fractions from lungs were subjected to western blot analysis, probing for RAGE (A, upper panel). PVDF membranes were stripped and re-probed for β-actin (A, lower panel) as a loading control. (B) Densitometry was performed on the film in *A* to quantify changes in RAGE band intensities, normalized to β-actin intensities. * $p<0.05$

In order to gauge of the kinetics of RAGE loss, a timecourse was done during the first week after bleomycin treatment. Figure 13 shows a significant decrease in RAGE levels by one day after bleomycin treatment, and these levels continue to decrease through day 7 after bleomycin treatment, when they reach their lowest values. These data indicate that loss of RAGE occurs promptly after bleomycin insult.

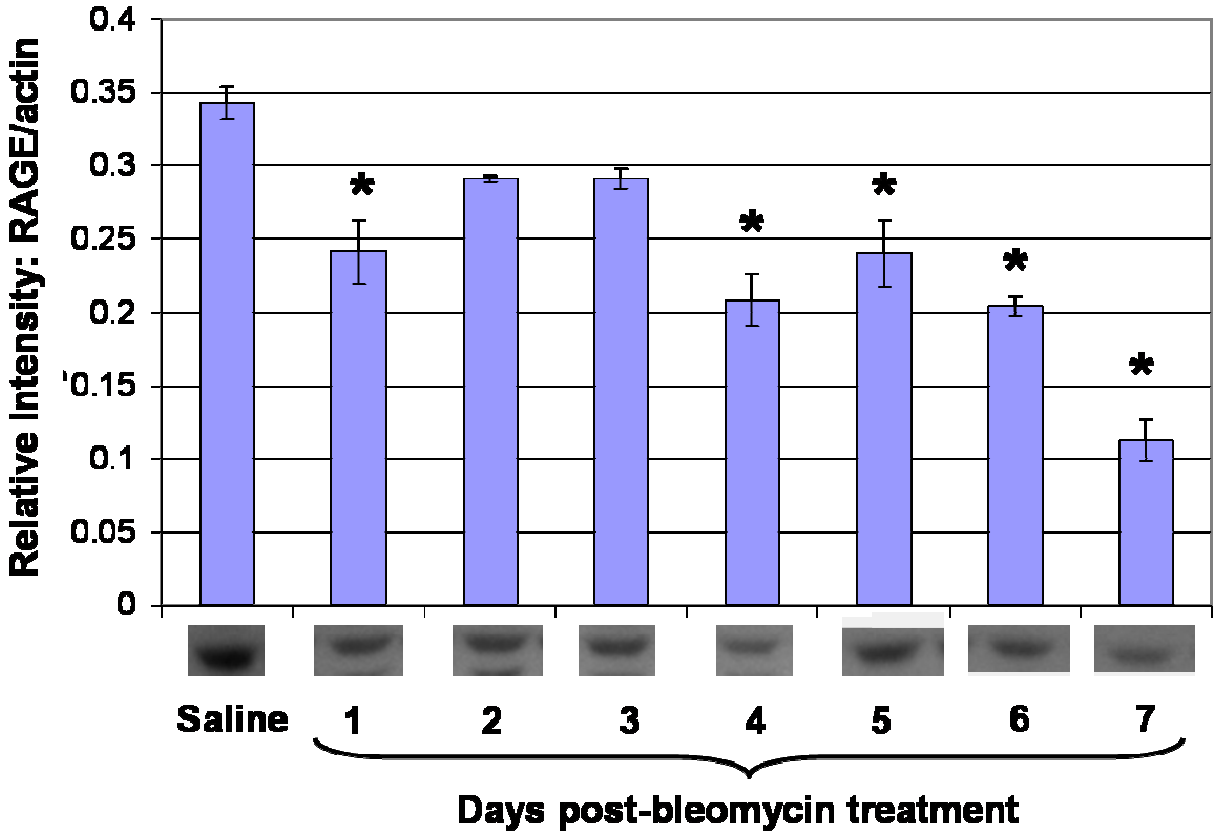

Figure 13. Seven-day bleomycin timecourse: loss of RAGE.

C57Bl/6 mice were treated with bleomycin on day 0, then sacrificed after the number of days indicated below the graph. Membrane fractions were isolated from lungs and analyzed by western blotting for RAGE. The PVDF membrane was stripped and re-probed for β-actin. Densitometry was performed and each lane's RAGE density was normalized by its actin density. Averaged normalized RAGE density is plotted for each timepoint. n=3 for each timepoint, and directly below the graph is one representative lane. *p<0.05

To investigate the effects of bleomycin treatment on sRAGE protein levels, we again used the seven-day timepoint. Soluble fractions were prepared from lungs of mice treated with bleomycin or saline seven days previously and subjected to western blot analysis for sRAGE. Figure 14 shows that, similar to RAGE, sRAGE protein is also reduced significantly at seven days post-bleomycin treatment.

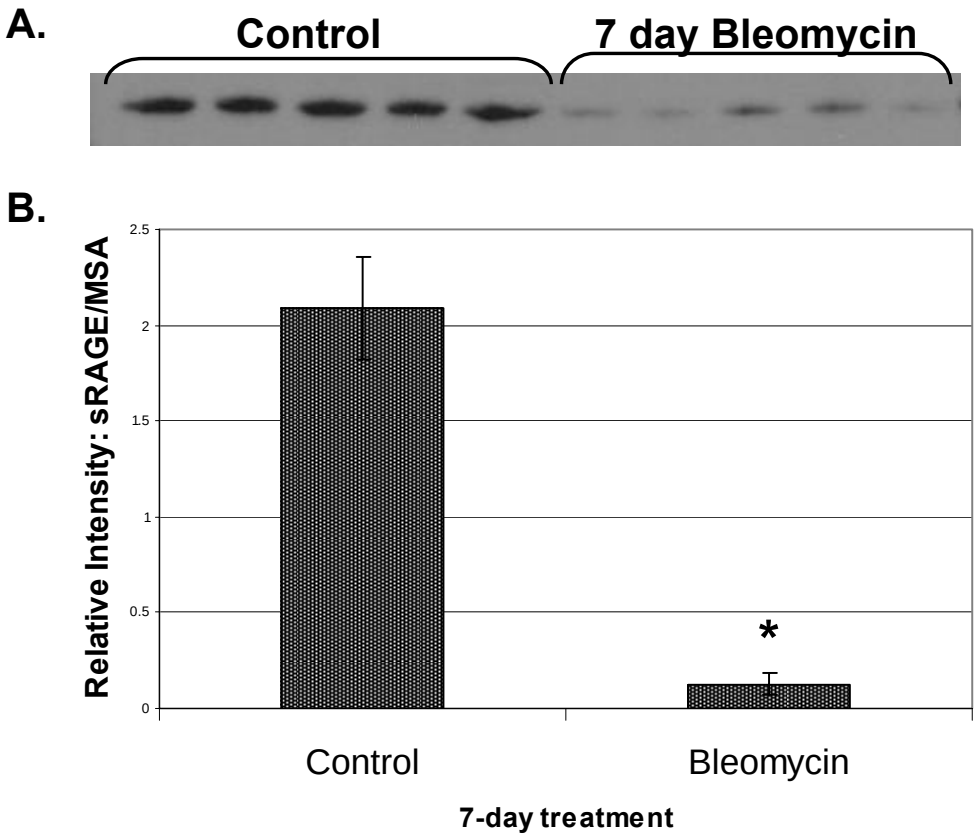

Figure 14. sRAGE is reduced in the lung seven days after bleomycin treatment.

Mice were treated with bleomycin or saline (controls) and seven days later were sacrificed. Soluble protein fractions were prepared from the lungs and equal protein was subjected to western blot analysis probing for sRAGE (A). The PVDF membrane was stripped and re-probed for mouse serum albumin (MSA) as a loading control. (B) Densitometry was performed on the film from *A* and sRAGE band density was normalized to MSA band density before being plotted. *p<0.05

To better describe the kinetics of sRAGE depletion during the first week after bleomycin injury, soluble protein fractions from the 7-day bleomycin timecourse were analyzed by western

blot for sRAGE at each timepoint (Figure 15). Although the trend for decreased sRAGE protein is apparent after one day, the difference is not significant until four days after bleomycin insult, and continues to decrease through day seven. The kinetics of sRAGE depletion are slightly slower than kinetics for the reduction of RAGE, but both appear to be early events after bleomycin injury.

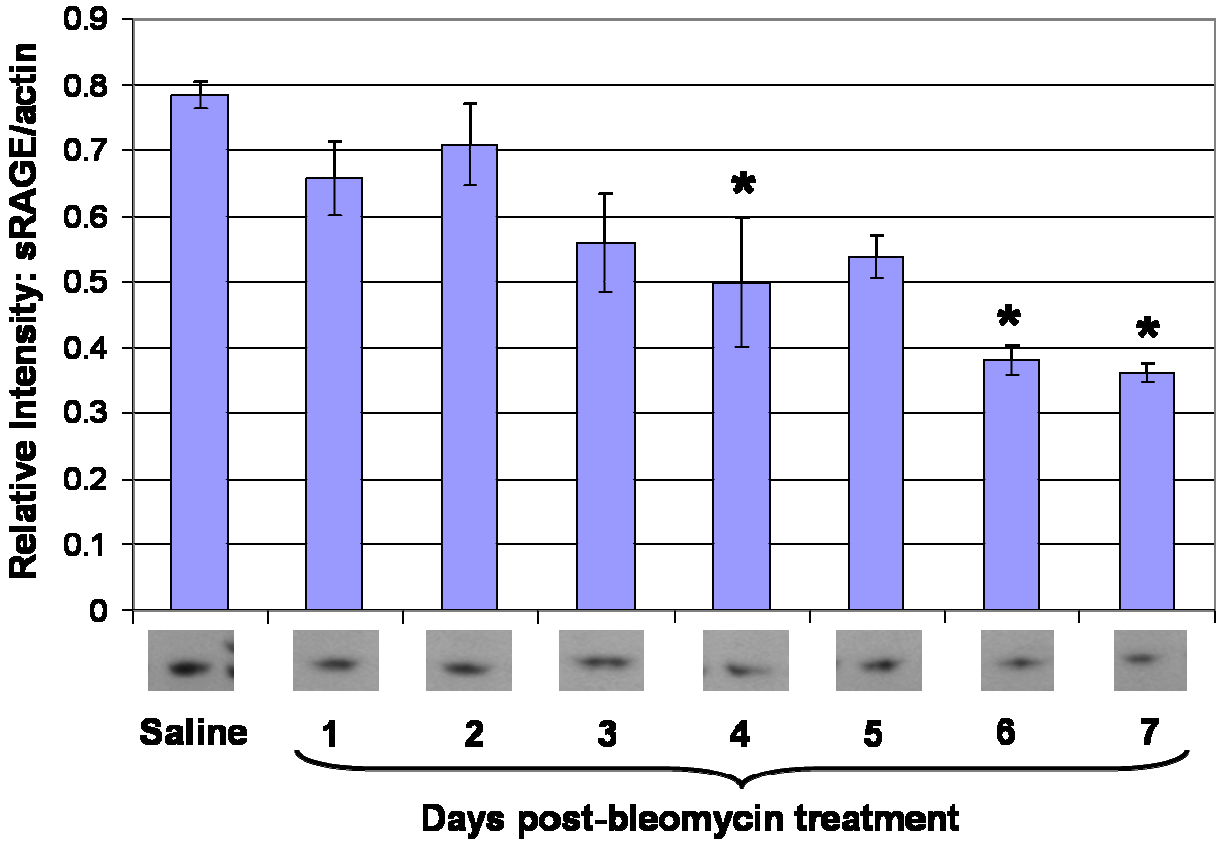

Figure 15. Seven-day bleomycin timecourse: depletion of sRAGE.

C57Bl/6 mice were treated with bleomycin on day 0, then sacrificed after the number of days indicated below the graph. Soluble protein fractions were isolated from lungs and analyzed by western blot for sRAGE. The PVDF membrane was stripped and re-probed for β-actin. Densitometry was performed and each lane's sRAGE density was normalized to its actin density. Averaged normalized sRAGE density is plotted for each timepoint. n=3 for each timepoint, and directly below the graph is one representative lane. *$p<0.05$

We also examined sRAGE expression at a later timepoint, 14 days. At this timepoint, there is no significant difference between saline- and bleomycin-treated mouse lungs in terms of

sRAGE protein expression (Figure 16), indicating a partial recovery from severe sRAGE depletion seen at 7 days post-bleomycin treatment (Figure 14).

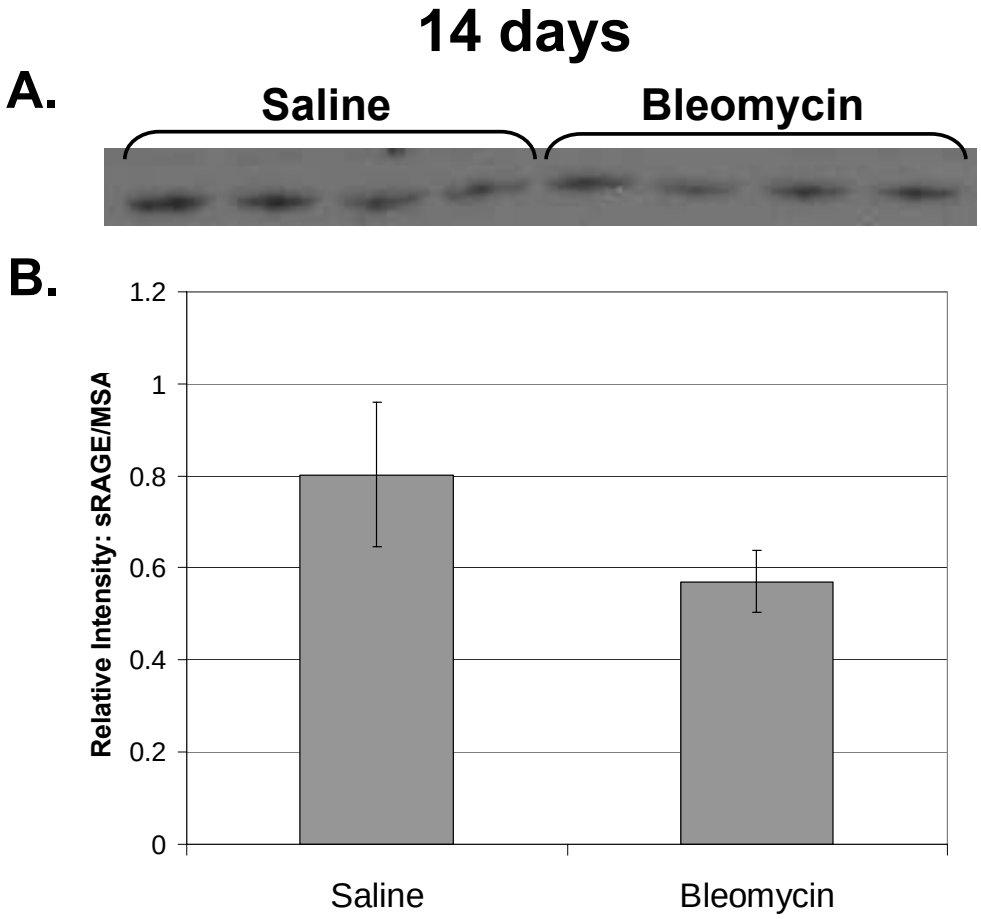

Figure 16. Partial recovery from sRAGE depletion 14 days after bleomycin injury.

Mice were treated with bleomycin or saline, and 14 days later were sacrificed. Soluble protein fractions were prepared from lungs and subjected to western blot analysis probing for sRAGE (A). The PVDF membrane was stripped and re-probed for MSA as a loading control. Densitometry was performed to quantify changes in sRAGE expression normalized to mouse serum albumin band intensities (B). p=0.24

To determine if reduction of RAGE and sRAGE at seven days post-bleomycin treatment can be explained by a decrease in RAGE mRNA, quantitative RT-PCR was performed on RNA from lungs of mice sacrificed seven days after bleomycin treatment (Figure 17). Quantitative RT-PCR analysis indicates that there is a trend of fewer RAGE transcripts seven days after

bleomycin treatment compared to saline controls, although the difference is not statistically significant. Because the 7-day timepoint is the one at which RAGE and sRAGE expression are lowest, it appears that RAGE transcript levels cannot account completely for decreased protein expression.

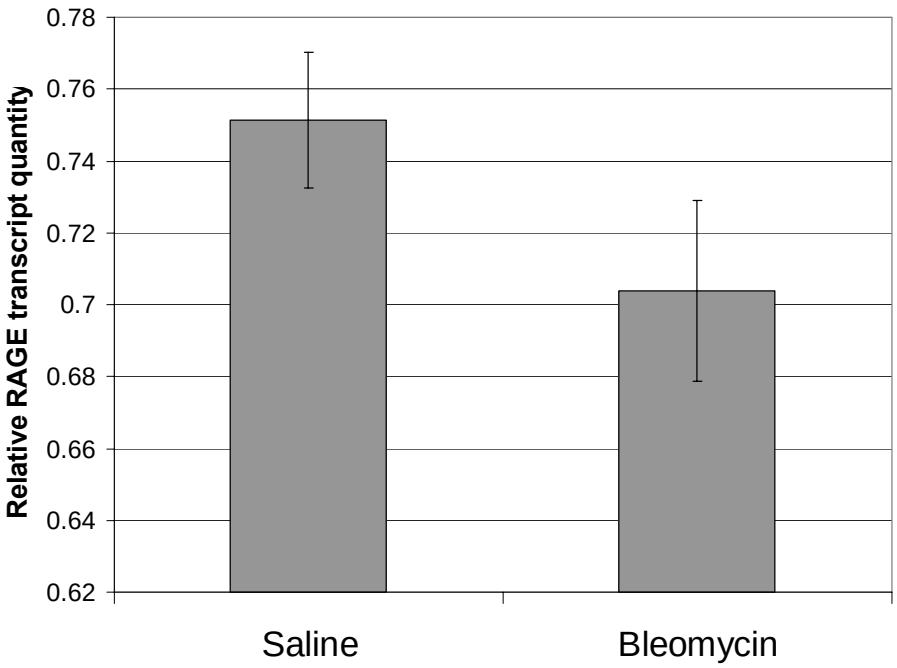

Figure 17. Trend for lower RAGE transcripts seven days after bleomycin injury.

Mice were treated with bleomycin or an equivalent volume of saline, and were sacrificed seven days later. Total RNA was isolated from lungs, and subjected to quantitative RT-PCR to quantify relative amounts of RAGE mRNA. Housekeeping reactions (G6PDH) were run in parallel for normalization of RAGE transcript crossing points. Plotted here is the *inverse* of the normalized RAGE crossing point to directly reflect the relative RAGE transcript quantity. The crossing point is the cycle number at which the RT-PCR product enters log phase amplification. p=0.20, n=3 for each treatment group.

6.2. RAGE AND sRAGE EXPRESSION IN ASBESTOS-INDUCED PULMONARY FIBROSIS

To determine if the changes seen in RAGE and sRAGE expression are specific to bleomycin-induced injury or are also generated in other injuries leading to pulmonary fibrosis, we utilized the asbestos-induced model of pulmonary fibrosis. This model is initiated by intratracheal instillation of asbestos. Injury after intratracheal asbestos exposure (0.1 mg crocidolyte asbestos) is evident by 24 hours post-treatment [194]. At this timepoint, there is a significant leukocyte infiltrate in the airspaces, predominantly composed of neutrophils, as well as some interstitial thickening. By 28 days post-exposure to asbestos, interstitial fibrosis is prominent, focused in areas where asbestos fibers have become visibly immobilized in the tissue (Fattman CL, *et al.*, Manuscript in preparation). In addition, there is still an active inflammatory response, indicated by the presence of elevated neutrophils in the airspaces. In the asbestos mouse model of pulmonary fibrosis, the negative control used is titanium dioxide, TiO_2, an inert particulate control [195]. It is also instilled intratracheally and ensures that any affects observed after asbestos treatment are not a response to particulate material in general.

To investigate the regulation of RAGE and sRAGE in the response to asbestos treatment, C57Bl/6 mice were treated with 0.1 mg crocidolyte asbestos (>10 μm in length) or TiO_2 and sacrificed 24 hours later. Soluble and membrane fractions were prepared from lungs and used to evaluate sRAGE (Figure 18) and RAGE (Figure 19) expression, respectively, by western blot analysis. These data show that in the early stages of asbestos injury, expression of both RAGE and sRAGE is significantly reduced.

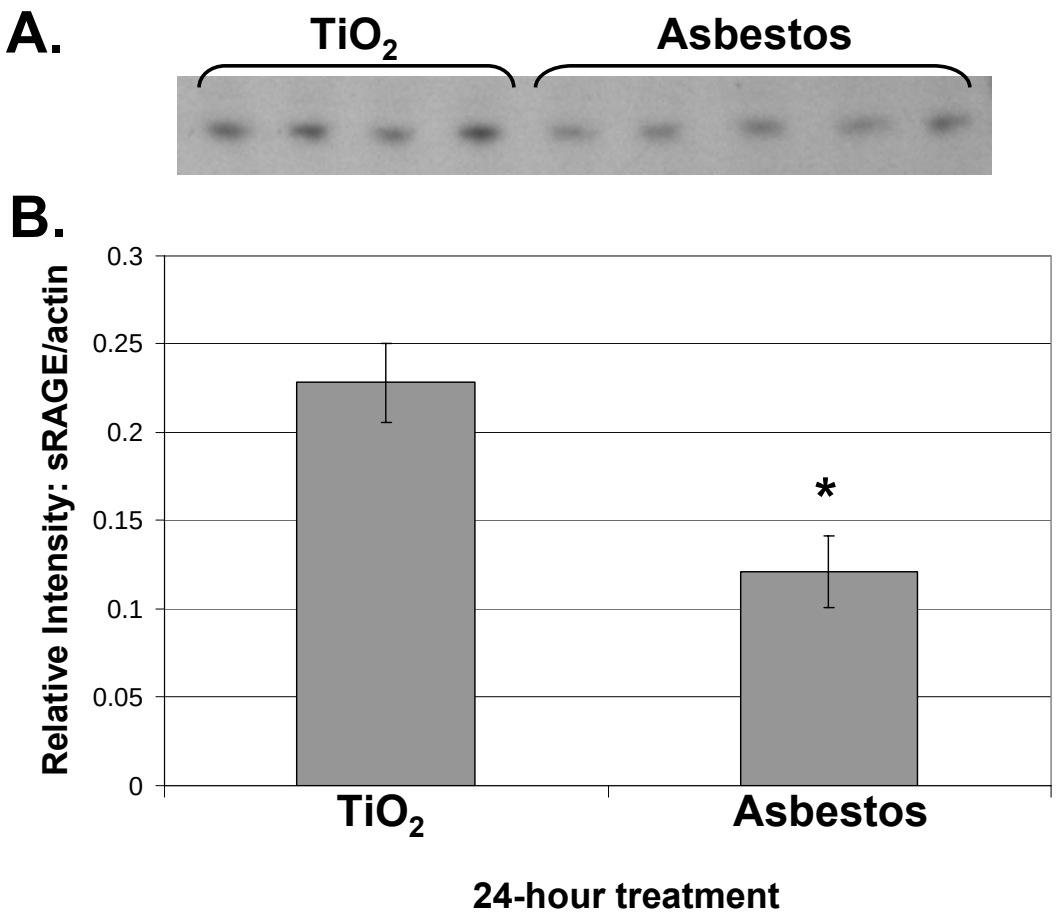

Figure 18. Downregulation of sRAGE 24 hours after asbestos exposure.

(A) C57Bl/6 mice received 0.1 mg crocidolyte asbestos (>10 μm in length) or TiO_2 by intratracheal instillation. Twenty-four hours later mice were sacrificed and soluble protein fractions were isolated from lungs and analyzed by western blot for sRAGE expression. PVDF membranes were stripped and re-probed for actin as a loading control. (B) Density of sRAGE bands, normalized to actin bands, is plotted. *$p<0.05$

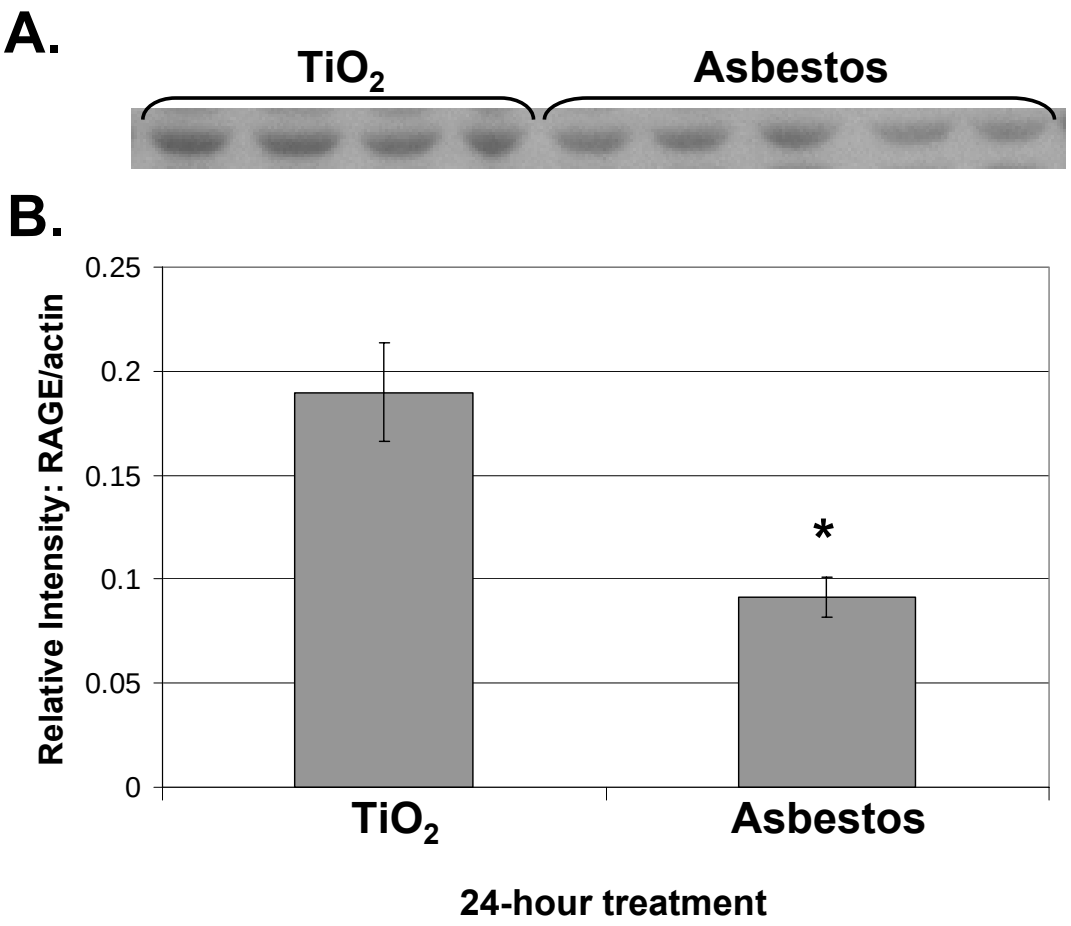

Figure 19. Downregulation of RAGE 24 hours after asbestos exposure.

(A) C57Bl/6 mice received 0.1 mg crocidolyte asbestos (>10 μm in length) or TiO_2 by intratracheal instillation. Twenty-four hours later mice were sacrificed and membrane protein fractions were isolated from lungs and analyzed by western blot for RAGE expression. PVDF membranes were stripped and re-probed for actin as a loading control. (B) Density of RAGE bands, normalized to actin bands, is plotted. *$p<0.05$

RAGE and sRAGE expression were also analyzed at a later timepoint, after significant fibrosis is established (28 days post-exposure). Mice were treated as described above and lungs were harvested 28 days later and used to prepare soluble and membrane protein fractions. As Figure 20 and Figure 21 show, RAGE and sRAGE expression is significantly downregulated in the later fibrotic stages of asbestos injury.

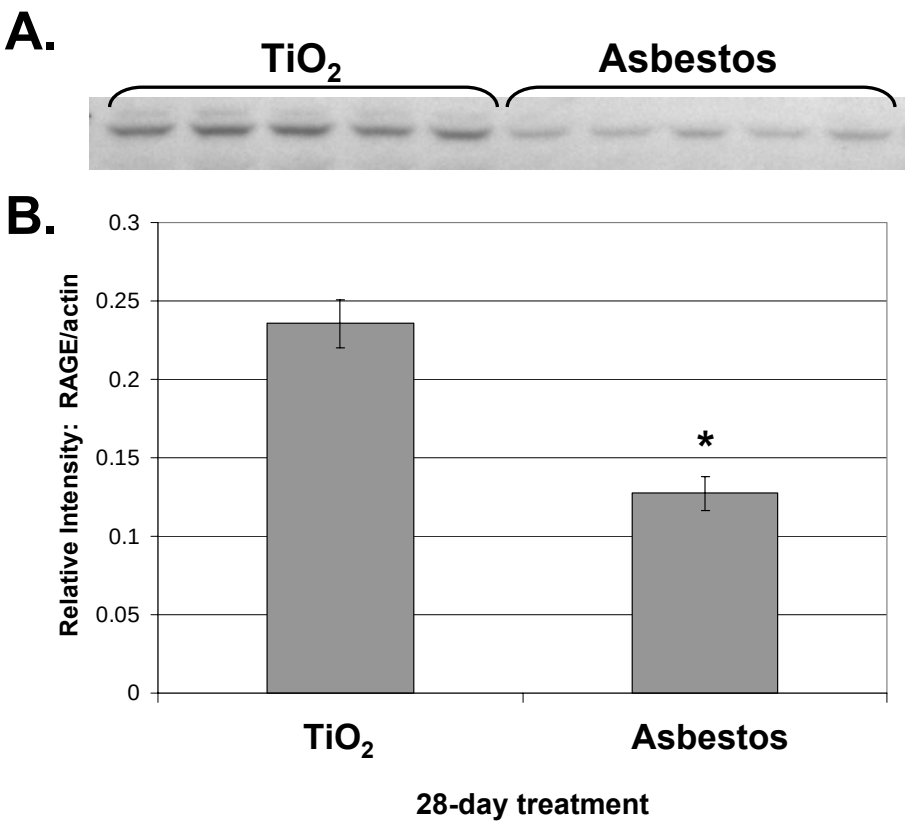

Figure 20. RAGE is downregulated 28 days after asbestos exposure.

(A) C57Bl/6 mice received 0.1 mg crocidolyte asbestos (>10 μm in length) or TiO_2 by intratracheal instillation. Twenty-eight days later mice were sacrificed and membrane protein fractions were isolated from lungs and analyzed by western blot for RAGE expression. PVDF membranes were stripped and re-probed for actin as a loading control. (B) Density of RAGE bands, normalized to actin bands, is plotted. *$p<0.05$

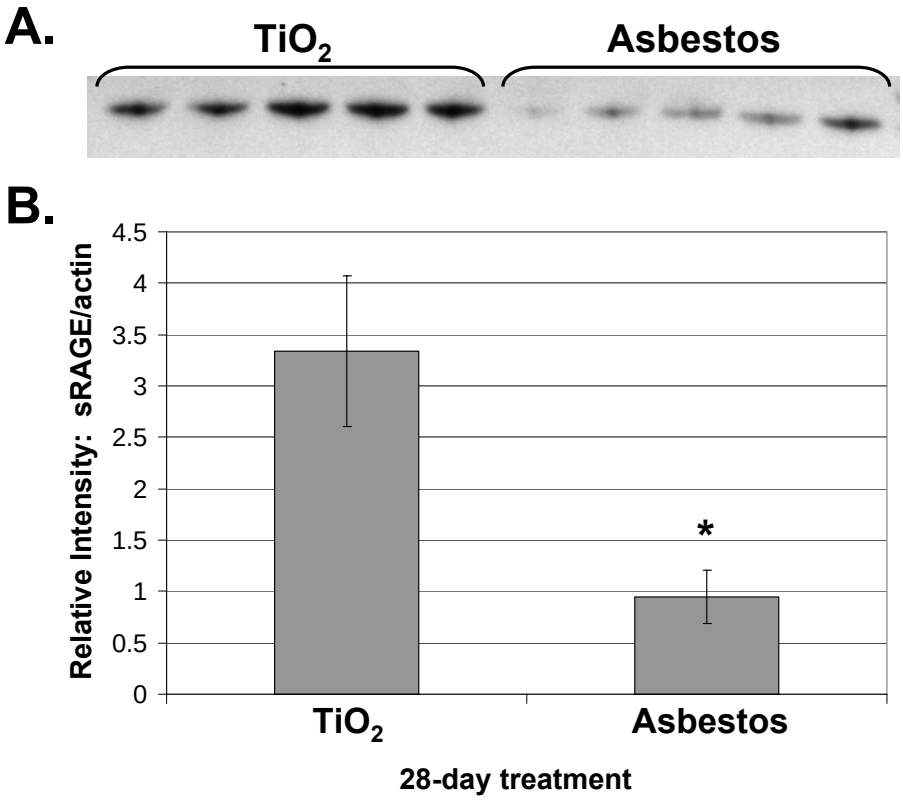

Figure 21. sRAGE is downregulated 28 days after asbestos exposure.

(A) C57Bl/6 mice received 0.1 mg crocidolyte asbestos (>10 μm in length) or TiO_2 by intratracheal instillation. Twenty-eight days later mice were sacrificed and soluble protein fractions were isolated from lungs and analyzed by western blot for sRAGE expression. PVDF membranes were stripped and re-probed for actin as a loading control. (B) Density of sRAGE bands, normalized to actin bands, is plotted. *$p<0.05$

6.3. RAGE AND sRAGE EXPRESSION IN IDIOPATHIC PULMONARY FIBROSIS

A critical test for any study focused on an animal model of a human disease is to see if observations made in the animal model extend to the human disease itself. Thus, it was important to determine if RAGE and sRAGE are reduced in human IPF as well as in both of these mouse models.

Human IPF tissues were obtained from the University of Pittsburgh Department of Pathology Tissue Bank and used for microarray analysis. In collaboration with the laboratory of

Dr. Naftali Kaminski, we found that RAGE transcripts are downregulated 4.65-fold in IPF lungs compared to normal lungs (Figure 22), leading it to be one of the most downregulated genes in patients with IPF.

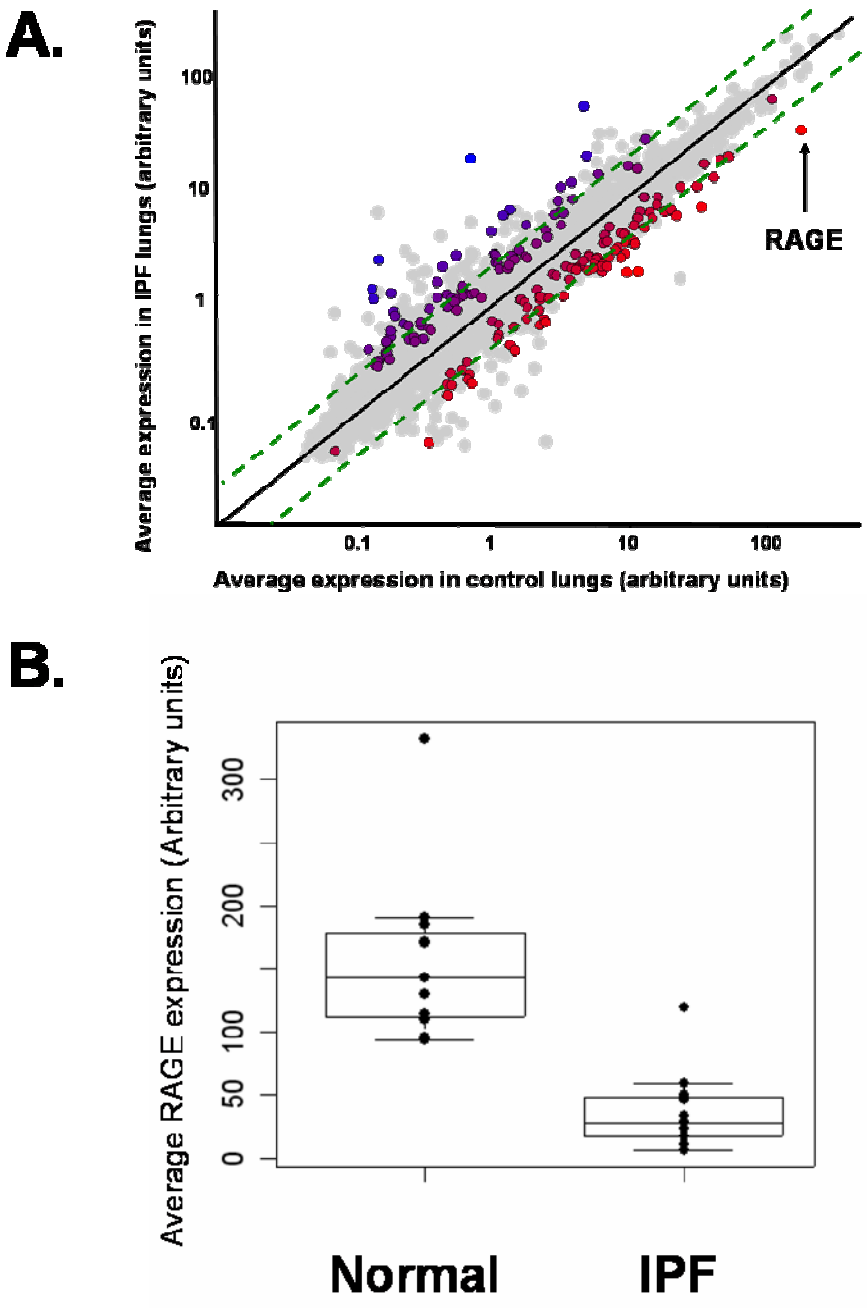

Figure 22. IPF microarray data: downregulation of RAGE transcripts.

(Figure 22, cont.) Lung tissues obtained from the tissue bank of the Department of Pathology at the University of Pittsburgh from either IPF patients or normal areas from lung cancer specimens ("Normal") were used for microarray analysis in collaboration with the laboratory of Dr. Naftali Kaminski. (A) Log scale scatter plot of the average intensity of all of the genes on the microarrays, where each dot represents a single gene and is plotted by its expression in normals (*x*-axis) by its expression in IPF lungs (*y*-axis). Points in gray represent genes whose differences did not reach significance. The oblique solid line indicates the line of equality, while each green dashed line indicates a two-fold change. RAGE was downregulated 4.65 fold (t-test, p=0.00000146; TNoM, p= 0.00000192). (B) Plot of RAGE transcripts in which each point represents an individual lung specimen.

To verify the microarray data, RAGE protein levels were examined by western blot analysis. Another set of human tissues was obtained from the tissue bank of the University of Pittsburgh Department of Pathology. Membrane and soluble protein fractions were prepared and analyzed by western blotting for RAGE and sRAGE, respectively. Figure 23 and Figure 24 show that RAGE and sRAGE protein expression is greatly reduced in the lungs from IPF patients, corroborating the microarray data and supporting the significance of our findings in the bleomycin and asbestos mouse models. These data further suggest the importance of RAGE (and sRAGE) in pulmonary fibrosis.

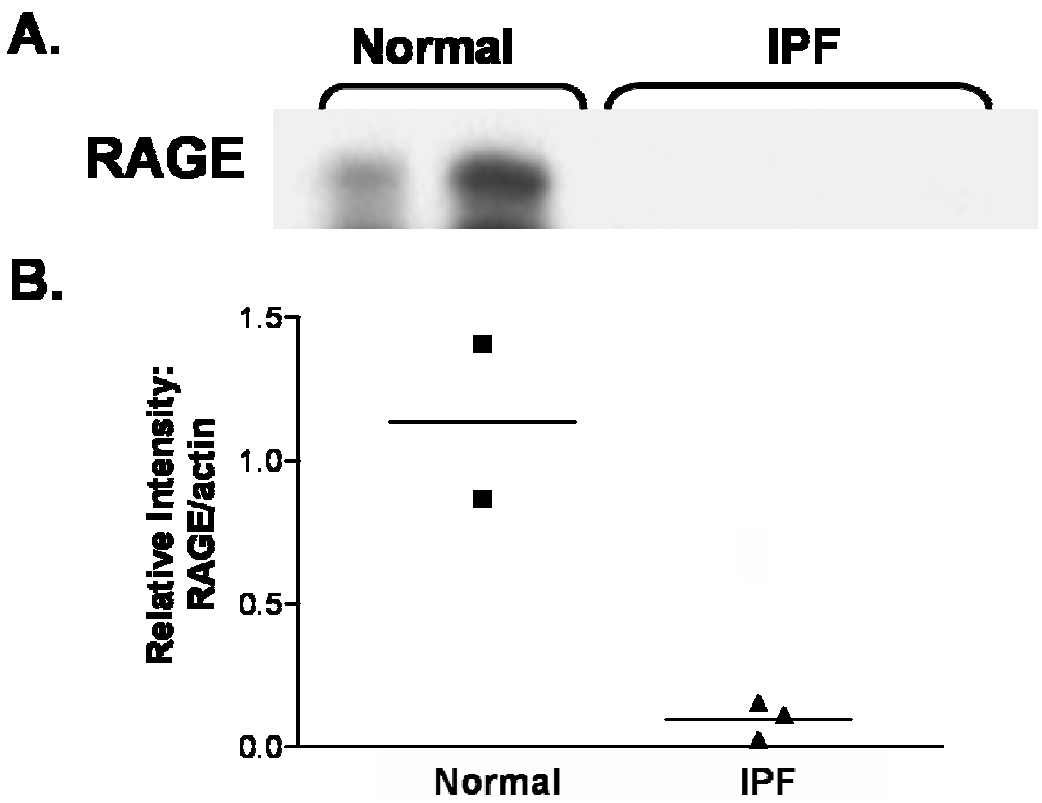

Figure 23. RAGE protein expression is reduced in IPF lungs.

Normal and IPF lung tissues were obtained from the University of Pittsburgh Department of Pathology tissue bank. (A) Membrane fractions were prepared from tissues and subjected to western blot analysis probing for RAGE. PVDF membranes were then stripped and re-probed for actin as a loading control. (B) RAGE band intensities normalized to actin band intensities are plotted, where each point represents one individual sample and the horizontal bars represent the means. $p<0.02$

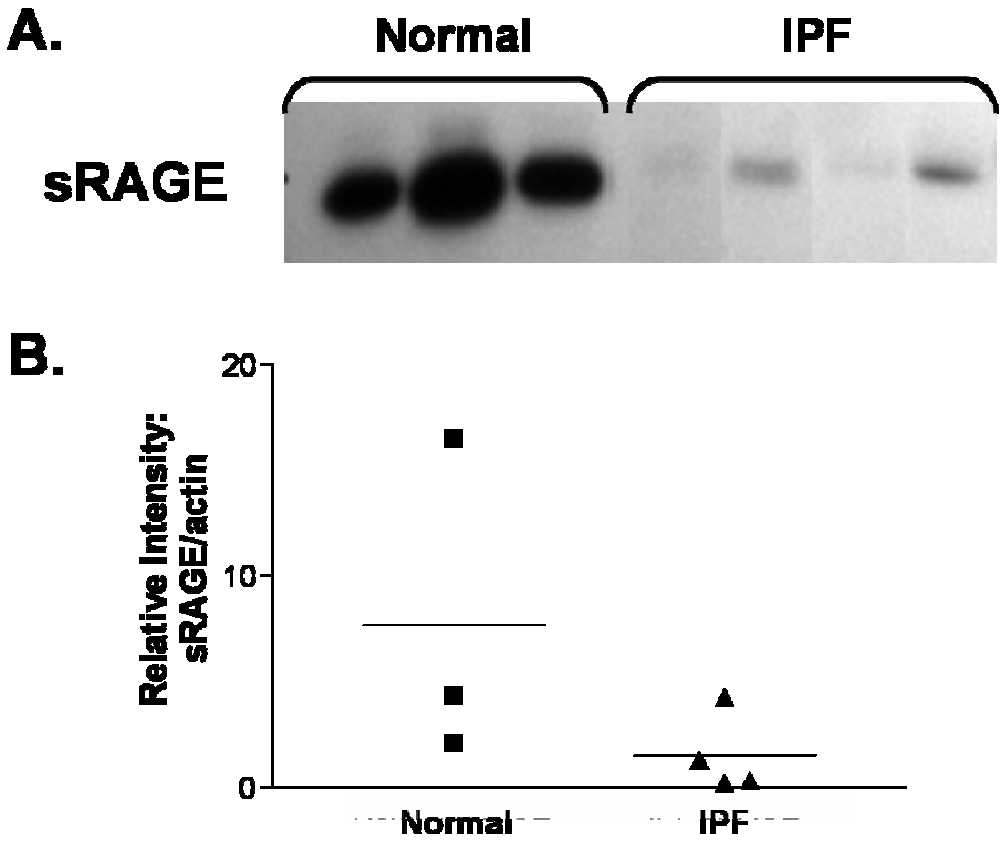

Figure 24. sRAGE protein expression is reduced in IPF lungs.

Normal and IPF lung tissues were obtained from the University of Pittsburgh Department of Pathology tissue bank. (A) Soluble fractions were prepared from tissues and subjected to western blot analysis probing for sRAGE. PVDF membranes were then stripped and re-probed for actin as a loading control. (B) sRAGE band intensities normalized to actin band intensities are plotted, where each point represents one individual sample and the horizontal bars represent the means.

6.4. ABSENCE OF RAGE EXPRESSION PROMOTES A FIBROTIC PHENOTYPE IN THE LUNG

Data shown above suggest that loss of RAGE and/or sRAGE may be a key step in the pathogenesis of pulmonary fibrosis. If this is true, then *the absence of RAGE should predispose an individual to pulmonary fibrosis*. RAGE-/- animals can help to address this question.

RAGE-/- mice have been generated by the laboratory of Dr. Bernd Arnold [189] (German Cancer Research Center, Heidelberg, Germany) using a Cre/*loxP* system that utilizes a Cre deleter transgene [196] to express Cre recombinase ubiquitously, and thus disrupt the RAGE gene ubiquitously. Studies done in collaboration with Dr. Angelika Bierhaus (University of Heidelberg, Germany) and Dr. Michael Kasper (Technical University of Dresden, Germany) have indicated that, as these RAGE-/- mice age, their lungs develop a phenotype with characteristics of pulmonary fibrosis.

As shown in Figure 25, by the age of 24 months, untreated RAGE-/- mouse lungs show an increase in staining in several molecules that have been reported to be upregulated in pulmonary fibrosis. TNF-α (Figure 25C and D) is a pro-inflammatory cytokine that is commonly implicated in the pathogenesis of pulmonary fibrosis, while collagen type I (Figure 25 E and F) is the principle ECM component that is excessively deposited in the interstitium in pulmonary fibrosis. RAGE-/- mouse lungs also contain areas that stain highly for α-smooth muscle actin (α-SMA) (a marker for myofibroblasts, Figure 25I), reminiscent of fibroblastic foci. Galectin-3 (Figure 25G and H) is another protein found to be upregulated in RAGE-/- mouse lungs, and it has been reported to be upregulated in a radiation-induced model of pulmonary fibrosis [197], although the role that galectin-3 plays in PF pathogenesis is incompletely defined. In addition, RAGE-/- mouse lungs demonstrated an increase in Ki67 staining (a marker of cellular proliferation found to be upregulated in alveolar epithelial cells and cells in fibroblastic foci [198]) and TUNEL staining (indicating DNA strand breaks associated with apoptosis) compared to wild-type mice (not shown). Overall, these data demonstrate that RAGE-/- mice are predisposed to a pulmonary fibrotic phenotype in the absence of any profibrotic injury or treatment.

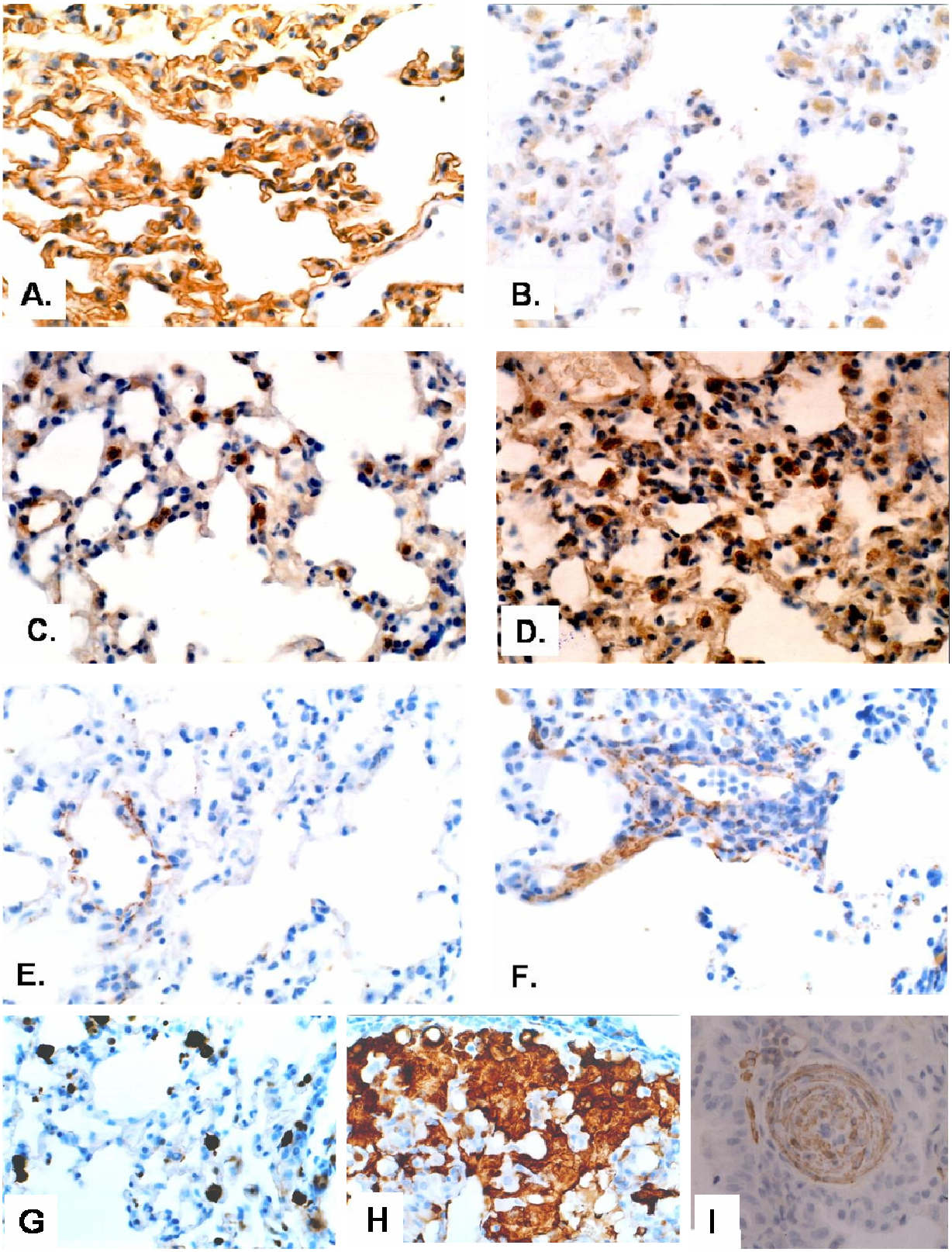

Figure 25. Immunohistochemical studies of RAGE-/- pulmonary phenotype.

(Figure 25, cont.) RAGE-/- mice (B, D, F, H, and I) or RAGE+/+ mice (A, C, E, and G) (19-24 months in age) were sacrificed and lungs were fixed and embedded in paraffin. Five micron sections were cut and stained for RAGE (A and B), TNF-α (C and D), collagen type I (E and F), galectin-3 (G and H),or α-SMA (M).

6.5. CONCLUSIONS

Under normal conditions, RAGE transcripts and protein have been shown to be highly expressed in the lung of humans, rats and mice [64, 76] (Figure 2 and Figure 3). These findings suggest that RAGE and sRAGE have a role in pulmonary homeostasis, and conversely, loss or reduction in these proteins may have a pathogenic effect in the lung. We originally hypothesized that during pulmonary fibrosis pathogenesis, RAGE (and sRAGE) regulation would be altered. To test this, we examined their expression in two models of pulmonary fibrosis.

We found significant reductions in RAGE and sRAGE protein levels in lungs in both the bleomycin- and asbestos-induced models of pulmonary fibrosis. In the asbestos model, reductions in both RAGE and sRAGE were significant by 24 hours post-exposure. In the bleomycin model, while RAGE reduction was significant by one day after treatment, the time for significant sRAGE protein reduction lagged. However, there was a trend of decreased sRAGE apparent by one day after treatment. These data indicate that RAGE and sRAGE loss are early events in the pathogenesis of PF in these animal models.

We also examined later timepoints. In the bleomycin model, we looked at the timepoint of seven days after injury and found that RAGE and sRAGE levels are still significantly reduced. At this timepoint is the transition from the inflammatory phase to the fibrotic phase in this model. This indicates that as the fibrotic phase begins to predominate, there is a depletion of RAGE and sRAGE in the lungs. However, this depletion cannot be completely explained by a reduction in RAGE transcripts because at this timepoint there is not a significant difference

between RAGE transcripts in the bleomycin-treated group and controls (although there was a trend). Post-transcriptional mechanisms are apparently contributing to the loss of RAGE isoforms. Interestingly, sRAGE levels appear to be approaching recovery later in the course of bleomycin injury, as there is no longer a significant difference between bleomycin-treated and control lungs 14 days after treatment. It is possible that the lack of significant difference between RAGE transcript levels at seven days post-treatment is foreshadowing the partial recovery of sRAGE protein seen at 14 days.

At the late timepoint in the asbestos model, 28 days post-exposure, both RAGE and sRAGE continue to be significantly reduced in the lungs. This is in contrast to the bleomycin model, in which sRAGE levels are no longer different between bleomycin-treated and control mice 14 days after treatment. Longer exposure times are needed for this model to determine if there is a recovery in RAGE and sRAGE levels at a later timepoint in this model.

It was important to validate our results in the animal models by examining IPF samples. In collaboration with Dr. Naftali Kaminski, we found that RAGE/sRAGE transcripts are significantly decreased in IPF lungs compared to normal lung tissue. In fact, it was one of the most-reduced transcripts in IPF lungs. In addition, we determined that RAGE and sRAGE protein levels are reduced in IPF lungs. Some of the IPF lung tissues used were derived from individuals who were undergoing lung transplantation, indicating that these tissues represented end-stage diesease. These data, combined with data from the animal models, suggest that RAGE and sRAGE are downregulated early in IPF pathogenesis, and this decrease is sustained through the course of the disease.

RAGE-/- mice further support the importance of a loss of RAGE or sRAGE for the pathogenesis of pulmonary fibrosis. These mice, when left untreated, develop characteristics of

pulmonary fibrosis. These characteristics include increased collagen type I deposition and foci that stain intensely for α-SMA. These findings suggest that lack of RAGE and sRAGE predispose mice to the development of pulmonary fibrisis and support our proposal that regulation of RAGE expression is a key aspect of pulmonary fibrosis pathogenesis.

7. INSIGHTS INTO THE ROLE OF RAGE LOSS IN PULMONARY FIBROSIS

7.1. MECHANISM OF THE LOSS OF RAGE

The cell type in the lung that appears to be principally responsible for RAGE expression is the AE-I cell [67]. As discussed in the Introduction, the AE-I cell type is one of the early targets of injury leading to pulmonary fibrosis [20, 22]. After these cells die, AE-II cells migrate and proliferate in attempt to cover the denuded basement membrane [20]. However, it has been determined by one study that AE-II cells do not express RAGE [67]. Thus, it is possible that loss of RAGE expression in the lung is primarily due to death of the major RAGE-expressing cell type, AE-I cells.

Another possibility is that the source of pulmonary injury, which comes into contact first with AE-I cells when inhaled or intratracheally instilled, directly downregulates RAGE expression by AE-I cells, independent of cell death. To test this, a human pulmonary epithelial cell line, A549 cells, were treated with asbestos or TiO_2, and their expression of RAGE was analyzed. Figure 26 shows that in response to 24 hours of asbestos treatment, A549 cells downregulate RAGE expression (sRAGE could not be detected in cell culture media). It is important to note that this result has not been completely consistent, so it is likely that if this mechanism is a component of RAGE loss, it is in addition to RAGE loss caused by AE-I cell death.

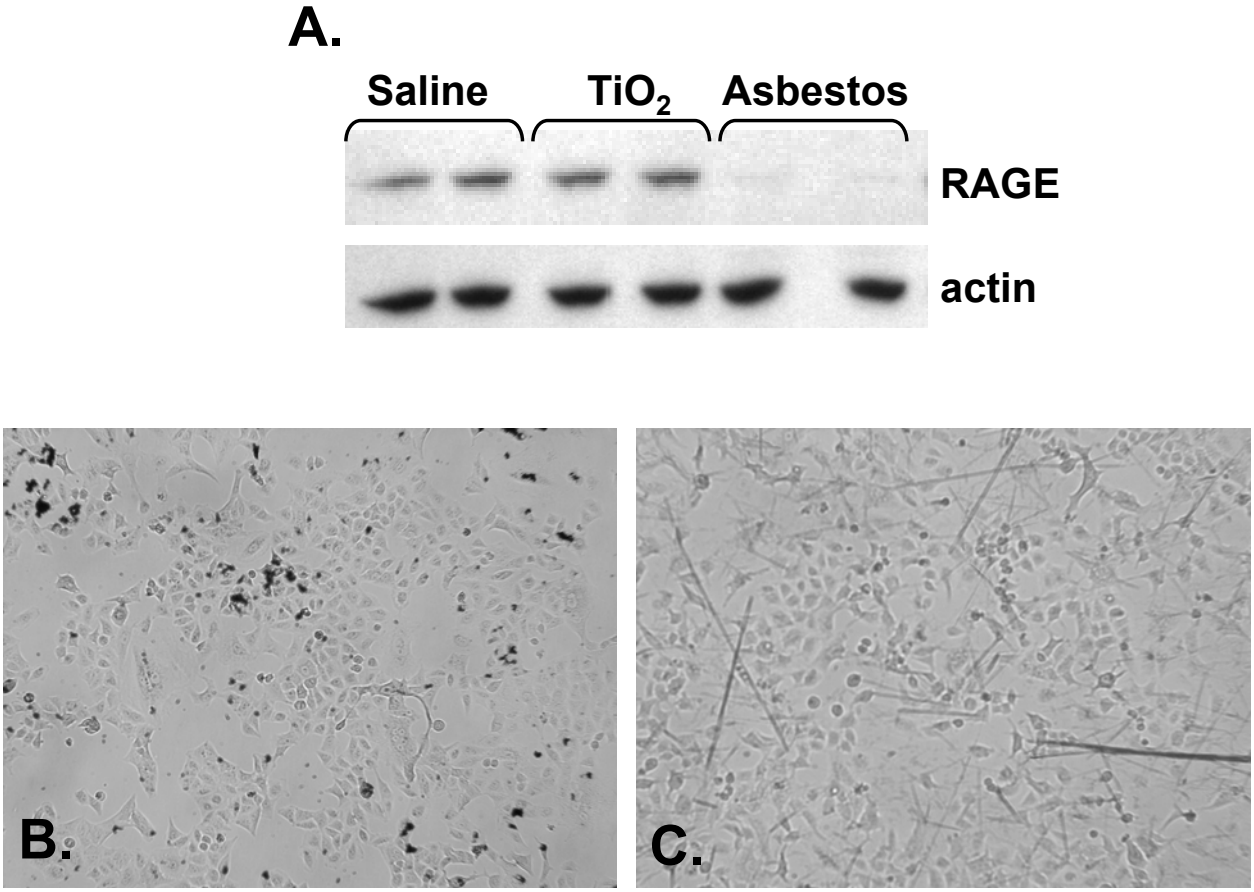

Figure 26. Asbestos treatment induces RAGE downregulation in A549 cells.

(A) Human pulmonary epithelial cell line A549 was treated with saline, TiO_2, or crocidolyte asbestos (5μg/cm^2) for 24 hours. Cells were harvested to recover whole cell lysates that were then subjected to western blot analysis probing for RAGE. The PVDF membrane was then stripped and re-probed for actin as a loading control. Photographs are shown of (B) TiO_2 treated cells and (C) crocidolyte astestos treated cells (40X magnification).

7.2. RELEASE OF HMGB1 BY STIMULATED MACROPHAGES

One potential problem with RAGE downregulation is that its ligands may bind other, perhaps more pathogenic, mediators. It is possible that one of the purposes that RAGE serves in the lung is to prevent its ligands from binding other proteins. To determine if pro-fibrotic stimuli can cause the accumulation of RAGE ligands, we used a murine pulmonary macrophage cell line,

MH-S. MH-S cells were treated with bleomycin or asbestos or relevant controls for 24 hours, following which the conditioned media were probed for HMGB1. Figure 27A demonstrates that following 24 hours of bleomycin or asbestos treatment, macrophages release HMGB1 into the medium. Macrophages can actively secrete HMGB1, but also necrotic cells passively release HMGB1 [103]. As Figure 27B-E show, massive cell death is not grossly apparent with either treatment, although apoptosis is evident in both, especially after bleomycin treatment. Notably, apoptotic cells do not release HMGB1 [103].

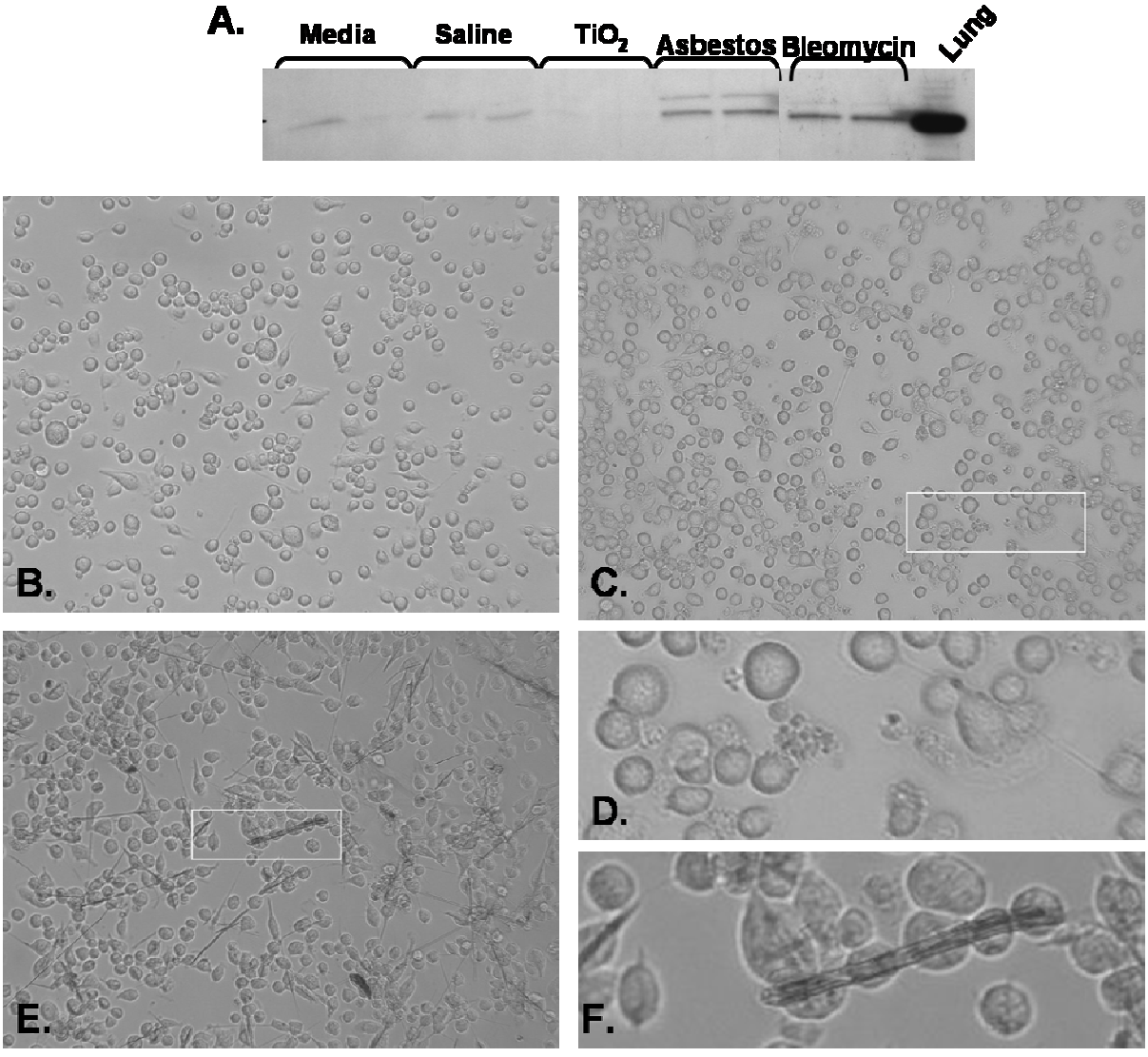

Figure 27. Release of HMGB1 by macrophages stimulated with asbestos or bleomycin.

(Figure 27, cont.) A murine pulmonary macrophage cell line was treated for 24 hours with 5.0 mU bleomycin, 5 μg/cm^2 asbestos, 5 μg/cm^2 TiO_2, or an equivalent volume of 0.9% saline or medium alone. Medium was collected from each well and equal volumes were subjected to western blot analysis, probing for HMGB1 release (A). Photographs (40X magnification) were taken prior to cell harvesting of (B) saline-treated, (C) bleomycin-treated, or (E) asbestos-treated cells. (D) Higher magnification of boxed area in *C* to show cells apparently undergoing apoptosis. (F) Higher magnification of boxed area in *E* to illustrate macrophages lined up along a thick bundle of asbestos fibers, and one cell that has ingested an entire short fiber (lower left).

7.3. AGE-TREATED FIBROBLASTS DOWNREGULATE α-SMA EXPRESSION

To determine the effect of RAGE ligands on pulmonary fibroblasts, a cell type that undergoes intense proliferation during pulmonary fibrosis pathogenesis, we used two human pulmonary fibroblast cell lines: LL-47 was derived from a normal human lung, and LL-29 was derived from an IPF lung (both cell lines were obtained from the American Type Culture Collection). Bovine serum albumin (BSA) was used to prepare AGEs (AGE-BSA) as described in Section 3.4.4. AGEs have a characteristic brown color, and AGE-BSA demonstrates decreased mobility in SDS-PAGE compared to nonglycated BSA (Figure 28). AGEs were chosen as the RAGE ligand for these experiments because large amounts can be produced inexpensively, and increased AGEs have been reported in pulmonary fibrosis [174]. In addition, studies in rat renal cells revealed that AGEs can induce epithelial to myofibroblast transdifferentiation that is RAGE-dependent [125]. Our objective was to determine if AGEs have an effect on pulmonary myofibroblast differentiation from fibroblasts.

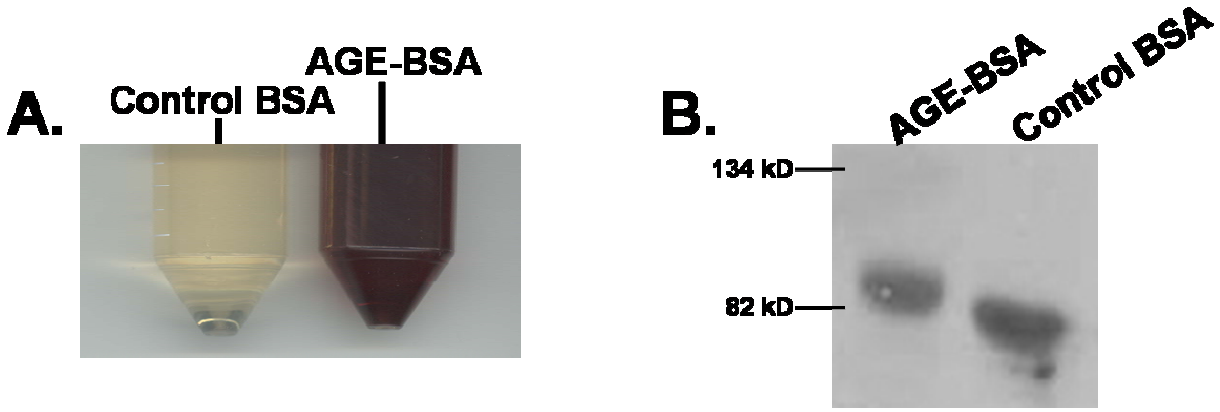

Figure 28. AGE-modified BSA preparation.

Bovine serum albumin (BSA) was modified by incubation with glucose or ribose to form advanced glycation end products (AGE-BSA). (A) Photograph of 50 mL conical tubes at the end of a 4-week incubation of BSA with ribose at 37°C, demonstrating the characteristic brown color of AGEs. Control BSA underwent the same incubation conditions, except that ribose was omitted from the tube. (B) AGE-BSA prepared by BSA incubation with glucose (or without glucose, Control BSA) for 10 weeks at 37°C was subjected to SDS-PAGE and western blot analysis probing for albumin. Covalent sugar modifications on AGE-BSA cause it to have slower mobility.

Pulmonary fibroblast cells were treated with AGE-BSA for six days, with replacement of medium every two days, and whole cell lysates were prepared and analyzed for α-SMA expression. Alpha-smooth muscle actin (α-SMA) is a marker for myofibroblasts, the cell type responsible for the majority of the collagen production and deposition in IPF [29]. Figure 29 demonstrates that AGE-BSA treatment of either pulmonary fibroblast cell line causes a decrease in α-SMA expression, reflecting a decrease in myofibroblast differentiation from these fibroblasts. This is not a perfect model because normal fibroblasts would not express α-SMA, yet these cell lines do show a basal level of α-SMA expression. Despite this problem, it is noteworthy that AGEs, a type of RAGE ligand, can cause downregulation of this myofibroblast marker.

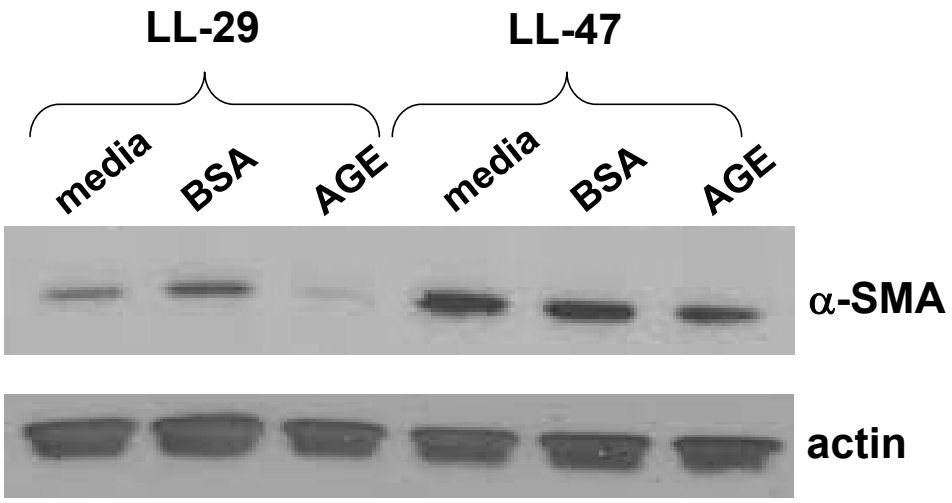

Figure 29. Downregulation of α-SMA by AGE-treated fibroblasts.

Two human pulmonary fibroblast cell lines were treated with AGE-BSA, control BSA or media alone for six days, with fresh media replacement every two days. Whole cell lysates were subjected to western blot analysis for α-SMA. The PVDF membrane was stripped and re-probed for actin as a loading control.

To be sure that this effect of AGE-BSA on fibroblasts is not due to a defect in the cells' ability to upregulate α-SMA, these cells were treated with TGF-β, which in known to cause differentiation of fibroblasts into myofibroblasts [199, 200], marked by upregulation of α-SMA. Figure 30 shows that these cells are capable of upregulating α-SMA with the proper stimulus.

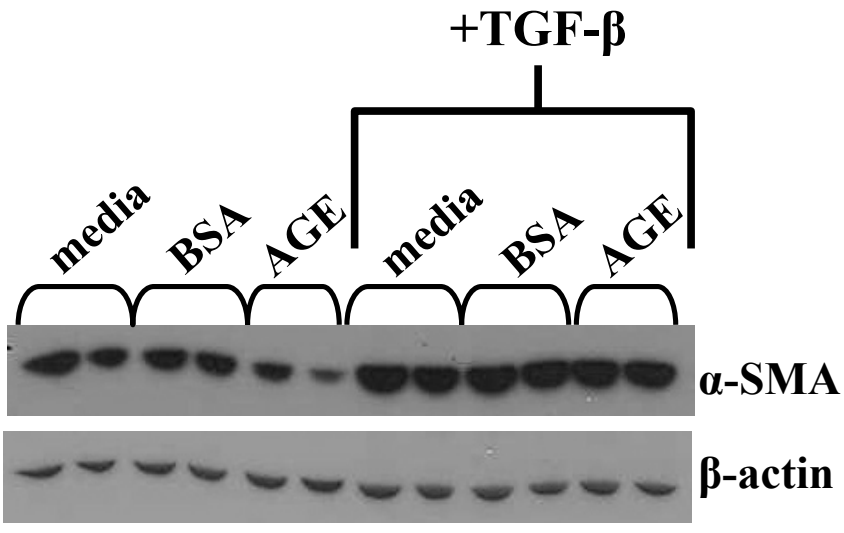

Figure 30. Fibroblast cell lines upregulate α-SMA with TGF-β treatment.

(Figure 30, cont.) LL-47 cells were treated for 6 days with 40 μM AGE-BSA, control BSA, or media alone in the presence or absence of 5 ng/ml TGF-β. Cell lysates were probed by western blot analysis for α-SMA (upper panel), and the PVDF membrane was stripped and re-probed for actin (lower panel) as a loading control. This cell line is thus able to upregulate α-SMA with the proper stimulus.

7.4. CONCLUSIONS

We have shown that RAGE and its soluble isoform, sRAGE, are downregulated promptly after injuries which lead to pulmonary fibrosis (Figure 13 and Figure 15), and that this downregulation appears to be sustained throughout the course of IPF pathogenesis (Figure 23 and Figure 24). To begin to describe possible causes and effects of this downregulation, we focused on cell culture approaches.

We found evidence that an alveolar epithelial cell line is capable of downregulating RAGE directly in response to crocidolyte asbestos fibers (Figure 26). However, we speculate that the major cause of RAGE downregulation during PF pathogenesis may be AE-I cell death. AE-I cells are described to be the cell type that contributes the most to overall RAGE expression in the lung [67], and these cells are also an early target for the injurious stimuli that lead to pulmonary fibrosis. Thus, death and removal of these cells likely accounts for a major component of RAGE loss in the lung during PF pathogenesis.

HMGB1 is a RAGE ligand that is expressed in the lung [74]. Its role as a cytokine in lung inflammation has been explored [105], but it has not been studied in the context of pulmonary fibrosis. HMGB1 can be actively released by activated inflammatory cells, and it can also be passively released from necrotic cells (but *not* apoptotic cells) [103]. To determine if exposure of macrophages to pro-fibrotic agents modulates HMGB1 release, we treated

macrophages with bleomycin and crodicolyte asbestos. We found that, in respose to either agent, release of HMGB1 by macrophages into the culture supernatant was increased (Figure 27). Although we cannot conclude at this point whether this release is active due to cellular activation, or passive due to possible necrosis, these results suggest that HMGB1 levels are increased in the lung during the pathogenesis of PF.

Notably, IPF pathogenesis is thought to have a significant oxidative component [170-172]. Because AGE formation is accelerated in oxidative environments, AGEs are likely to accumulate in the lung during IPF pathogenesis. Indeed, AGE immunoreactivity has been reported in IPF [174]. In addition, associations between having diabetes (in which AGE accumulation is well-documented) and the risk for developing IPF have been reported [175]. Thus, it is likely that at least two RAGE ligands are accumulating in IPF, but the levels of RAGE and sRAGE are significantly reduced.

Fibroblasts also express RAGE. Because these cells undergo intense proliferation during the pathogenesis of PF, and because there are potentially at least two RAGE ligands upregulated in pulmonary fibrosis (HMGB1, above; AGEs [174]) we wanted to determine the effect of RAGE ligands on these cells. We showed that when human pulmonary fibroblast cell lines are treated with AGEs, α-SMA is downregulated, suggesting a shift away from myofibroblast differentiation. These cell lines express RAGE, so we hypothesize that this effect is RAGE-mediated. If this is true, and if RAGE is also downregulated in fibroblasts during PF pathogenesis, then loss of RAGE may promote myofibroblast differentiation and the resultant deposition of excess ECM components, contractility of lung parenchyma and tissue remodeling (Figure 31).

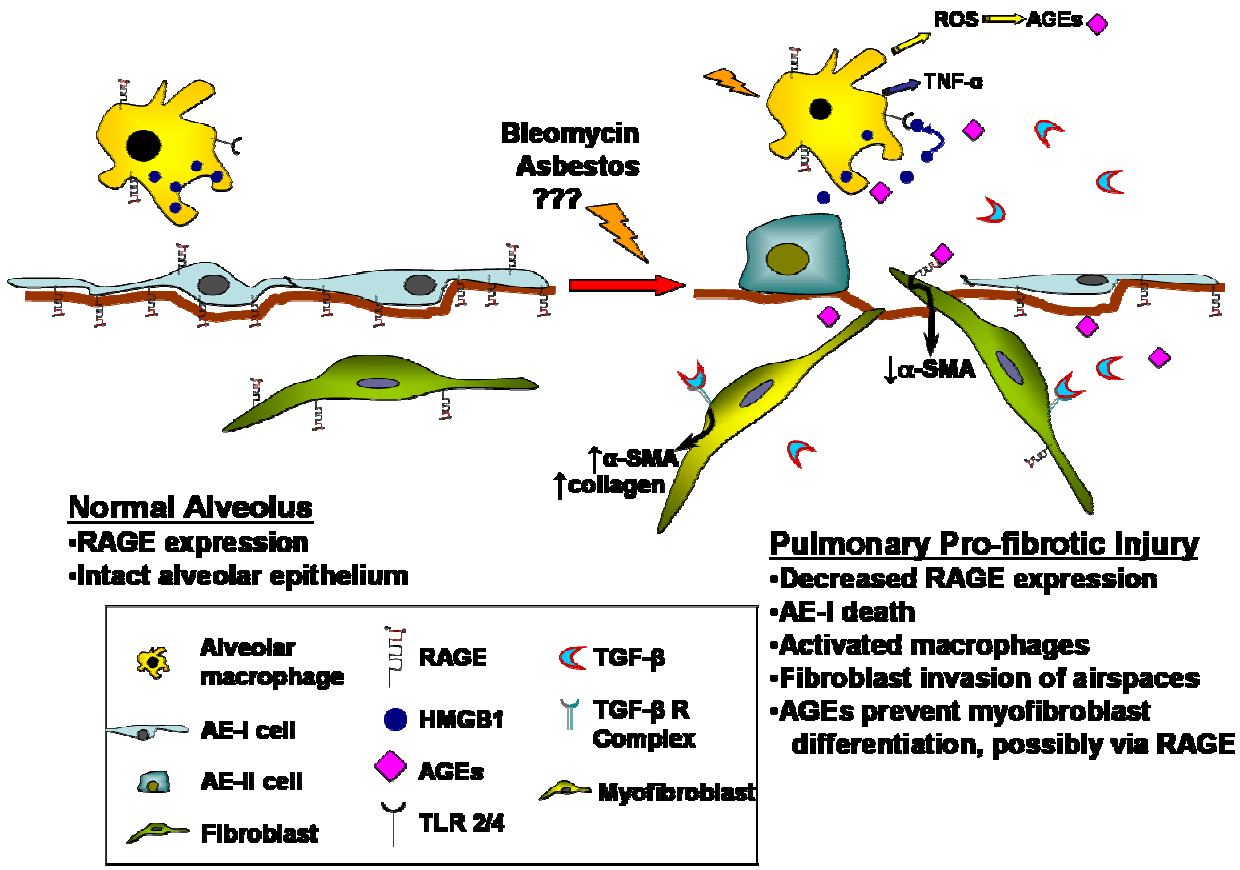

Figure 31. Hypothesis: Loss of RAGE and accumulation of its ligands in PF pathogenesis.

Pulmonary injury, such as that initiated by bleomycin or asbestos, leads to RAGE downregulation. This is likely to be at least partially due to death of AE-I cells. Injury also leads to macrophage activation and the release of cytokines including TGF-β and HMGB1, as well as reactive oxygen species (ROS). This oxidative environment also elevates AGE generation, leading to the presence of more RAGE ligands. RAGE-expressing fibroblasts invading the denuded alveolar basement membrane may bind AGEs (and perhaps HMGB1) in the ECM or alveolar lining fluid which act to suppress myofibroblast differentiation (α-SMA expression), whereas fibroblasts that lose RAGE expression may lack this suppression and more readily differentiate into myofibroblasts in response to TGF-β and other pro-fibrotic cytokines. Further, in the setting of decreased RAGE expression, HMGB1 may be more likely to bind toll-like receptors 2 or 4 (TLR2/4) on macrophages to promote inflammation that will enhance fibrosis.

TGF-β, an orchestrating cytokine in IPF pathogenesis, induces myofibroblast differentiation [199, 200]. If RAGE mediates suppression of myofibroblast differentiation by AGEs, this would implicate RAGE as a counteracting factor to certain pro-fibrotic TGF-β

effects. Thus, the extent of myofibroblast differentiation may reflect a balance between TGF-β-mediated signaling and its suppression by RAGE-mediated signaling (Figure 31).

8. DISCUSSION AND FUTURE DIRECTIONS

IPF is a devastating disease with high morbidity and mortality, for which there is currently no effective therapy. Importantly, molecular details of IPF pathogenesis remain largely unknown. In this dissertation, we hypothesized that RAGE may play a central role in the pathogenesis IPF. To test this hypothesis, we used a combination of two mouse models of pulmonary fibrosis, the bleomycin model and the asbestos model. Specifically, the experiments described were carried out with the following goals: 1) to describe the production of sRAGE in the mouse to enhance its use as a research tool, 2) to investigate the regulation of both RAGE isoforms in pulmonary fibrosis using animal models and tissue from IPF patients, and 3) to propose a mechanism for the effects of RAGE regulation in the pathogenesis of IPF. The following conclusions were made from these studies: 1) mouse sRAGE is produced by proteolytic truncation of RAGE, in contrast to the alternative splicing mechanism utilized in humans, 2) RAGE and sRAGE expression are downregulated in both mouse models, as well as in human IPF, and 3) loss of pulmonary RAGE may contribute to the development of pulmonary fibrosis. Thus, reduction in RAGE expression may be a key event in the pathogenesis of idiopathic pulmonary fibrosis.

8.1. MOUSE sRAGE BIOSYNTHESIS AND CHARACTERIZATION

sRAGE, like RAGE, is expressed at high levels in the mouse lung. Because we hypothesized that this isoform may also have a role in IPF pathogenesis, it was important to fully describe this protein in terms of its biosynthesis, as well as its biochemical structure.

8.1.1. Implications of mouse sRAGE biosynthesis

We presented evidence that sRAGE biosynthesis in the mouse contrasts with that in humans. In humans, sRAGE is produced by alternative splicing of the RAGE transcript [70, 72]. In mice, there are no alternative RAGE transcripts, and peptide sequencing and mass spectroscopy analyses indicate that the carboxy-terminus of sRAGE does not have a unique amino acid sequence from RAGE but rather is truncated. In addition, matrix metalloproteinase-9 has been identified as a protease that can execute RAGE truncation [193].

Although the primary mechanism of sRAGE biosynthesis in mice differs from that in humans, it is likely that truncation may also occur in humans, in addition to the alternative splicing mechanism. Matrix metalloproteinase-9 is well-conserved between humans and mice [201], so it is also likely that MMP-9 can mediate a similar truncation in humans. It is important to note that despite this difference in sRAGE biosynthesis, sRAGE is still abundant in normal lungs of both mice and humans (see Chapter 6).

One consequence of the lack of an alternative splicing mechanism in sRAGE biosynthesis in mice is that differential expression of RAGE and sRAGE on the transcript level cannot be quantitated. Instead, expression strictly on the protein level must be used to analyze differences in the levels of these isoforms.

8.1.2. Structural characterization of mouse sRAGE

sRAGE has proven to be a valuable tool in studies of RAGE-mediated diseases. Because our experiments included the use of mouse models, we sought to better characterize sRAGE from the mouse.

We began this characterization of mouse sRAGE with its purification from mouse lungs. We found that sRAGE binds heparin, suggesting that *in vivo* it binds heparan sulfate, localizing

sRAGE in the ECM and cell surfaces. It is interesting to consider the possibility that ligand binding could cause a conformational change in sRAGE that could alter its heparin affinity, perhaps allowing sRAGE-ligand complexes to be released from the surrounding ECM and enter the bloodstream to be cleared. It has been postulated that sRAGE-ligand complexes are eliminated from the blood via the spleen and/or liver [124]. Further studies are needed to determine if loss of ECM affinity upon ligand binding is a component of sRAGE physiology. Because of our findings that the extracellular sequence of RAGE is the same as sRAGE in mice, we speculate that membrane-bound RAGE also has heparin affinity, and that RAGE may mediate some cell-matrix interactions. The domain of RAGE/sRAGE involved in heparin binding has yet to be defined.

Another structural feature of mouse sRAGE that we chose to examine was its glycosylation pattern. We found that mouse sRAGE is *N*-glycosylated at two sites in the V-like immunoglobulin domain, which is the domain shown to be involved in ligand binding [71]. Thus, it is likely that these carbohydrate groups are involved in sRAGE-ligand interactions. This is important information for us to consider as we intend to establish a sRAGE expression system in the future (see Section 8.1.3).

8.1.3. Future Directions: husRAGE expression system

A valuable tool for RAGE studies would be a sRAGE expression system. During efforts to determine if there is an alternative mouse RAGE transcript, we were able to detect and clone an alternative RAGE transcript from a human cDNA library. This clone (human sRAGE, or husRAGE) nearly matched that found by Malherbe *et al.* [70] to be a secretory form of human RAGE (in other words, sRAGE) (Figure 32). Through the V-like domain, there is only one difference between the sequence reported by Malherbe and colleagues [70] and our husRAGE

sequence ("X" residue, located at the second position in the V-like domain), and this directly corresponds to three nucleotide residues that could not be resolved during sequencing. Thus, this difference is likely due to a technical problem rather than a true difference in sequence. The signal peptide sequence differs from that published by Malherbe *et al.* [70], however. To make sure that this does not affect the secretion of husRAGE, we inserted the husRAGE sequence into a mammalian expression vector (pcDNA3.1^{+}) and transfected human 293T cells with this construct. The media was probed by western blotting and husRAGE was successfully detected (Figure 33), so this difference in the signal peptide does not appear to affect husRAGE secretion.

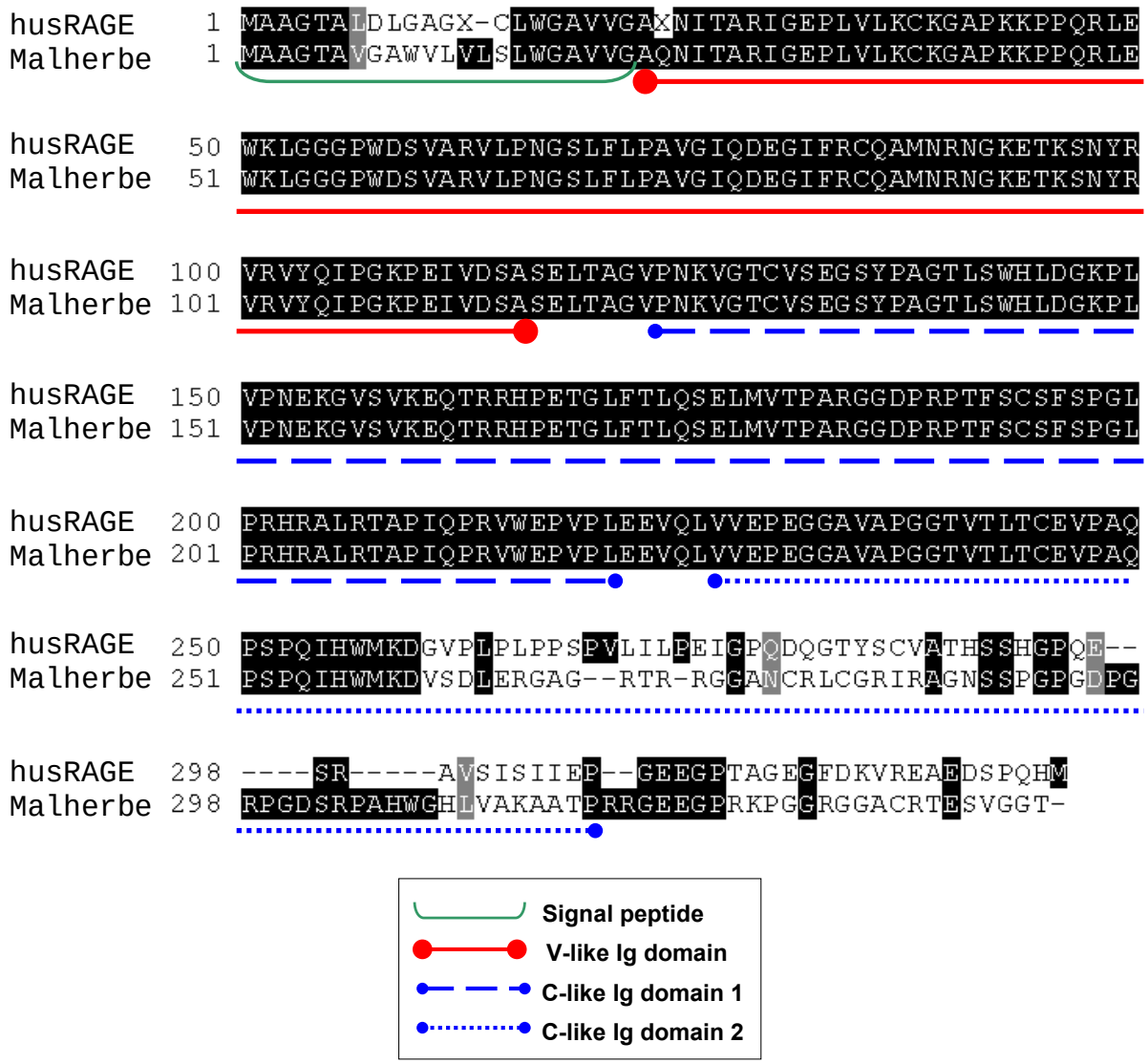

Figure 32. Alignment of husRAGE and hRAGEsec.

husRAGE was cloned from a commercial human cDNA library and sequenced. The ORF Finder program (http://www.ncbi.nlm.nih.gov/gorf/gorf.html) was used to generate the predicted open reading frame amino acid sequence, which was compared to the sequence for hRAGEsec, the secreted RAGE isoform described by Malherbe *et al.* [70] ("Malherbe" sequence). Residues shaded in *black* indicate a match, while residues shaded in *gray* indicate a conservative change in residue. The signal peptide and immunoglobulin (Ig) domains are indicated under the Malherbe sequence (see legend).

Figure 33. husRAGE is secreted into culture medium.

Human 293T cells were transfected with the husRAGE-pcDNA3.1^{+} vector, and three days later cell culture medium was subjected to western blot analysis probing for sRAGE. Mouse sRAGE was loaded as a positive control for western blotting.

Although we have been successful at expressing husRAGE, we have not been successful at purifying it from culture media because it precipitates out of solution. As a future direction, husRAGE will be inserted into a vector with a FLAG tag (Sigma) (pFLAG-CMV-5 Expression Vector, Figure 34). One advantage of this system is that it may help prevent protein precipitation because the tag is hydrophilic. Also, the tag will greatly assist in husRAGE purification from culture medium using a column with immobilized anti-FLAG antibodies. Finally, the tag is short (8 amino acids), and thus should affect protein function minimally.

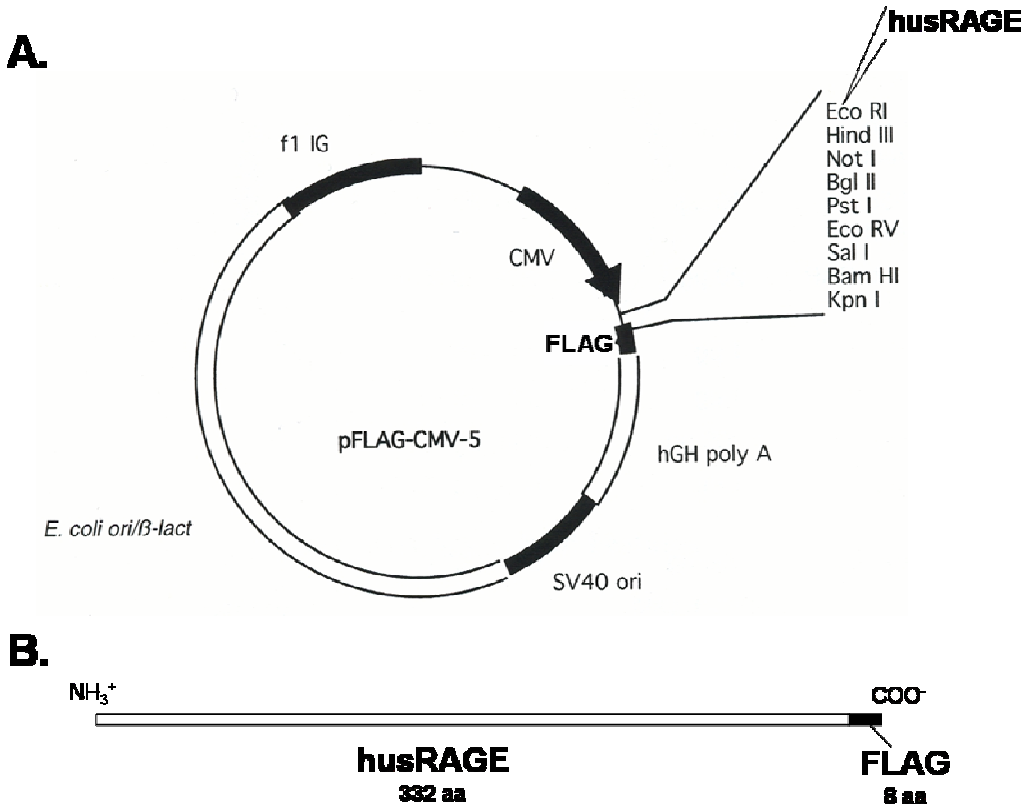

Figure 34. The pFLAG-CMV-5 Expression Vector.

The FLAG expression system (Sigma) will be used to generate a mammalian expression system for husRAGE. (A) pFLAG-CMV-5 expression vector map (modified from www.sigmaaldrich.com). husRAGE cDNA will be inserted into the EcoRI restriction site as indicated schematically. (B) Schematic of husRAGE translated sequence. The FLAG tag (8 amino acids) will be on the carboxy-terminus of husRAGE.

The FLAG tag can be added to the amino- or carboxy-terminus of the protein. Because the amino-terminus is where ligand binding occurs, we will first attempt to tag husRAGE at the carboxy-terminus. RAGE-ligand binding assays [190] will also be employed to assure proper ligand-binding function of husRAGE.

Once established, this protein expression system will be useful in determining the effects of blockade of RAGE signaling. husRAGE will be used in cell culture to prevent ligand-RAGE interactions and help determine which cellular outcomes are RAGE-mediated. In addition, it can

be used *in vivo* to help determine the role of RAGE blockade in our bleomycin and asbestos models of pulmonary fibrosis.

8.2. RAGE AND sRAGE REGULATION IN IDIOPATHIC PULMONARY FIBROSIS

8.2.1. RAGE and sRAGE are downregulated during pulmonary fibrosis pathogenesis

In both the bleomycin-induced and the asbestos-induced mouse models of pulmonary fibrosis, we found significant reductions in RAGE and sRAGE protein levels at two timepoints in each model. Interestingly, in both models, a significant decrease in RAGE was evident by 1 day after injury (Figure 13 and Figure 19). This indicates that the loss of RAGE is an early event in the pathogenesis of these models of pulmonary fibrosis. This loss of RAGE may contribute to the ensuing injury and fibrosis. While sRAGE is significantly reduced by 24 hours after asbestos treatment, decreases in sRAGE in the bleomycin model do not become significant until 4 days after treatment (although there is a trend of decreased sRAGE after 24 hours). The decrease in sRAGE may be delayed compared to RAGE since sRAGE is produced by proteolytic truncation of RAGE in mice (see Chapter 5).

We also looked at later timepoints after injury. In the bleomycin model, the timepoint of transition from inflammatory phase to fibrotic phase is around day 7. At this timepoint, there is also a significant decrease in both RAGE isoforms (Figure 12 and Figure 14). Thus, RAGE and sRAGE loss is evident throughout the inflammatory phase. In the asbestos model, significant fibrosis has occurred by day 28 after injury with some residual inflammation. This is a late stage of the asbestos model. At this timepoint, RAGE and sRAGE continue to show signs of depletion from the lung tissue (Figure 18 and Figure 19).

On the other hand, at a later stage of bleomycin-induced pulmonary fibrosis (14 days) when most of the fibrosis has occurred, sRAGE protein shows a trend for reduction that does not reach significance (Figure 16). In addition, RAGE transcripts at 7 days post-bleomycin injury show a nonsignificant decrease compared to control animals (Figure 17). It is possible that at this point (day 7), when RAGE and sRAGE protein levels are very low, recovery mechanisms are being initiated to increase RAGE isoforms back toward their baseline levels. At day 14 when the differences in sRAGE levels between control and bleomycin-treated mouse lungs are not significant, we may be seeing the effect of these slow recovery mechanisms in their attempt to compensate for RAGE depletion. As discussed above, bleomycin-induced pulmonary fibrosis in animal models has been shown to resolve [51], and we speculate that eventual compensation for RAGE and sRAGE loss may be a component of the resolution process that is initiated as bleomycin is slowly degraded in the lung.

On the other hand, there are no reports of asbestos-induced pulmonary fibrosis undergoing resolution. In fact, long-term models of asbestos pulmonary injury indicate that fibrosis does not resolve, but instead leads to an increased the risk of mesothelioma development [202, 203]. We found that at a late timepoint in asbestos-mediated disease (day 28), RAGE and sRAGE protein levels remain significantly reduced (Figure 20 and Figure 21). It is interesting to speculate that one difference between these two models in terms of their ability to resolve injury lies in their ability to compensate for RAGE/sRAGE depletion. In the bleomycin model, where mice can resolve their injury after sufficient time, RAGE appears to be approaching control levels at later stages of the disease. In the asbestos model, in which resolution has not been shown, there is no evidence of recovery of RAGE/sRAGE expression. Investigating RAGE and

sRAGE protein and transcript expression at more timepoints in the bleomycin and asbestos models will help address this hypothesis.

Importantly, our data from these animal models is supported by data derived from IPF in humans. RAGE/sRAGE transcript levels are significantly reduced in the lungs of IPF patients (Figure 22). On the protein level, RAGE and sRAGE are reduced as well (Figure 23 and Figure 24). By the time that patients present with symptoms of pulmonary fibrosis, the disease is well advanced. Thus, samples used for human IPF analysis described here represent late stages of IPF. It is interesting that RAGE/sRAGE transcripts and protein are reduced in these samples because this, combined with data from our animal models, suggests that an alteration in RAGE and sRAGE expression occuring at early stages of the disease persists through the late stages of the disease. This supports the proposition discussed above that the apparent inability to restore RAGE/sRAGE expression after pulmonary injury in the asbestos model may correspond to the inability to resolve pulmonary injury.

Another interesting contribution to these data comes from RAGE-/- mice. With time, and in the absence of exogenous injury, these mice develop characteristics of pulmonary fibrosis (Figure 25). These characteristics include upregulation of a subset of molecules that have been observed to be upregulated in experimental models of pulmonary fibrosis, including α-smooth muscle actin, TNF-α , Ki67, and galectin-3 [20, 197, 198]. This suggests that lack of RAGE and sRAGE is sufficient to cause a fibrotic phenotype in the lung.

One interesting protein that is highly upregulated in RAGE knockouts is galectin-3 (Figure 25H). This lectin can be found in the cytoplasm, on the cell surface, or secreted into the extracellular matrix [204]. It has been shown to bind AGEs and mediate their uptake [205], as well as binding other carbohydrates, and is implicated in modulating cell-cell and cell-matrix

interactions. Galectin-3 was also found to be dramatically increased shortly after irradiation-induced pulmonary fibrosis in macrophages and the expanding alveolar epithelium [197]. Although its effect on pulmonary pathology has not been fully described, galectin-3 has been proposed to be involved in alveolar epithelial regeneration during injury and repair. Because the ligand specificity of RAGE and galectin-3 partially overlap, it is interesting to consider that a balance between their expression is important in a setting such as pulmonary fibrosis. Galectin-3 is upregulated in diabetic complications where AGE concentration is high, as is RAGE. However, in PF, it seems that galectin-3 is upregulated but RAGE is downregulated. This observation may support the recurring theme of differential RAGE biology in the lung compared to other tissues.

Taken together, these data indicate that RAGE expression in the lung is *protective* against fibrotic changes. There are two possible explanations for how RAGE could have a protective role against PF pathogenesis: 1) RAGE-mediated signaling in the lung is beneficial, or 2) the presence of RAGE and/or sRAGE in the lung prevents RAGE ligands from binding other pathogenic receptors or mediators. Studies described in Future Directions (section 8.2.2) will help distinguish between these two possibilities.

8.2.2. Future Directions: Animal models

Two of the major conclusions from this body of work are that RAGE and sRAGE expression are downregulated during pathogenesis of animal models of PF as well as human IPF, and that the absence of RAGE appears to promote a fibrotic phenotype in the lung. Both of these results suggest that RAGE and/or sRAGE expression in the lung are protective against fibrotic damage, but the mechanism of protection by RAGE and/or sRAGE needs to be described.

There are two ways in which RAGE could act as a protective molecule: 1) RAGE-mediated signaling is beneficial in the lung, or 2) the presence of RAGE or sRAGE prevents RAGE ligands from binding other pathogenic mediators. In the future, excess pulmonary sRAGE will be used to discern between these possibilities in mouse models. This is an excellent tool for this purpose of distinguishing between possibility (1) and (2). If RAGE-mediated signaling is necessary for its protective effects (1), then excess sRAGE will block this signaling and thereby exacerbate pulmonary injury. However, if pulmonary protection by RAGE is mediated by its ability to sequester its ligands from other, more pathogenic mediators (2), then excess sRAGE will function to further sequester these ligands, and thereby improve disease outcome.

Excess pulmonary sRAGE will be obtained using two approaches. In one approach, exogenous sRAGE will be administered. As described in Section 8.1.3 (Future Directions: husRAGE expression system), a mammalian expression system is being developed for human sRAGE (husRAGE). Once this system is established, we will be able to isolate functional husRAGE from culture medium and administer it to mice treated with bleomycin or asbestos. husRAGE will be given once daily [77, 80] via the intratracheal route. By administering intratracheally, the protein will be delivered directly into the lungs.

Notably, we have used this approach before in preliminary studies. In one experiment, the sRAGE used was purified from mouse lungs as described in Chapter 5 and was administered intraperitoneally once per day. In another experiment, we obtained mouse recombinant sRAGE from Dr. Ann-Marie Schmidt (Columbia University, New York) and administered this intratracheally once per day. In both cases, mice were treated with bleomycin and the experiment ran until day 7. Assessment parameters we used were histological grading and

hydroxyproline quantification. Hydroxyproline is a modified form of the amino acid praline that is found abundantly in collagen chains, and thus is commonly used as an indicator of the extent of fibrosis [206]. In both experiments, sRAGE administration appeared to exacerbate injury (Figure 35). However, endotoxin testing of the sRAGE samples used after the completion of these experiments revealed that these sRAGE preparations were contaminated with endotoxin. Therefore, solid conclusions cannot be made from these results. However, uninjured mice treated with sRAGE did not demonstrate pathology after seven daily treatments of contaminated sRAGE (Figure 35B), which seems to suggest that the effect of sRAGE exacerbating bleomycin injury was real. Nevertheless, these experiments need to be repeated with LPS-free sRAGE.

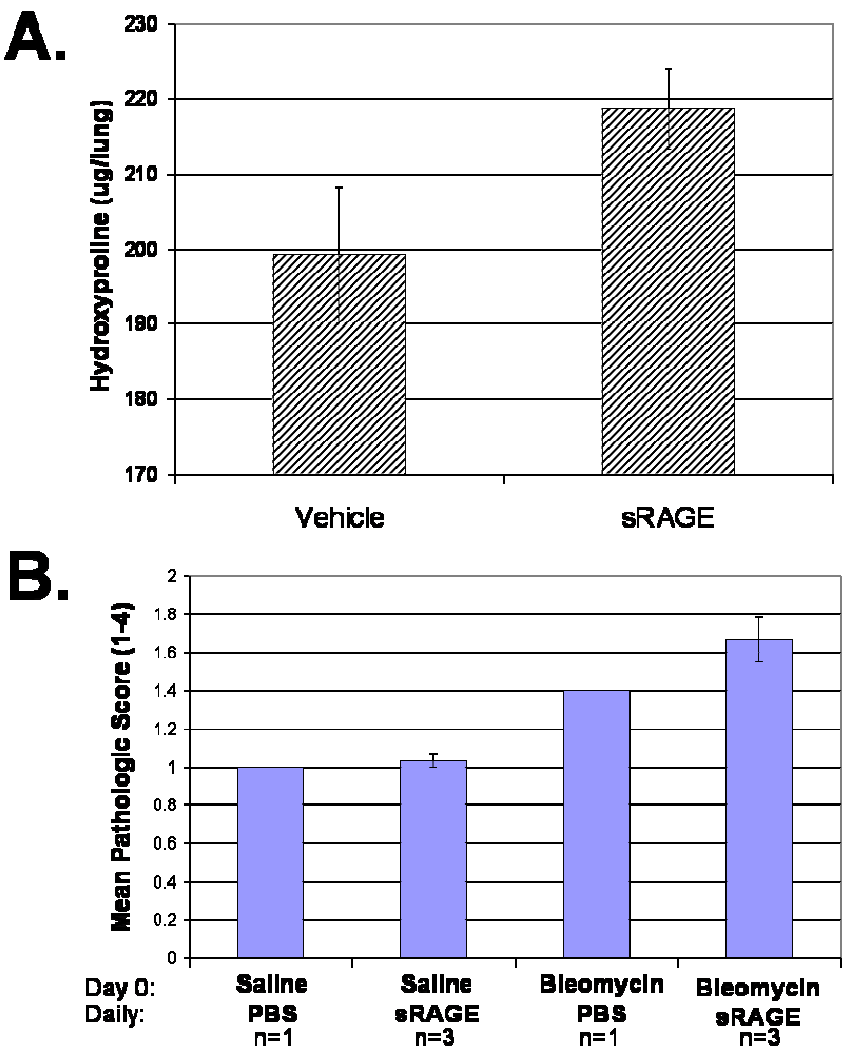

Figure 35. Exogenous sRAGE exacerbates bleomycin-induced pulmonary injury.

(A) C57Bl/6 mice were treated with 0.12 U bleomycin intratracheally on day 0, and either 60 μg sRAGE (purified from mouse lungs) or an equivalent volume of vehicle (PBS) daily until day 7, when they were sacrificed. Hydroxyproline content of lungs was quantified [206] as an index of fibrosis. p=0.14. (B) C57Bl/6 mice were treated with 0.5 U bleomycin or an equivalent volume of 0.9% saline on day 0, and either 60 μg sRAGE (recombinant mouse sRAGE acquired from Dr. Ann-Marie Schmidt, Columbia University) or an equivalent volume of vehicle (PBS) daily until day 7, when they were sacrificed. Lungs were formalin fixed and paraffin-embedded. Five micron sections were cut and stained with hematoxylin and eosin. Histological grading was performed by a pathologist blinded to treatment group, who scored ten fields from each slide according to the degree of injury (inflammatory infiltrate and fibrosis) on a scale of 1-4 (where 1 indicates no injury).

The other approach that will be used in the future to determine the effects of excess sRAGE on bleomycin- and asbestos-induced pulmonary fibrosis is an inducible transgenic approach (Figure 36), accomplished by mating two specific mouse strains together. In one mouse strain, the promoter for Clara cell secretory protein will be used to express the reverse tetracycline responsive transactivator specifically in AE-II cells and some non-ciliated bronchial and bronchiolar epithelial cells [207]. In the other strain, the tetracycline operator with a tetracycline-responsive element (tetO) will regulate transcription of husRAGE cDNA. When these two strains are crossed, we will have an inducible husRAGE transgenic that will express husRAGE in AE-II cells only after doxycycline administration [207]. These inducible transgenic mice will then be treated with bleomycin or asbestos and evaluated for exacerbation of fibrosis or slowing of disease progression.

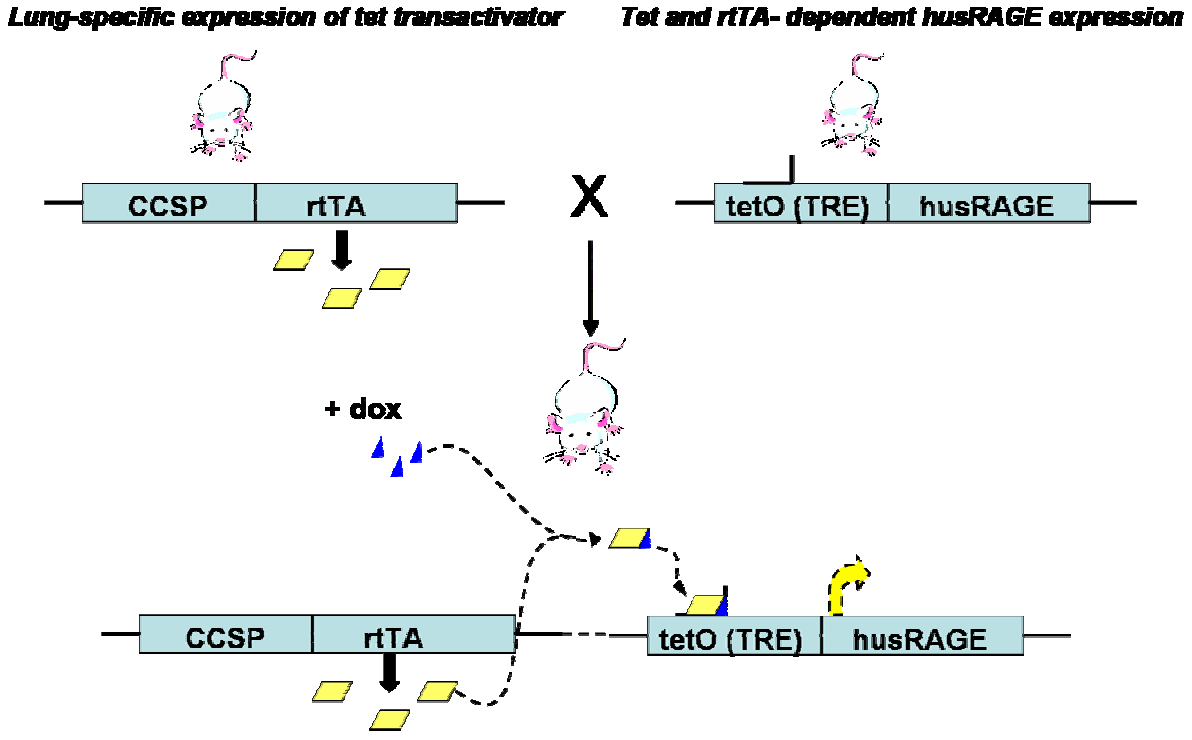

Figure 36. husRAGE inducible transgenic scheme.

Mice transgenic for husRAGE will be generated in collaboration with Dr. Barry Stripp and Dr. Susan Reynolds (University of Pittsburgh, Environmental and Occupational Health).

(Figure 36, cont.) The first construct includes the reverse tetracycline responsive transactivator (rtTA) under the control of the Clara cell secretory protein promoter (CCSP), driving expression of the transactivator only in AE-II cells and some bronchiolar epithelial cells. The second construct includes the husRAGE cDNA under the control of the tetracycline operator with a tetracycline-responsive element (tetO). Mouse strains with each of these constructs are crossed to generate an inducible transgenic line. In the inducible transgenic mice, when doxycycline (dox, a tetracycline analog) is administered, dox binds the transactivator and binds to tetO to drive husRAGE expression. The transactivator will not bind the tetO in the absence of dox.

8.2.3. Cell Culture Studies

Using cell culture approaches, we found evidence of HMGB1 release by macrophages exposed to pulmonary fibrotic stimuli, as well as evidence of a protective role of RAGE. After being cultured in the presence of asbestos or bleomycin for 24 hours, pulmonary murine macrophages released HMGB1 into culture medium (Figure 27). Once released from macrophages, HMGB1 may act in an autocrine or paracrine fashion. In addition to RAGE, macrophages and neutrophils express toll-like receptors 2 and 4, which also bind HMGB1, to initiate pro-inflammatory signaling [134]. In fact, toll-like receptors 2 and 4 have recently been shown to be more effective at mediating HMGB1-induced NF-κB activation in macrophages than RAGE [134]. Thus, the presence of RAGE or sRAGE may reduce HMGB1-toll-like receptor interactions that cause enhanced release of inflammatory mediators including TNF-α and IL-1. In addition, HMGB1-induced cytokine release is delayed and sustained [104, 208], compared to that induced by TNF-α, thus contributing to a chronic inflammatory state that may augment injury. In terms of HMGB1-induced pro-inflammatory effects, RAGE may be the less-damaging alternative to toll-like receptors 2 and 4, and loss of RAGE (and sRAGE) may promote further inflammation and tissue injury.

In terms of pulmonary fibroblast biology, we found that culturing a cell line of this type with AGEs resulted in a decrease in α-SMA, the marker for myofibroblasts (Figure 29). This

implies that signaling initiated by AGEs suppresses myofibroblast differentiation. We speculate that this suppression is mediated via RAGE, and experiments detailed in the following section will help to determine if this is the case. One concern with this study, however, is that α-SMA is expressed at baseline in these cells, whereas fibroblasts *in vivo* would not express α-SMA. Notably, serum starvation of these cells does not abolish α-SMA expression. Thus, these studies need to be repeated in another cell line that does not demonstrate baseline expression of α-SMA (see below).

8.2.4. Future Directions: *In vitro* studies

For the fibroblast experiments in culture, one important future direction is to show that the effects of AGEs on myofibroblast differentiation are RAGE-mediated. Once our husRAGE expression system is established, we can use husRAGE for this purpose. In addition to using husRAGE, we will use commercially available neutralizing RAGE antibodies that have been described [137]. Also, Dr. Angelika Bierhaus (University of Heidelberg, Germany) has primary fibroblasts isolated from RAGE knockout mice, and these fibroblasts would be another valuable tool for determining if AGE effects are RAGE-mediated. Finally, a recent paper demonstrated the use of a fibroblast cell line that expressed very little α-SMA under baseline conditions [209], and the use of this cell line instead of the ones described above may be more similar to the case *in vivo*, in which normal fibroblasts do not express α-SMA. Once all of these issues are resolved, we would like to perform these experiments in primary human lung fibroblasts that do not express α-SMA under normal conditions, and also look at other parameters including collagen production and TGF-β synthesis by these cells.

Ultimately, we would like to explain the apparent discrepancy between the role of RAGE in the lung compared to other tissues. The fact that RAGE and sRAGE are downregulated in

IPF, where there is likely elevation of RAGE ligands ([174] and Figure 27), suggests that there is a different signaling cascade operating in the lung. This lung-specific signaling does not appear to involve the positive feedback loop that has been characterized in studies of other tissues. One way to begin looking at such signaling pathways would be by proteomic approaches such as two-dimensional electrophoresis. By comparing AGE-treated pulmonary fibroblasts and vascular endothelial cells (in which RAGE expression is upregulated in response to its ligands and RAGE-mediated signaling triggers cellular activation [86, 91, 93, 97, 121, 137]), it may be possible to identify molecules that are involved in RAGE-mediated signaling in one cell type but not the other. Thus, we may begin to explain another interesting facet of RAGE biology.

8.3. CLINICAL IMPLICATIONS

In this project we identified a novel target for IPF therapeutics, the receptor for advanced glycation end products. Although RAGE biology has been well-studied in other diseases, particularly diabetic complications, studies in the lung have been limited.

We found evidence that the loss of RAGE expression in the lung promotes pulmonary fibrosis, and this reduction appears to be sustained through end-stages of the disease. Future studies will be aimed at determining the mechanism of the protective role of RAGE in the lung. At this point, there seem to be two possible explanations: 1) RAGE signaling is protective, and 2) RAGE expression in the lung prevents RAGE ligands from interacting with other more pathogenic mediators. The design of therapeutic approaches targeted to RAGE biology will depend on which of these possibilities represents the case *in vivo*.

If future studies determine that RAGE signaling is protective, therapeutic strategies may be aimed at increasing RAGE-mediated signaling, perhaps by administration of RAGE ligands.

This poses an immediate complication, however, because the presence of RAGE ligands in other tissues induces pro-inflammatory RAGE signaling [80, 97, 137]. Thus, these ligands can not be systemically administered, but rather must be delivered directly to the lung. In addition, the ligand used in such approaches should not be HMGB1 because this protein causes lung inflammation [105, 208, 210], likely, it seems, by its interactions with toll-like receptors 2 and 4 [134]. Also, S100/calgranulins are associated with inflammatory responses [80, 84, 153], and AGEs have long-term structural effects on blood vessels [110] which could cause complications if they reach the pulmonary vasculature. Thus, it is likely that a synthetic RAGE agonist would be the best option, however one has not yet been identified.

On the other hand, if it is determined that the expression of RAGE/sRAGE in the lung is indirectly protective by preventing association of ligands with other more pathogenic mediators, sRAGE administration would be an appropriate therapeutic approach. In addition, this molecule could theoretically be given systemically, being delivered to the lung via the circulation, or administered by aerosolization from an inhaler.

RAGE is a fascinating protein with many facets to its biology. Here we describe a novel role for RAGE as a protective molecule in the lung. Whereas in the wide range of RAGE-mediated pathologies in other tissues, RAGE *upregulation* seems to invoke disease progression, RAGE *downregulation* in the lung seems to promote IPF pathogenesis. Importantly, our studies on RAGE have identified a novel modulator of IPF that may provide more insight into its pathogenesis, a focus of study that continues to have just as many questions as answers.

BIBLIOGRAPHY

1. West, J.B., *Respiratory Physiology: The Essentials*. Sixth ed. 2000, Philadelphia: Lippincott Williams & Wilkins.

2. Crystal, R.G., Oxidants and respiratory tract epithelial injury: pathogenesis and strategies for therapeutic intervention. *Am J Med*, 1991. **91**(3C): p. 39S-44S.

3. Weibel, E.R., Morphometric estimation of pulmonary diffusion capacity. I. Model and method. *Respir Physiol*, 1970. **11**(1): p. 54-75.

4. Chang, L.Y., L.H. Overby, A.R. Brody, and J.D. Crapo, Progressive lung cell reactions and extracellular matrix production after a brief exposure to asbestos. *Am J Pathol*, 1988. **131**(1): p. 156-70.

5. Davis, G.S., Pathogenesis of silicosis: current concepts and hypotheses. *Lung*, 1986. **164**(3): p. 139-54.

6. Rudders, R.A. and G.T. Hensley, Bleomycin pulmonary toxicity. *Chest*, 1973. **63**(4): p. 627-8.

7. Pickrell, J.A., D.V. Harris, F.F. Hahn, J.J. Belasich, and R.K. Jones, Biological alterations resulting from chronic lung irradiation. III. Effect of partial 30Co thoracic irradiation upon pulmonary collagen metabolism and fractionation in syrian hamsters. *Radiat Res*, 1975. **62**(1): p. 133-44.

8. Nogee, L.M., A.E. Dunbar, 3rd, S.E. Wert, F. Askin, A. Hamvas, and J.A. Whitsett, A mutation in the surfactant protein C gene associated with familial interstitial lung disease. *N Engl J Med*, 2001. **344**(8): p. 573-9.

9. Amin, R.S., S.E. Wert, R.P. Baughman, J.F. Tomashefski, Jr., L.M. Nogee, A.S. Brody, W.M. Hull, and J.A. Whitsett, Surfactant protein deficiency in familial interstitial lung disease. *J Pediatr*, 2001. **139**(1): p. 85-92.

10. Nogee, L.M., A.E. Dunbar, 3rd, S. Wert, F. Askin, A. Hamvas, and J.A. Whitsett, Mutations in the surfactant protein C gene associated with interstitial lung disease. *Chest*, 2002. **121**(3 Suppl): p. 20S-21S.

11. Thomas, A.Q., K. Lane, J. Phillips, 3rd, M. Prince, C. Markin, M. Speer, D.A. Schwartz, R. Gaddipati, A. Marney, J. Johnson, R. Roberts, J. Haines, M. Stahlman, and J.E. Loyd,

Heterozygosity for a surfactant protein C gene mutation associated with usual interstitial pneumonitis and cellular nonspecific interstitial pneumonitis in one kindred. *Am J Respir Crit Care Med*, 2002. **165**(9): p. 1322-8.

12. Crystal, R.G., P.B. Bitterman, S.I. Rennard, A.J. Hance, and B.A. Keogh, Interstitial lung diseases of unknown cause. Disorders characterized by chronic inflammation of the lower respiratory tract. *N Engl J Med*, 1984. **310**(4): p. 235-44.

13. Gross, T.J. and G.W. Hunninghake, Idiopathic pulmonary fibrosis. *N Engl J Med*, 2001. **345**(7): p. 517-25.

14. Mason, R.J., M.I. Schwarz, G.W. Hunninghake, and R.A. Musson, NHLBI Workshop Summary. Pharmacological therapy for idiopathic pulmonary fibrosis. Past, present, and future. *Am J Respir Crit Care Med*, 1999. **160**(5 Pt 1): p. 1771-7.

15. Lynch, J.P., 3rd, E. White, and K. Flaherty, Corticosteroids in idiopathic pulmonary fibrosis. *Curr Opin Pulm Med*, 2001. **7**(5): p. 298-308.

16. Flaherty, K.R., G.B. Toews, J.P. Lynch, 3rd, E.A. Kazerooni, B.H. Gross, R.L. Strawderman, K. Hariharan, A. Flint, and F.J. Martinez, Steroids in idiopathic pulmonary fibrosis: a prospective assessment of adverse reactions, response to therapy, and survival. *Am J Med*, 2001. **110**(4): p. 278-82.

17. Coultas, D.B., R.E. Zumwalt, W.C. Black, and R.E. Sobonya, The epidemiology of interstitial lung diseases. *Am J Respir Crit Care Med*, 1994. **150**(4): p. 967-72.

18. Panos, R.J., R.L. Mortenson, S.A. Niccoli, and T.E. King, Jr., Clinical deterioration in patients with idiopathic pulmonary fibrosis: causes and assessment. *Am J Med*, 1990. **88**(4): p. 396-404.

19. Bjoraker, J.A., J.H. Ryu, M.K. Edwin, J.L. Myers, H.D. Tazelaar, D.R. Schroeder, and K.P. Offord, Prognostic significance of histopathologic subsets in idiopathic pulmonary fibrosis. *Am J Respir Crit Care Med*, 1998. **157**(1): p. 199-203.

20. Phan, S.H. and R.S. Thrall, eds. *Pulmonary Fibrosis*. Lung Biology in Health and Disease, ed. C. Lenfant. Vol. 80. 1995, Marcel Dekker, Inc.: New York.

21. Kawanami, O., V.J. Ferrans, and R.G. Crystal, Structure of alveolar epithelial cells in patients with fibrotic lung disorders. *Lab Invest*, 1982. **46**(1): p. 39-53.

22. Myers, J.L. and A.L. Katzenstein, Epithelial necrosis and alveolar collapse in the pathogenesis of usual interstitial pneumonia. *Chest*, 1988. **94**(6): p. 1309-11.

23. Uhal, B.D., I. Joshi, A.L. True, S. Mundle, A. Raza, A. Pardo, and M. Selman, Fibroblasts isolated after fibrotic lung injury induce apoptosis of alveolar epithelial cells in vitro. *Am J Physiol*, 1995. **269**(6 Pt 1): p. L819-28.

24. Idell, S., K.K. James, E.G. Levin, B.S. Schwartz, N. Manchanda, R.J. Maunder, T.R. Martin, J. McLarty, and D.S. Fair, Local abnormalities in coagulation and fibrinolytic pathways predispose to alveolar fibrin deposition in the adult respiratory distress syndrome. *J Clin Invest*, 1989. **84**(2): p. 695-705.

25. Last, J.A., A.D. Siefkin, and K.M. Reiser, Type I collagen content is increased in lungs of patients with adult respiratory distress syndrome. *Thorax*, 1983. **38**(5): p. 364-8.

26. Raghu, G., L.J. Striker, L.D. Hudson, and G.E. Striker, Extracellular matrix in normal and fibrotic human lungs. *Am Rev Respir Dis*, 1985. **131**(2): p. 281-9.

27. Katzenstein, A.L. and J.L. Myers, Idiopathic pulmonary fibrosis: clinical relevance of pathologic classification. *Am J Respir Crit Care Med*, 1998. **157**(4 Pt 1): p. 1301-15.

28. Phan, S.H., The myofibroblast in pulmonary fibrosis. *Chest*, 2002. **122**(6 Suppl): p. 286S-289S.

29. Zhang, K., M.D. Rekhter, D. Gordon, and S.H. Phan, Myofibroblasts and their role in lung collagen gene expression during pulmonary fibrosis. A combined immunohistochemical and in situ hybridization study. *Am J Pathol*, 1994. **145**(1): p. 114-25.

30. Adler, K.B., R.B. Low, K.O. Leslie, J. Mitchell, and J.N. Evans, Contractile cells in normal and fibrotic lung. *Lab Invest*, 1989. **60**(4): p. 473-85.

31. Zhang, K., K.C. Flanders, and S.H. Phan, Cellular localization of transforming growth factor-beta expression in bleomycin-induced pulmonary fibrosis. *Am J Pathol*, 1995. **147**(2): p. 352-61.

32. Zhang, K., M. Gharaee-Kermani, M.L. Jones, J.S. Warren, and S.H. Phan, Lung monocyte chemoattractant protein-1 gene expression in bleomycin-induced pulmonary fibrosis. *J Immunol*, 1994. **153**(10): p. 4733-41.

33. Kuhn, C. and J.A. McDonald, The roles of the myofibroblast in idiopathic pulmonary fibrosis. Ultrastructural and immunohistochemical features of sites of active extracellular matrix synthesis. *Am J Pathol*, 1991. **138**(5): p. 1257-65.

34. Reynolds, H.Y., J.D. Fulmer, J.A. Kazmierowski, W.C. Roberts, M.M. Frank, and R.G. Crystal, Analysis of cellular and protein content of broncho-alveolar lavage fluid from patients with idiopathic pulmonary fibrosis and chronic hypersensitivity pneumonitis. *J Clin Invest*, 1977. **59**(1): p. 165-75.

35. Ward, P.A. and G.W. Hunninghake, Lung inflammation and fibrosis. *Am J Respir Crit Care Med*, 1998. **157**(4 Pt 2): p. S123-9.

36. Kovacs, E.J., Fibrogenic cytokines: the role of immune mediators in the development of scar tissue. *Immunol Today*, 1991. **12**(1): p. 17-23.

37. Keogh, B.A. and R.G. Crystal, Alveolitis: the key to the interstitial lung disorders. *Thorax*, 1982. **37**(1): p. 1-10.

38. Selman, M., T.E. King, and A. Pardo, Idiopathic pulmonary fibrosis: prevailing and evolving hypotheses about its pathogenesis and implications for therapy. *Ann Intern Med*, 2001. **134**(2): p. 136-51.

39. Munger, J.S., X. Huang, H. Kawakatsu, M.J. Griffiths, S.L. Dalton, J. Wu, J.F. Pittet, N. Kaminski, C. Garat, M.A. Matthay, D.B. Rifkin, and D. Sheppard, The integrin alpha v beta 6 binds and activates latent TGF beta 1: a mechanism for regulating pulmonary inflammation and fibrosis. *Cell*, 1999. **96**(3): p. 319-28.

40. Broekelmann, T.J., A.H. Limper, T.V. Colby, and J.A. McDonald, Transforming growth factor beta 1 is present at sites of extracellular matrix gene expression in human pulmonary fibrosis. *Proc Natl Acad Sci U S A*, 1991. **88**(15): p. 6642-6.

41. Allen, J.T., R.A. Knight, C.A. Bloor, and M.A. Spiteri, Enhanced insulin-like growth factor binding protein-related protein 2 (Connective tissue growth factor) expression in patients with idiopathic pulmonary fibrosis and pulmonary sarcoidosis. *Am J Respir Cell Mol Biol*, 1999. **21**(6): p. 693-700.

42. Hardman, J.G., L.E. Limbird, and A.G. Gilman, eds. *Goodman & Gilman's the pharmacological basis of therapeutics*. 10th ed. 2001, McGraw-Hill: New York.

43. D'Andrea, A.D. and W.A. Haseltine, Sequence specific cleavage of DNA by the antitumor antibiotics neocarzinostatin and bleomycin. *Proc Natl Acad Sci U S A*, 1978. **75**(8): p. 3608-12.

44. Lazo, J.S., D.G. Hoyt, S.M. Sebti, and B.R. Pitt, Bleomycin: a pharmacologic tool in the study of the pathogenesis of interstitial pulmonary fibrosis. *Pharmacol Ther*, 1990. **47**(3): p. 347-58.

45. Lazo, J.S. and C.J. Humphreys, Lack of metabolism as the biochemical basis of bleomycin-induced pulmonary toxicity. *Proc Natl Acad Sci U S A*, 1983. **80**(10): p. 3064-8.

46. Snider, G.L., B.R. Celli, R.H. Goldstein, J.J. O'Brien, and E.C. Lucey, Chronic interstitial pulmonary fibrosis produced in hamsters by endotracheal bleomycin. Lung volumes, volume-pressure relations, carbon monoxide uptake, and arterial blood gas studied. *Am Rev Respir Dis*, 1978. **117**(2): p. 289-97.

47. Starcher, B.C., C. Kuhn, and J.E. Overton, Increased elastin and collagen content in the lungs of hamsters receiving an intratracheal injection of bleomycin. *Am Rev Respir Dis*, 1978. **117**(2): p. 299-305.

48. Schrier, D.J., R.G. Kunkel, and S.H. Phan, The role of strain variation in murine bleomycin-induced pulmonary fibrosis. *Am Rev Respir Dis*, 1983. **127**(1): p. 63-6.

49. Fattman, C.L., C.T. Chu, S.M. Kulich, J.J. Enghild, and T.D. Oury, Altered expression of extracellular superoxide dismutase in mouse lung after bleomycin treatment. *Free Radic Biol Med*, 2001. **31**(10): p. 1198-207.

50. Vyalov, S.L., G. Gabbiani, and Y. Kapanci, Rat alveolar myofibroblasts acquire alpha-smooth muscle actin expression during bleomycin-induced pulmonary fibrosis. *Am J Pathol*, 1993. **143**(6): p. 1754-65.

51. Brown, R.F., R.B. Drawbaugh, and T.C. Marrs, An investigation of possible models for the production of progressive pulmonary fibrosis in the rat. The effects of repeated intratracheal instillation of bleomycin. *Toxicology*, 1988. **51**(1): p. 101-10.

52. Mossman, B.T. and J.B. Gee, Asbestos-related diseases. *N Engl J Med*, 1989. **320**(26): p. 1721-30.

53. Ashcroft, T. and A.G. Heppleston, The optical and electron microscopic determination of pulmonary asbestos fibre concentration and its relation to the human pathological reaction. *J Clin Pathol*, 1973. **26**(3): p. 224-34.

54. Davis, J.M., S.T. Beckett, R.E. Bolton, P. Collings, and A.P. Middleton, Mass and number of fibres in the pathogenesis of asbestos-related lung disease in rats. *Br J Cancer*, 1978. **37**(5): p. 673-88.

55. Davis, J.M. and A.D. Jones, Comparisons of the pathogenicity of long and short fibres of chrysotile asbestos in rats. *Br J Exp Pathol*, 1988. **69**(5): p. 717-37.

56. Mossman, B.T., J. Bignon, M. Corn, A. Seaton, and J.B. Gee, Asbestos: scientific developments and implications for public policy. *Science*, 1990. **247**(4940): p. 294-301.

57. Rom, W.N., W.D. Travis, and A.R. Brody, Cellular and molecular basis of the asbestos-related diseases. *Am Rev Respir Dis*, 1991. **143**(2): p. 408-22.

58. Brody, A.R., L.H. Hill, B. Adkins, Jr., and R.W. O'Connor, Chrysotile asbestos inhalation in rats: deposition pattern and reaction of alveolar epithelium and pulmonary macrophages. *Am Rev Respir Dis*, 1981. **123**(6): p. 670-9.

59. Craighead, J.E., J.L. Abraham, A. Churg, F.H. Green, J. Kleinerman, P.C. Pratt, T.A. Seemayer, V. Vallyathan, and H. Weill, The pathology of asbestos-associated diseases of the lungs and pleural cavities: diagnostic criteria and proposed grading schema. Report of the Pneumoconiosis Committee of the College of American Pathologists and the National Institute for Occupational Safety and Health. *Arch Pathol Lab Med*, 1982. **106**(11): p. 544-96.

60. Schmidt, A.M., M. Vianna, M. Gerlach, J. Brett, J. Ryan, J. Kao, C. Esposito, H. Hegarty, W. Hurley, M. Clauss, and et al., Isolation and characterization of two binding proteins for advanced glycosylation end products from bovine lung which are present on the endothelial cell surface. *J Biol Chem*, 1992. **267**(21): p. 14987-97.

61. Schmidt, A.M., R. Mora, R. Cao, S.D. Yan, J. Brett, R. Ramakrishnan, T.C. Tsang, M. Simionescu, and D. Stern, The endothelial cell binding site for advanced glycation end products consists of a complex: an integral membrane protein and a lactoferrin-like polypeptide. *J Biol Chem*, 1994. **269**(13): p. 9882-8.

62. Neeper, M., A.M. Schmidt, J. Brett, S.D. Yan, F. Wang, Y.C. Pan, K. Elliston, D. Stern, and A. Shaw, Cloning and expression of a cell surface receptor for advanced glycosylation end products of proteins. *J Biol Chem*, 1992. **267**(21): p. 14998-5004.

63. Huttunen, H.J., C. Fages, and H. Rauvala, Receptor for advanced glycation end products (RAGE)-mediated neurite outgrowth and activation of NF-kappaB require the cytoplasmic domain of the receptor but different downstream signaling pathways. *Journal of Biological Chemistry*, 1999. **274**(28): p. 19919-24.

64. Brett, J., A.M. Schmidt, S.D. Yan, Y.S. Zou, E. Weidman, D. Pinsky, R. Nowygrod, M. Neeper, C. Przysiecki, A. Shaw, and et al., Survey of the distribution of a newly characterized receptor for advanced glycation end products in tissues. *Am J Pathol*, 1993. **143**(6): p. 1699-712.

65. Owen, W.F., Jr., F.F. Hou, R.O. Stuart, J. Kay, J. Boyce, G.M. Chertow, and A.M. Schmidt, Beta 2-microglobulin modified with advanced glycation end products modulates collagen synthesis by human fibroblasts. *Kidney Int*, 1998. **53**(5): p. 1365-73.

66. Collison, K.S., R.S. Parhar, S.S. Saleh, B.F. Meyer, A.A. Kwaasi, M.M. Hammami, A.M. Schmidt, D.M. Stern, and F.A. Al-Mohanna, RAGE-mediated neutrophil dysfunction is evoked by advanced glycation end products (AGEs). *J Leukoc Biol*, 2002. **71**(3): p. 433-44.

67. Fehrenbach, H., M. Kasper, T. Tschernig, M.S. Shearman, D. Schuh, and M. Muller, Receptor for advanced glycation endproducts (RAGE) exhibits highly differential cellular and subcellular localisation in rat and human lung. *Cell Mol Biol (Noisy-le-grand)*, 1998. **44**(7): p. 1147-57.

68. Schmidt, A.M., S.D. Yan, J. Brett, R. Mora, R. Nowygrod, and D. Stern, Regulation of human mononuclear phagocyte migration by cell surface-binding proteins for advanced glycation end products. *J Clin Invest*, 1993. **91**(5): p. 2155-68.

69. Huang, J.S., J.Y. Guh, H.C. Chen, W.C. Hung, Y.H. Lai, and L.Y. Chuang, Role of receptor for advanced glycation end-product (RAGE) and the JAK/STAT-signaling pathway in AGE-induced collagen production in NRK-49F cells. *J Cell Biochem*, 2001. **81**(1): p. 102-13.

70. Malherbe, P., J.G. Richards, H. Gaillard, A. Thompson, C. Diener, A. Schuler, and G. Huber, cDNA cloning of a novel secreted isoform of the human receptor for advanced glycation end products and characterization of cells co-expressing cell-surface scavenger receptors and Swedish mutant amyloid precursor protein. *Brain Research. Molecular Brain Research*, 1999. **71**(2): p. 159-70.

71. Kislinger, T., C. Fu, B. Huber, W. Qu, A. Taguchi, S. Du Yan, M. Hofmann, S.F. Yan, M. Pischetsrieder, D. Stern, and A.M. Schmidt, N(epsilon)-(carboxymethyl)lysine adducts of proteins are ligands for receptor for advanced glycation end products that activate cell signaling pathways and modulate gene expression. *J Biol Chem*, 1999. **274**(44): p. 31740-9.

72. Yonekura, H., Y. Yamamoto, S. Sakurai, R.G. Petrova, M.J. Abedin, H. Li, K. Yasui, M. Takeuchi, Z. Makita, S. Takasawa, H. Okamoto, T. Watanabe, and H. Yamamoto, Novel splice variants of the receptor for advanced glycation end-products expressed in human vascular endothelial cells and pericytes, and their putative roles in diabetes-induced vascular injury. *Biochem J*, 2003. **370**(Pt 3): p. 1097-109.

73. Chavakis, T., A. Bierhaus, N. Al-Fakhri, D. Schneider, S. Witte, T. Linn, M. Nagashima, J. Morser, B. Arnold, K.T. Preissner, and P.P. Nawroth, The pattern recognition receptor (RAGE) is a counterreceptor for leukocyte integrins: a novel pathway for inflammatory cell recruitment. *J Exp Med*, 2003. **198**(10): p. 1507-15.

74. Hori, O., J. Brett, T. Slattery, R. Cao, J. Zhang, J.X. Chen, M. Nagashima, E.R. Lundh, S. Vijay, D. Nitecki, and et al., The receptor for advanced glycation end products (RAGE) is a cellular binding site for amphoterin. Mediation of neurite outgrowth and co-expression of rage and amphoterin in the developing nervous system. *J Biol Chem*, 1995. **270**(43): p. 25752-61.

75. Huttunen, H.J., J. Kuja-Panula, and H. Rauvala, Receptor for advanced glycation end products (RAGE) signaling induces CREB-dependent chromogranin expression during neuronal differentiation. *J Biol Chem*, 2002. **277**(41): p. 38635-46.

76. Katsuoka, F., Y. Kawakami, T. Arai, H. Imuta, M. Fujiwara, H. Kanma, and K. Yamashita, Type II alveolar epithelial cells in lung express receptor for advanced glycation end products (RAGE) gene. *Biochemical & Biophysical Research Communications*, 1997. **238**(2): p. 512-6.

77. Park, L., K.G. Raman, K.J. Lee, Y. Lu, L.J. Ferran, Jr., W.S. Chow, D. Stern, and A.M. Schmidt, Suppression of accelerated diabetic atherosclerosis by the soluble receptor for advanced glycation endproducts. *Nat Med*, 1998. **4**(9): p. 1025-31.

78. Tsuji, H., N. Iehara, T. Masegi, M. Imura, J. Ohkawa, H. Arai, K. Ishii, T. Kita, and T. Doi, Ribozyme targeting of receptor for advanced glycation end products in mouse mesangial cells. *Biochem Biophys Res Commun*, 1998. **245**(2): p. 583-8.

79. Yamamoto, Y., I. Kato, T. Doi, H. Yonekura, S. Ohashi, M. Takeuchi, T. Watanabe, S. Yamagishi, S. Sakurai, S. Takasawa, H. Okamoto, and H. Yamamoto, Development and prevention of advanced diabetic nephropathy in RAGE-overexpressing mice. *J Clin Invest*, 2001. **108**(2): p. 261-8.

80. Hofmann, M.A., S. Drury, C. Fu, W. Qu, A. Taguchi, Y. Lu, C. Avila, N. Kambham, A. Bierhaus, P. Nawroth, M.F. Neurath, T. Slattery, D. Beach, J. McClary, M. Nagashima, J. Morser, D. Stern, and A.M. Schmidt, RAGE mediates a novel proinflammatory axis: a

central cell surface receptor for S100/calgranulin polypeptides. *Cell*, 1999. **97**(7): p. 889-901.

81. Taguchi, A., D.C. Blood, G. del Toro, A. Canet, D.C. Lee, W. Qu, N. Tanji, Y. Lu, E. Lalla, C. Fu, M.A. Hofmann, T. Kislinger, M. Ingram, A. Lu, H. Tanaka, O. Hori, S. Ogawa, D.M. Stern, and A.M. Schmidt, Blockade of RAGE-amphoterin signalling suppresses tumour growth and metastases. *Nature*, 2000. **405**(6784): p. 354-60.

82. Yan, S.D., X. Chen, J. Fu, M. Chen, H. Zhu, A. Roher, T. Slattery, L. Zhao, M. Nagashima, J. Morser, A. Migheli, P. Nawroth, D. Stern, and A.M. Schmidt, RAGE and amyloid-beta peptide neurotoxicity in Alzheimer's disease. *Nature*, 1996. **382**(6593): p. 685-91.

83. Takada, M., K. Hirata, T. Ajiki, Y. Suzuki, and Y. Kuroda, Expression of receptor for advanced glycation end products (RAGE) and MMP-9 in human pancreatic cancer cells. *Hepatogastroenterology*, 2004. **51**(58): p. 928-30.

84. Schmidt, A.M., S.D. Yan, S.F. Yan, and D.M. Stern, The biology of the receptor for advanced glycation end products and its ligands. *Biochimica et Biophysica Acta*, 2000. **1498**(2-3): p. 99-111.

85. Cataldegirmen, G., S. Zeng, N. Feirt, N. Ippagunta, H. Dun, W. Qu, Y. Lu, L.L. Rong, M.A. Hofmann, T. Kislinger, S.I. Pachydaki, D.G. Jenkins, A. Weinberg, J. Lefkowitch, X. Rogiers, S.F. Yan, A.M. Schmidt, and J.C. Emond, RAGE limits regeneration after massive liver injury by coordinated suppression of TNF-alpha and NF-kappaB. *J Exp Med*, 2005. **201**(3): p. 473-84.

86. Schmidt, A.M., M. Hasu, D. Popov, J.H. Zhang, J. Chen, S.D. Yan, J. Brett, R. Cao, K. Kuwabara, G. Costache, and et al., Receptor for advanced glycation end products (AGEs) has a central role in vessel wall interactions and gene activation in response to circulating AGE proteins. *Proc Natl Acad Sci U S A*, 1994. **91**(19): p. 8807-11.

87. Mackic, J.B., M. Stins, J.G. McComb, M. Calero, J. Ghiso, K.S. Kim, S.D. Yan, D. Stern, A.M. Schmidt, B. Frangione, and B.V. Zlokovic, Human blood-brain barrier receptors for Alzheimer's amyloid-beta 1- 40. Asymmetrical binding, endocytosis, and transcytosis at the apical side of brain microvascular endothelial cell monolayer. *J Clin Invest*, 1998. **102**(4): p. 734-43.

88. Ishihara, K., K. Tsutsumi, S. Kawane, M. Nakajima, and T. Kasaoka, The receptor for advanced glycation end-products (RAGE) directly binds to ERK by a D-domain-like docking site. *FEBS Lett*, 2003. **550**(1-3): p. 107-13.

89. Lander, H.M., J.M. Tauras, J.S. Ogiste, O. Hori, R.A. Moss, and A.M. Schmidt, Activation of the receptor for advanced glycation end products triggers a p21(ras)-dependent mitogen-activated protein kinase pathway regulated by oxidant stress. *Journal of Biological Chemistry*, 1997. **272**(28): p. 17810-4.

90. Yeh, C.H., L. Sturgis, J. Haidacher, X.N. Zhang, S.J. Sherwood, R.J. Bjercke, O. Juhasz, M.T. Crow, R.G. Tilton, and L. Denner, Requirement for p38 and p44/p42 mitogen-activated protein kinases in RAGE-mediated nuclear factor-kappaB transcriptional activation and cytokine secretion. *Diabetes*, 2001. **50**(6): p. 1495-504.

91. Wautier, M.P., O. Chappey, S. Corda, D.M. Stern, A.M. Schmidt, and J.L. Wautier, Activation of NADPH oxidase by AGE links oxidant stress to altered gene expression via RAGE. *American Journal of Physiology - Endocrinology & Metabolism*, 2001. **280**(5): p. E685-94.

92. Li, J. and A.M. Schmidt, Characterization and functional analysis of the promoter of RAGE, the receptor for advanced glycation end products. *J Biol Chem*, 1997. **272**(26): p. 16498-506.

93. Tanaka, N., H. Yonekura, S. Yamagishi, H. Fujimori, Y. Yamamoto, and H. Yamamoto, The receptor for advanced glycation end products is induced by the glycation products themselves and tumor necrosis factor-alpha through nuclear factor-kappa B, and by 17beta-estradiol through Sp-1 in human vascular endothelial cells. *Journal of Biological Chemistry*, 2000. **275**(33): p. 25781-90.

94. Bierhaus, A., S. Schiekofer, M. Schwaninger, M. Andrassy, P.M. Humpert, J. Chen, M. Hong, T. Luther, T. Henle, I. Kloting, M. Morcos, M. Hofmann, H. Tritschler, B. Weigle, M. Kasper, M. Smith, G. Perry, A.M. Schmidt, D.M. Stern, H.U. Haring, E. Schleicher, and P.P. Nawroth, Diabetes-associated sustained activation of the transcription factor nuclear factor-kappaB. *Diabetes*, 2001. **50**(12): p. 2792-808.

95. Ritthaler, U., Y. Deng, Y. Zhang, J. Greten, M. Abel, B. Sido, J. Allenberg, G. Otto, H. Roth, A. Bierhaus, and et al., Expression of receptors for advanced glycation end products in peripheral occlusive vascular disease. *Am J Pathol*, 1995. **146**(3): p. 688-94.

96. Soulis, T., V. Thallas, S. Youssef, R.E. Gilbert, B.G. McWilliam, R.P. Murray-McIntosh, and M.E. Cooper, Advanced glycation end products and their receptors co-localise in rat organs susceptible to diabetic microvascular injury. *Diabetologia*, 1997. **40**(6): p. 619-28.

97. Basta, G., G. Lazzerini, M. Massaro, T. Simoncini, P. Tanganelli, C. Fu, T. Kislinger, D.M. Stern, A.M. Schmidt, and R. De Caterina, Advanced glycation end products activate endothelium through signal-transduction receptor RAGE: a mechanism for amplification of inflammatory responses. *Circulation*, 2002. **105**(7): p. 816-22.

98. Lu, C., J.C. He, W. Cai, H. Liu, L. Zhu, and H. Vlassara, Advanced glycation endproduct (AGE) receptor 1 is a negative regulator of the inflammatory response to AGE in mesangial cells. *Proc Natl Acad Sci U S A*, 2004. **101**(32): p. 11767-72.

99. Shaw, S.S., A.M. Schmidt, A.K. Banes, X. Wang, D.M. Stern, and M.B. Marrero, S100B-RAGE-mediated augmentation of angiotensin II-induced activation of JAK2 in vascular smooth muscle cells is dependent on PLD2. *Diabetes*, 2003. **52**(9): p. 2381-8.

100. Kislinger, T., C. Fu, B. Huber, W. Qu, A. Taguchi, S. Du Yan, M. Hofmann, S.F. Yan, M. Pischetsrieder, D. Stern, and A.M. Schmidt, Nepsilon -(Carboxymethyl)Lysine Adducts of Proteins Are Ligands for Receptor for Advanced Glycation End Products That Activate Cell Signaling Pathways and Modulate Gene Expression. *J. Biol. Chem.*, 1999. **274**(44): p. 31740-31749.

101. King, G.L. and M. Brownlee, The cellular and molecular mechanisms of diabetic complications. *Endocrinol Metab Clin North Am*, 1996. **25**(2): p. 255-70.

102. Dukic-Stefanovic, S., J. Gasic-Milenkovic, W. Deuther-Conrad, and G. Munch, Signal transduction pathways in mouse microglia N-11 cells activated by advanced glycation endproducts (AGEs). *J Neurochem*, 2003. **87**(1): p. 44-55.

103. Scaffidi, P., T. Misteli, and M.E. Bianchi, Release of chromatin protein HMGB1 by necrotic cells triggers inflammation. *Nature*, 2002. **418**(6894): p. 191-5.

104. Wang, H., O. Bloom, M. Zhang, J.M. Vishnubhakat, M. Ombrellino, J. Che, A. Frazier, H. Yang, S. Ivanova, L. Borovikova, K.R. Manogue, E. Faist, E. Abraham, J. Andersson, U. Andersson, P.E. Molina, N.N. Abumrad, A. Sama, and K.J. Tracey, HMG-1 as a late mediator of endotoxin lethality in mice. *Science*, 1999. **285**(5425): p. 248-51.

105. Abraham, E., J. Arcaroli, A. Carmody, H. Wang, and K.J. Tracey, HMG-1 as a mediator of acute lung inflammation. *J Immunol*, 2000. **165**(6): p. 2950-4.

106. Yan, S.D., H. Zhu, A. Zhu, A. Golabek, H. Du, A. Roher, J. Yu, C. Soto, A.M. Schmidt, D. Stern, and M. Kindy, Receptor-dependent cell stress and amyloid accumulation in systemic amyloidosis. *Nat Med*, 2000. **6**(6): p. 643-51.

107. Ruderman, N.B., J.R. Williamson, and M. Brownlee, Glucose and diabetic vascular disease. *Faseb J*, 1992. **6**(11): p. 2905-14.

108. Bunn, H.F. and P.J. Higgins, Reaction of monosaccharides with proteins: possible evolutionary significance. *Science*, 1981. **213**(4504): p. 222-4.

109. Thorpe, S.R. and J.W. Baynes, Role of the Maillard reaction in diabetes mellitus and diseases of aging. *Drugs Aging*, 1996. **9**(2): p. 69-77.

110. Brownlee, M., Biochemistry and molecular cell biology of diabetic complications. *Nature*, 2001. **414**(6865): p. 813-20.

111. Schmidt, A.M., S.D. Yan, J.L. Wautier, and D. Stern, Activation of receptor for advanced glycation end products: a mechanism for chronic vascular dysfunction in diabetic vasculopathy and atherosclerosis. *Circulation Research*, 1999. **84**(5): p. 489-97.

112. Dyer, D.G., J.A. Dunn, S.R. Thorpe, K.E. Bailie, T.J. Lyons, D.R. McCance, and J.W. Baynes, Accumulation of Maillard reaction products in skin collagen in diabetes and aging. *J Clin Invest*, 1993. **91**(6): p. 2463-9.

113. Fu, M.X., K.J. Wells-Knecht, J.A. Blackledge, T.J. Lyons, S.R. Thorpe, and J.W. Baynes, Glycation, glycoxidation, and cross-linking of collagen by glucose. Kinetics, mechanisms, and inhibition of late stages of the Maillard reaction. *Diabetes*, 1994. **43**(5): p. 676-83.

114. Thornalley, P.J., Cell activation by glycated proteins. AGE receptors, receptor recognition factors and functional classification of AGEs. *Cell Mol Biol (Noisy-le-grand)*, 1998. **44**(7): p. 1013-23.

115. Miyata, T., O. Hori, J. Zhang, S.D. Yan, L. Ferran, Y. Iida, and A.M. Schmidt, The receptor for advanced glycation end products (RAGE) is a central mediator of the interaction of AGE-beta2microglobulin with human mononuclear phagocytes via an oxidant-sensitive pathway. Implications for the pathogenesis of dialysis-related amyloidosis. *J Clin Invest*, 1996. **98**(5): p. 1088-94.

116. Yan, S.F., R. Ramasamy, Y. Naka, and A.M. Schmidt, Glycation, inflammation, and RAGE: a scaffold for the macrovascular complications of diabetes and beyond. *Circ Res*, 2003. **93**(12): p. 1159-69.

117. Giardino, I., D. Edelstein, and M. Brownlee, Nonenzymatic glycosylation in vitro and in bovine endothelial cells alters basic fibroblast growth factor activity. A model for intracellular glycosylation in diabetes. *J Clin Invest*, 1994. **94**(1): p. 110-7.

118. Tanaka, S., G. Avigad, B. Brodsky, and E.F. Eikenberry, Glycation induces expansion of the molecular packing of collagen. *J Mol Biol*, 1988. **203**(2): p. 495-505.

119. Haitoglou, C.S., E.C. Tsilibary, M. Brownlee, and A.S. Charonis, Altered cellular interactions between endothelial cells and nonenzymatically glucosylated laminin/type IV collagen. *J Biol Chem*, 1992. **267**(18): p. 12404-7.

120. Bucala, R., K.J. Tracey, and A. Cerami, Advanced glycosylation products quench nitric oxide and mediate defective endothelium-dependent vasodilatation in experimental diabetes. *J Clin Invest*, 1991. **87**(2): p. 432-8.

121. Wautier, J.L., C. Zoukourian, O. Chappey, M.P. Wautier, P.J. Guillausseau, R. Cao, O. Hori, D. Stern, and A.M. Schmidt, Receptor-mediated endothelial cell dysfunction in diabetic vasculopathy. Soluble receptor for advanced glycation end products blocks hyperpermeability in diabetic rats. *Journal of Clinical Investigation*, 1996. **97**(1): p. 238-43.

122. Ando, K., M. Beppu, K. Kikugawa, R. Nagai, and S. Horiuchi, Membrane proteins of human erythrocytes are modified by advanced glycation end products during aging in the circulation. *Biochem Biophys Res Commun*, 1999. **258**(1): p. 123-7.

123. Viberti, G.C., Increased capillary permeability in diabetes mellitus and its relationship to microvascular angiopathy. *Am J Med*, 1983. **75**(5B): p. 81-4.

124. Renard, C., O. Chappey, M.P. Wautier, M. Nagashima, E. Lundh, J. Morser, L. Zhao, A.M. Schmidt, J.M. Scherrmann, and J.L. Wautier, Recombinant advanced glycation end product receptor pharmacokinetics in normal and diabetic rats. *Mol Pharmacol*, 1997. **52**(1): p. 54-62.

125. Oldfield, M.D., L.A. Bach, J.M. Forbes, D. Nikolic-Paterson, A. McRobert, V. Thallas, R.C. Atkins, T. Osicka, G. Jerums, and M.E. Cooper, Advanced glycation end products cause epithelial-myofibroblast transdifferentiation via the receptor for advanced glycation end products (RAGE). *J Clin Invest*, 2001. **108**(12): p. 1853-63.

126. Li, J.H., W. Wang, X.R. Huang, M. Oldfield, A.M. Schmidt, M.E. Cooper, and H.Y. Lan, Advanced glycation end products induce tubular epithelial-myofibroblast transition through the RAGE-ERK1/2 MAP kinase signaling pathway. *Am J Pathol*, 2004. **164**(4): p. 1389-97.

127. Fehrenbach, H., R. Weiskirchen, M. Kasper, and A.M. Gressner, Up-regulated expression of the receptor for advanced glycation end products in cultured rat hepatic stellate cells during transdifferentiation to myofibroblasts. *Hepatology*, 2001. **34**(5): p. 943-52.

128. Sakaguchi, T., S.F. Yan, S.D. Yan, D. Belov, L.L. Rong, M. Sousa, M. Andrassy, S.P. Marso, S. Duda, B. Arnold, B. Liliensiek, P.P. Nawroth, D.M. Stern, A.M. Schmidt, and Y. Naka, Central role of RAGE-dependent neointimal expansion in arterial restenosis. *J Clin Invest*, 2003. **111**(7): p. 959-72.

129. Zhou, Z., K. Wang, M.S. Penn, S.P. Marso, M.A. Lauer, F. Forudi, X. Zhou, W. Qu, Y. Lu, D.M. Stern, A.M. Schmidt, A.M. Lincoff, and E.J. Topol, Receptor for AGE (RAGE) mediates neointimal formation in response to arterial injury. *Circulation*, 2003. **107**(17): p. 2238-43.

130. Maher, J.F. and D. Nathans, Multivalent DNA-binding properties of the HMG-1 proteins. *Proc Natl Acad Sci U S A*, 1996. **93**(13): p. 6716-20.

131. Parkkinen, J., E. Raulo, J. Merenmies, R. Nolo, E.O. Kajander, M. Baumann, and H. Rauvala, Amphoterin, the 30-kDa protein in a family of HMG1-type polypeptides. Enhanced expression in transformed cells, leading edge localization, and interactions with plasminogen activation. *J Biol Chem*, 1993. **268**(26): p. 19726-38.

132. Rauvala, H. and R. Pihlaskari, Isolation and some characteristics of an adhesive factor of brain that enhances neurite outgrowth in central neurons. *J Biol Chem*, 1987. **262**(34): p. 16625-35.

133. Daston, M.M. and N. Ratner, Amphoterin (P30, HMG-1) and RIP are early markers of oligodendrocytes in the developing rat spinal cord. *J Neurocytol*, 1994. **23**(5): p. 323-32.

134. Park, J.S., D. Svetkauskaite, Q. He, J.Y. Kim, D. Strassheim, A. Ishizaka, and E. Abraham, Involvement of toll-like receptors 2 and 4 in cellular activation by high mobility group box 1 protein. *J Biol Chem*, 2004. **279**(9): p. 7370-7.

135. Yang, H., H. Wang, and K.J. Tracey, HMG-1 rediscovered as a cytokine. *Shock*, 2001. **15**(4): p. 247-53.

136. Treutiger, C.J., G.E. Mullins, A.S. Johansson, A. Rouhiainen, H.M. Rauvala, H. Erlandsson-Harris, U. Andersson, H. Yang, K.J. Tracey, J. Andersson, and J.E. Palmblad, High mobility group 1 B-box mediates activation of human endothelium. *J Intern Med*, 2003. **254**(4): p. 375-85.

137. Fiuza, C., M. Bustin, S. Talwar, M. Tropea, E. Gerstenberger, J.H. Shelhamer, and A.F. Suffredini, Inflammation-promoting activity of HMGB1 on human microvascular endothelial cells. *Blood*, 2003. **101**(7): p. 2652-60.

138. Liliensiek, B., M.A. Weigand, A. Bierhaus, W. Nicklas, M. Kasper, S. Hofer, J. Plachky, H.J. Grone, F.C. Kurschus, A.M. Schmidt, S.D. Yan, E. Martin, E. Schleicher, D.M. Stern, G.G. Hammerling, P.P. Nawroth, and B. Arnold, Receptor for advanced glycation end products (RAGE) regulates sepsis but not the adaptive immune response. *J Clin Invest*, 2004. **113**(11): p. 1641-50.

139. Heizmann, C.W., G. Fritz, and B.W. Schafer, S100 proteins: structure, functions and pathology. *Front Biosci*, 2002. **7**: p. d1356-68.

140. Hsieh, H.L., B.W. Schafer, B. Weigle, and C.W. Heizmann, S100 protein translocation in response to extracellular S100 is mediated by receptor for advanced glycation endproducts in human endothelial cells. *Biochem Biophys Res Commun*, 2004. **316**(3): p. 949-59.

141. Huttunen, H.J., J. Kuja-Panula, G. Sorci, A.L. Agneletti, R. Donato, and H. Rauvala, Coregulation of neurite outgrowth and cell survival by amphoterin and S100 proteins through receptor for advanced glycation end products (RAGE) activation. *Journal of Biological Chemistry*, 2000. **275**(51): p. 40096-105.

142. Passey, R.J., K. Xu, D.A. Hume, and C.L. Geczy, S100A8: emerging functions and regulation. *J Leukoc Biol*, 1999. **66**(4): p. 549-56.

143. Arumugam, T., D.M. Simeone, A.M. Schmidt, and C.D. Logsdon, S100P stimulates cell proliferation and survival via receptor for activated glycation end products (RAGE). *J Biol Chem*, 2004. **279**(7): p. 5059-65.

144. Belot, N., R. Pochet, C.W. Heizmann, R. Kiss, and C. Decaestecker, Extracellular S100A4 stimulates the migration rate of astrocytic tumor cells by modifying the organization of their actin cytoskeleton. *Biochim Biophys Acta*, 2002. **1600**(1-2): p. 74-83.

145. Wicki, R., B.W. Schafer, P. Erne, and C.W. Heizmann, Characterization of the human and mouse cDNAs coding for S100A13, a new member of the S100 protein family. *Biochem Biophys Res Commun*, 1996. **227**(2): p. 594-9.

146. Ridinger, K., B.W. Schafer, I. Durussel, J.A. Cox, and C.W. Heizmann, S100A13. Biochemical characterization and subcellular localization in different cell lines. *J Biol Chem*, 2000. **275**(12): p. 8686-94.

147. Vogl, T., C. Propper, M. Hartmann, A. Strey, K. Strupat, C. van den Bos, C. Sorg, and J. Roth, S100A12 is expressed exclusively by granulocytes and acts independently from MRP8 and MRP14. *J Biol Chem*, 1999. **274**(36): p. 25291-6.

148. Shashoua, V.E., G.W. Hesse, and B.W. Moore, Proteins of the brain extracellular fluid: evidence for release of S-100 protein. *J Neurochem*, 1984. **42**(6): p. 1536-41.

149. Kligman, D. and D.R. Marshak, Purification and characterization of a neurite extension factor from bovine brain. *Proc Natl Acad Sci U S A*, 1985. **82**(20): p. 7136-9.

150. Van Eldik, L.J., B. Christie-Pope, L.M. Bolin, E.M. Shooter, and W.O. Whetsell, Jr., Neurotrophic activity of S-100 beta in cultures of dorsal root ganglia from embryonic chick and fetal rat. *Brain Res*, 1991. **542**(2): p. 280-5.

151. Hu, J., F. Castets, J.L. Guevara, and L.J. Van Eldik, S100 beta stimulates inducible nitric oxide synthase activity and mRNA levels in rat cortical astrocytes. *J Biol Chem*, 1996. **271**(5): p. 2543-7.

152. Goova, M.T., J. Li, T. Kislinger, W. Qu, Y. Lu, L.G. Bucciarelli, S. Nowygrod, B.M. Wolf, X. Caliste, S.F. Yan, D.M. Stern, and A.M. Schmidt, Blockade of receptor for advanced glycation end-products restores effective wound healing in diabetic mice. *American Journal of Pathology*, 2001. **159**(2): p. 513-25.

153. Foell, D., T. Kucharzik, M. Kraft, T. Vogl, C. Sorg, W. Domschke, and J. Roth, Neutrophil derived human S100A12 (EN-RAGE) is strongly expressed during chronic active inflammatory bowel disease. *Gut*, 2003. **52**(6): p. 847-53.

154. Foell, D., S. Seeliger, T. Vogl, H.G. Koch, H. Maschek, E. Harms, C. Sorg, and J. Roth, Expression of S100A12 (EN-RAGE) in cystic fibrosis. *Thorax*, 2003. **58**(7): p. 613-7.

155. Magi, B., L. Bini, M.G. Perari, A. Fossi, J.C. Sanchez, D. Hochstrasser, S. Paesano, R. Raggiaschi, A. Santucci, V. Pallini, and P. Rottoli, Bronchoalveolar lavage fluid protein composition in patients with sarcoidosis and idiopathic pulmonary fibrosis: A two-dimensional electrophoretic study. *Electrophoresis*, 2002. **23**(19): p. 3434-44.

156. Masters, C.L., G. Simms, N.A. Weinman, G. Multhaup, B.L. McDonald, and K. Beyreuther, Amyloid plaque core protein in Alzheimer disease and Down syndrome. *Proc Natl Acad Sci U S A*, 1985. **82**(12): p. 4245-9.

157. Selkoe, D.J., Toward a comprehensive theory for Alzheimer's disease. Hypothesis: Alzheimer's disease is caused by the cerebral accumulation and cytotoxicity of amyloid beta-protein. *Ann N Y Acad Sci*, 2000. **924**: p. 17-25.

158. Yankner, B.A., L.K. Duffy, and D.A. Kirschner, Neurotrophic and neurotoxic effects of amyloid beta protein: reversal by tachykinin neuropeptides. *Science*, 1990. **250**(4978): p. 279-82.

159. Hadding, A., B. Kaltschmidt, and C. Kaltschmidt, Overexpression of receptor of advanced glycation end products hypersensitizes cells for amyloid beta peptide-induced cell death. *Biochim Biophys Acta*, 2004. **1691**(1): p. 67-72.

160. Hensley, K., J.M. Carney, M.P. Mattson, M. Aksenova, M. Harris, J.F. Wu, R.A. Floyd, and D.A. Butterfield, A model for beta-amyloid aggregation and neurotoxicity based on free radical generation by the peptide: relevance to Alzheimer disease. *Proc Natl Acad Sci U S A*, 1994. **91**(8): p. 3270-4.

161. Verdier, Y. and B. Penke, Binding sites of amyloid beta-peptide in cell plasma membrane and implications for Alzheimer's disease. *Curr Protein Pept Sci*, 2004. **5**(1): p. 19-31.

162. Deane, R., S. Du Yan, R.K. Submamaryan, B. LaRue, S. Jovanovic, E. Hogg, D. Welch, L. Manness, C. Lin, J. Yu, H. Zhu, J. Ghiso, B. Frangione, A. Stern, A.M. Schmidt, D.L. Armstrong, B. Arnold, B. Liliensiek, P. Nawroth, F. Hofman, M. Kindy, D. Stern, and B. Zlokovic, RAGE mediates amyloid-beta peptide transport across the blood-brain barrier and accumulation in brain. *Nat Med*, 2003. **9**(7): p. 907-13.

163. Prusiner, S.B., Shattuck lecture--neurodegenerative diseases and prions. *N Engl J Med*, 2001. **344**(20): p. 1516-26.

164. Sasaki, N., M. Takeuchi, H. Chowei, S. Kikuchi, Y. Hayashi, N. Nakano, H. Ikeda, S. Yamagishi, T. Kitamoto, T. Saito, and Z. Makita, Advanced glycation end products (AGE) and their receptor (RAGE) in the brain of patients with Creutzfeldt-Jakob disease with prion plaques. *Neurosci Lett*, 2002. **326**(2): p. 117-20.

165. Thabut, G., H. Mal, Y. Castier, O. Groussard, O. Brugiere, R. Marrash-Chahla, G. Leseche, and M. Fournier, Survival benefit of lung transplantation for patients with idiopathic pulmonary fibrosis. *J Thorac Cardiovasc Surg*, 2003. **126**(2): p. 469-75.

166. Schmidt, A.M., S.D. Yan, S.F. Yan, and D.M. Stern, The multiligand receptor RAGE as a progression factor amplifying immune and inflammatory responses. *J Clin Invest*, 2001. **108**(7): p. 949-55.

167. Simm, A., B. Bartling, and R.E. Silber, RAGE: a new pleiotropic antagonistic gene? *Ann N Y Acad Sci*, 2004. **1019**: p. 228-31.

168. Dahlin, K., E.M. Mager, L. Allen, Z. Tigue, L. Goodglick, M. Wadehra, and L. Dobbs, Identification of genes differentially expressed in rat alveolar type I cells. *Am J Respir Cell Mol Biol*, 2004. **31**(3): p. 309-16.

169. Shirasawa, M., N. Fujiwara, S. Hirabayashi, H. Ohno, J. Iida, K. Makita, and Y. Hata, Receptor for advanced glycation end-products is a marker of type I lung alveolar cells. *Genes Cells*, 2004. **9**(2): p. 165-74.

170. Rahman, I., E. Skwarska, M. Henry, M. Davis, C.M. O'Connor, M.X. FitzGerald, A. Greening, and W. MacNee, Systemic and pulmonary oxidative stress in idiopathic pulmonary fibrosis. *Free Radic Biol Med*, 1999. **27**(1-2): p. 60-8.

171. Behr, J., B. Degenkolb, F. Krombach, and C. Vogelmeier, Intracellular glutathione and bronchoalveolar cells in fibrosing alveolitis: effects of N-acetylcysteine. *Eur Respir J*, 2002. **19**(5): p. 906-11.

172. Fattman, C.L., L.Y. Chang, T.A. Termin, L. Petersen, J.J. Enghild, and T.D. Oury, Enhanced bleomycin-induced pulmonary damage in mice lacking extracellular superoxide dismutase. *Free Radic Biol Med*, 2003. **35**(7): p. 763-71.

173. Baynes, J.W., Role of oxidative stress in development of complications in diabetes. *Diabetes*, 1991. **40**(4): p. 405-12.

174. Matsuse, T., E. Ohga, S. Teramoto, M. Fukayama, R. Nagai, S. Horiuchi, and Y. Ouchi, Immunohistochemical localisation of advanced glycation end products in pulmonary fibrosis. *J Clin Pathol*, 1998. **51**(7): p. 515-9.

175. Enomoto, T., J. Usuki, A. Azuma, T. Nakagawa, and S. Kudoh, Diabetes mellitus may increase risk for idiopathic pulmonary fibrosis. *Chest*, 2003. **123**(6): p. 2007-11.

176. Popov, D. and M. Simionescu, Alterations of lung structure in experimental diabetes, and diabetes associated with hyperlipidaemia in hamsters. *Eur Respir J*, 1997. **10**(8): p. 1850-8.

177. Kuniyasu, H., Y. Chihara, and H. Kondo, Differential effects between amphoterin and advanced glycation end products on colon cancer cells. *Int J Cancer*, 2003. **104**(6): p. 722-7.

178. Kuniyasu, H., N. Oue, A. Wakikawa, H. Shigeishi, N. Matsutani, K. Kuraoka, R. Ito, H. Yokozaki, and W. Yasui, Expression of receptors for advanced glycation end-products (RAGE) is closely associated with the invasive and metastatic activity of gastric cancer. *J Pathol*, 2002. **196**(2): p. 163-70.

179. Miki, S., S. Kasayama, Y. Miki, Y. Nakamura, M. Yamamoto, B. Sato, and T. Kishimoto, Expression of receptors for advanced glycosylation end products on renal cell carcinoma cells in vitro. *Biochem Biophys Res Commun*, 1993. **196**(2): p. 984-9.

180. Hofmann, H.S., G. Hansen, S. Burdach, B. Bartling, R.E. Silber, and A. Simm, Discrimination of human lung neoplasm from normal lung by two target genes. *Am J Respir Crit Care Med*, 2004. **170**(5): p. 516-9.

181. Bartling, B., H.S. Hofmann, B. Weigle, R.E. Silber, and A. Simm, Down-regulation of the receptor for advanced glycation end-products (RAGE) supports non-small cell lung carcinoma. *Carcinogenesis*, 2005. **26**(2): p. 293-301.

182. Schraml, P., R. Shipman, M. Colombi, and C.U. Ludwig, Identification of genes differentially expressed in normal lung and non-small cell lung carcinoma tissue. *Cancer Res*, 1994. **54**(19): p. 5236-40.

183. Wendt, T.M., N. Tanji, J. Guo, T.R. Kislinger, W. Qu, Y. Lu, L.G. Bucciarelli, L.L. Rong, B. Moser, G.S. Markowitz, G. Stein, A. Bierhaus, B. Liliensiek, B. Arnold, P.P. Nawroth, D.M. Stern, V.D. D'Agati, and A.M. Schmidt, RAGE drives the development of glomerulosclerosis and implicates podocyte activation in the pathogenesis of diabetic nephropathy. *Am J Pathol*, 2003. **162**(4): p. 1123-37.

184. De Vriese, A.S., A. Flyvbjerg, S. Mortier, R.G. Tilton, and N.H. Lameire, Inhibition of the interaction of AGE-RAGE prevents hyperglycemia-induced fibrosis of the peritoneal membrane. *J Am Soc Nephrol*, 2003. **14**(8): p. 2109-18.

185. Jendrisak, J., *The Use of Polyethyleneimine in Protein Purification*, in *Protein Purification: Micro to Macro: proceedings of a Cetus- UCLA symposium held at Frisco, Colorado, March 29-April 4, 1987*, R. Burgess, Editor. 1987, A. R. Liss, Inc.: New York. p. 75-97.

186. Chomczynski, P. and N. Sacchi, Single-step method of RNA isolation by acid guanidinium thiocyanate-phenol-chloroform extraction. *Anal Biochem*, 1987. **162**(1): p. 156-9.

187. Perkins, D.N., D.J. Pappin, D.M. Creasy, and J.S. Cottrell, Probability-based protein identification by searching sequence databases using mass spectrometry data. *Electrophoresis*, 1999. **20**(18): p. 3551-67.

188. Kaminski, N. and N. Friedman, Practical approaches to analyzing results of microarray experiments. *Am J Respir Cell Mol Biol*, 2002. **27**(2): p. 125-32.

189. Constien, R., A. Forde, B. Liliensiek, H.J. Grone, P. Nawroth, G. Hammerling, and B. Arnold, Characterization of a novel EGFP reporter mouse to monitor Cre recombination as demonstrated by a Tie2 Cre mouse line. *Genesis*, 2001. **30**(1): p. 36-44.

190. Valencia, J.V., S.C. Weldon, D. Quinn, G.H. Kiers, J. DeGroot, J.M. TeKoppele, and T.E. Hughes, Advanced glycation end product ligands for the receptor for advanced glycation end products: biochemical characterization and formation kinetics. *Anal Biochem*, 2004. **324**(1): p. 68-78.

191. Soulis-Liparota, T., M. Cooper, D. Papazoglou, B. Clarke, and G. Jerums, Retardation by aminoguanidine of development of albuminuria, mesangial expansion, and tissue fluorescence in streptozocin-induced diabetic rat. *Diabetes*, 1991. **40**(10): p. 1328-34.

192. Srikrishna, G., H.J. Huttunen, L. Johansson, B. Weigle, Y. Yamaguchi, H. Rauvala, and H.H. Freeze, N -Glycans on the receptor for advanced glycation end products influence amphoterin binding and neurite outgrowth. *J Neurochem*, 2002. **80**(6): p. 998-1008.

193. Devaux, Y., R.M. Senior, and P. Ray, RAGE: A New Target for MMP-9 in the Regulation of Inflammatory Response in the Lung during Oxidative Stress. *American Journal of Respiratory and Critical Care Medicine*, 2004. **169**(7): p. A456.

194. Tan, R.J., C.L. Fattman, S.C. Watkins, and T.D. Oury, Redistribution of pulmonary EC-SOD after exposure to asbestos. *J Appl Physiol*, 2004. **97**(5): p. 2006-13.

195. Kamp, D.W., V. Panduri, S.A. Weitzman, and N. Chandel, Asbestos-induced alveolar epithelial cell apoptosis: role of mitochondrial dysfunction caused by iron-derived free radicals. *Mol Cell Biochem*, 2002. **234-235**(1-2): p. 153-60.

196. Schwenk, F., U. Baron, and K. Rajewsky, A cre-transgenic mouse strain for the ubiquitous deletion of loxP-flanked gene segments including deletion in germ cells. *Nucleic Acids Res*, 1995. **23**(24): p. 5080-1.

197. Kasper, M. and R.C. Hughes, Immunocytochemical evidence for a modulation of galectin 3 (Mac-2), a carbohydrate binding protein, in pulmonary fibrosis. *J Pathol*, 1996. **179**(3): p. 309-16.

198. Selman, M., V. Ruiz, S. Cabrera, L. Segura, R. Ramirez, R. Barrios, and A. Pardo, TIMP-1, -2, -3, and -4 in idiopathic pulmonary fibrosis. A prevailing nondegradative lung microenvironment? *Am J Physiol Lung Cell Mol Physiol*, 2000. **279**(3): p. L562-74.

199. Desmouliere, A., A. Geinoz, F. Gabbiani, and G. Gabbiani, Transforming growth factor-beta 1 induces alpha-smooth muscle actin expression in granulation tissue myofibroblasts and in quiescent and growing cultured fibroblasts. *J Cell Biol*, 1993. **122**(1): p. 103-11.

200. Mattey, D.L., P.T. Dawes, N.B. Nixon, and H. Slater, Transforming growth factor beta 1 and interleukin 4 induced alpha smooth muscle actin expression and myofibroblast-like differentiation in human synovial fibroblasts in vitro: modulation by basic fibroblast growth factor. *Ann Rheum Dis*, 1997. **56**(7): p. 426-31.

201. Masure, S., G. Nys, P. Fiten, J. Van Damme, and G. Opdenakker, Mouse gelatinase B. cDNA cloning, regulation of expression and glycosylation in WEHI-3 macrophages and gene organisation. *Eur J Biochem*, 1993. **218**(1): p. 129-41.

202. Hesterberg, T.W., C. Axten, E.E. McConnell, G. Oberdorster, J. Everitt, W.C. Miiller, J. Chevalier, G.R. Chase, and P. Thevenaz, Chronic inhalation study of fiber glass and amosite asbestos in hamsters: twelve-month preliminary results. *Environ Health Perspect*, 1997. **105 Suppl 5**: p. 1223-9.

203. McConnell, E.E., C. Axten, T.W. Hesterberg, J. Chevalier, W.C. Miiller, J. Everitt, G. Oberdorster, G.R. Chase, P. Thevenaz, and P. Kotin, Studies on the inhalation toxicology of two fiberglasses and amosite asbestos in the Syrian golden hamster. Part II. Results of chronic exposure. *Inhal Toxicol*, 1999. **11**(9): p. 785-835.

204. Kikuchi, Y., S. Kobayashi, N. Hemmi, R. Ikee, N. Hyodo, T. Saigusa, T. Namikoshi, M. Yamada, S. Suzuki, and S. Miura, Galectin-3-positive cell infiltration in human diabetic nephropathy. *Nephrol Dial Transplant*, 2004. **19**(3): p. 602-7.

205. Vlassara, H., Y.M. Li, F. Imani, D. Wojciechowicz, Z. Yang, F.T. Liu, and A. Cerami, Identification of galectin-3 as a high-affinity binding protein for advanced glycation end products (AGE): a new member of the AGE-receptor complex. *Mol Med*, 1995. **1**(6): p. 634-46.

206. Woessner, J.F., The determination of hydroxyproline in tissue and protein samples containing small proportions of this imino acid. *Archives of Biochemistry and Biophysics*, 1961. **93**: p. 440-447.

207. Perl, A.K., J.W. Tichelaar, and J.A. Whitsett, Conditional gene expression in the respiratory epithelium of the mouse. *Transgenic Res*, 2002. **11**(1): p. 21-9.

208. Wang, H., H. Yang, C.J. Czura, A.E. Sama, and K.J. Tracey, HMGB1 as a late mediator of lethal systemic inflammation. *Am J Respir Crit Care Med*, 2001. **164**(10 Pt 1): p. 1768-73.

209. Kolodsick, J.E., M. Peters-Golden, J. Larios, G.B. Toews, V.J. Thannickal, and B.B. Moore, Prostaglandin E2 inhibits fibroblast to myofibroblast transition via E. prostanoid receptor 2 signaling and cyclic adenosine monophosphate elevation. *Am J Respir Cell Mol Biol*, 2003. **29**(5): p. 537-44.

210. Lutz, W. and J. Stetkiewicz, High mobility group box 1 protein as a late-acting mediator of acute lung inflammation. *Int J Occup Med Environ Health*, 2004. **17**(2): p. 245-54.